

**DESIGN AND SYNTHESIS OF NOVEL YELLOW AND  
GREEN LIGHT EMITTING ORGANIC MATERIALS  
FOR APPLICATION IN NON-LINEAR OPTICS AND  
RELATED STUDIES**

*Thesis submitted to the  
Cochin University of Science and Technology  
In partial fulfilment of the requirements for the degree of*

*Doctor of Philosophy  
in  
Chemistry*

*In the Faculty of Science  
By*

**Nithya C.**

*(Reg. No: 4042)*

*Under the supervision of*

**Dr. Prathapan S.**



**DEPARTMENT OF APPLIED CHEMISTRY  
COCHIN UNIVERSITY OF SCIENCE AND TECHNOLOGY  
KOCHI- 682 022, KERALA, INDIA**

*March 2017*



*Dedicated to my family, teachers and well-wishers.....*



*When you want something,*

*all the universe conspires in helping you to achieve it*

*~ Paulo Coelho*





**Department of Applied Chemistry**  
**Cochin University of Science and Technology**  
**Kochi 682 022, India**

---

**Dr. Prathapan S.**  
**Associate Professor**  
Ph:-0484-2575804  
email: prathapan@cusat.ac.in

20-03-2017

## *Certificate*

*This is to certify that the thesis entitled "DESIGN AND SYNTHESIS OF NOVEL YELLOW AND GREEN LIGHT EMITTING ORGANIC MATERIALS FOR APPLICATION IN NON-LINEAR OPTICS AND RELATED STUDIES" submitted by Ms. Nithya C., in partial fulfillment of the requirements for the degree of Doctor of Philosophy, to the Cochin University of Science and Technology, Kochi-22, is an authentic record of the original research work carried out by her under my guidance and supervision. The results embodied in this thesis, in full or in part, have not been submitted for the award of any other degree. All the relevant corrections and modifications suggested by the audience and recommended by the doctoral committee of the candidate during the presynopsis seminar have been incorporated in the thesis.*

Kochi 22  
March, 2017

**Prathapan S.**  
(Supervisor)





## DECLARATION

I hereby declare that the work presented in the thesis entitled **“DESIGN AND SYNTHESIS OF NOVEL YELLOW AND GREEN LIGHT EMITTING ORGANIC MATERIALS FOR APPLICATION IN NON-LINEAR OPTICS AND RELATED STUDIES”** is the result of genuine research carried out by me under the supervision of **Dr. PRATHAPAN S.**, Associate Professor of Organic Chemistry, Department of Applied Chemistry, Cochin University of Science and Technology, Kochi-22, and the same has not been submitted elsewhere for the award of any other degree.

*Kochi-22*  
*March 2017*

*Nithya C.*



## *ACKNOWLEDGEMENTS*

*This thesis is the pinnacle of my journey of Ph.D, and though my name is highlighted in the front page of this dissertation, there are great many people including my family members, teachers, friends and other well-wishers who have contributed for the accomplishment of this huge task,*

*First and foremost, I thank God almighty for showers of blessings on me and leading me on the right path for successful completion of my research work,*

*My deepest gratitude goes to my supervising guide, Dr. Prathapan S., for all his support, encouragement and patience throughout my research career as his student.*

*He uplifted me during the tough times of my research work, helped me out to solve many of my questions and queries for achieving my goal. All his expertise, timely involvement, advices and criticisms helped me to complete my research work in time.*

*It has been a greatly enriching experience to work under his guidance and I consider myself lucky enough to work under his supervision.*

*I extend my sincere thanks to Prof. K. Girish Kumar, Head, Department of Applied Chemistry and former heads of the department, Prof. K. Sreekumar, Dr. N. Manoj and Prof. M. R. Prathapachandra Kurup for providing me all the facilities here in this department. Dr. P. A. Unnikrishnan, my Doctoral Committee member, is also greatly acknowledged for all his concern and support. I acknowledge my sincere thanks to all the teaching and non-teaching staffs of the Department of Applied chemistry.*

*I offer my whole hearted thanks to Prof. M. R. Prathapachandra Kurup and Dr. M. Sithambaresan for helping me out with Single Crystal X-ray diffraction analysis in solving crystal data's and with publication of the results.*

*I specially thank Dr. Mahesh Kumar M. V. for helping me with computational calculations. In his busy schedule, he found time to resolve problems with some of*

*my experimental data's and interpreting the results theoretically. I sincerely acknowledge him for his support and patience.*

*My research work was carried out in collaboration with Department of Physics and my heartfelt thank goes to Dr. S. Jayalekshmi, Professor, Department of Physics, for providing me all the facilities there in the Department. I am deeply indebted to my husband Dr. Anand B. Puthirath, Tata Institute of fundamental Research, for helping me with many important characterizations including device fabrication. He had been a pillar support in my research career and moreover a good adviser to my research problems. I also thank Mr. Abhilash, Department of Physics, for helping me with sample analyses.*

*I gratefully acknowledge Dr. Reji Philip, Raman Research Institute (RRI), Bangalore, for carrying out non-linear optical studies of my compounds. I thank Dr. P. R. Rajamohanan, NCL Pune for various characterisations.*

*My thanks also goes to Saif STIC, CUSAT, SCTIMST, Thiruvananthapuram, CECRI, Karaikudi and IISER Thiruvananthapuram for various spectral analysis.*

*My thanks are also due to Dr. Shibu Eapen, Dr. Adarsh, K. J. and Mr. Saji, STIC CUSAT for helping me with SCXRD, TGA, DSC and NMR analyses.*

*I remember late Mr. Vishnu, P. Alpha chemicals and Diagnostics for supplying chemicals in time.*

*The financial assistance received from Department of Science & Technology-Innovation in Science Pursuit for Inspired Research (DST-INSPIRE), New Delhi is gratefully acknowledged.*

*I extend my heartfelt thanks to my seniors in the lab, Dr. Jomon, Dr. Sandhya, Dr. Vidya, Dr. Sajitha, Dr. Eason, Dr. Reshma, Dr. Rakesh for their support. I specially mention Dr. Jomon who had always extended his helping hands for all my doubts and queries. My labmates Saumya, Kala, Ligi, Jesna, Lekshmi, Tomson, Shan, Vineetha, Parvathy, Ashwathy, Jyothy, Amritha, Cisy, Jith, Rani, Nishad,*

*Kiran, Suma, Ashwathy C. S, Seena and all the friends of other groups in Department of Applied Chemistry and Department of Physics are deeply acknowledged for their boundless support and for making the atmosphere here fruitful and interesting. My friends and roommates in Athulya hostel Anju, Anjali, Bhavya, Sowmya, Jinisha should be mentioned specially for making my hostel life joyful.*

*Without my family, I would never be able to fulfill my dreams. My Amma, Achan, Chechi, Chetan and my little pearl Adhi all have encouraged and inspired me to fulfill my dreams. They have supported me emotionally, believed me and always expected the best from me. They gave me freedom to choose what I desired. I always wish to dedicate all my achievements to my family. I also thank all my in laws, mother-in-law, father-in-law, brother-in-law and sister-in-law for their support.*

*I am deeply indebted to my loving husband, Anand, he was always with me at times when I struggled with my work. His unfailing love, care and affection made the completion of this thesis possible. I greatly value his contribution and his patience, for he has answered all my questions without any hesitations. He boosted up my confidence at times when I was really frustrated. Many thanks to my soul mate for being with me always.*

*Nithya C.*



## PREFACE

In the present context, research has been extensively intensified in the field of light emitting polymers of which thiophene based ones have received much attention owing to their interesting optical properties. Thiophenes, in fact, have paved the way to achieve great milestones in the field of optoelectronics. Not only the polymers but even oligomers, currently being mentioned as “third generation” of organic conjugated polymers consisting of thiophene units are widely exploited in the various fields like fabrication of transistors, capacitors, polymeric light emitting diodes etc. Apart from polymers, oligomers have the special advantage of strong interchain interactions which make them applicable in the foresaid areas. Thiophene rings owing to their electron rich nature can be converted easily to other highly conducting forms. In addition, their electronic properties can be tuned widely offering flexibility to explore different areas. Thiophenes are considered to be the ideal building blocks in transition metal catalyzed cross coupling reactions. Their indistinguishable and unique electronic, optical, redox and self-assembling properties makes them promising candidates for organic electronics.

The thesis entitled: “**DESIGN AND SYNTHESIS OF NOVEL YELLOW AND GREEN LIGHT EMITTING ORGANIC MATERIALS FOR APPLICATION IN NON-LINER OPTICS AND RELATED STUDIES**” is mainly focused on the synthesis of some novel light emitting organic materials and to highlight the possibility of exploiting them in various fields like non-linear optics and polymeric light emitting diodes (PLED’s) etc. Bisthiophene cycloalkanones are

chosen as basic skeleton for synthesis since they are typical donor-acceptor systems and to best of our knowledge none of them have been used effectively in the field of optoelectronics. These compounds are known to possess various biological activities like antitumor, anticancer, antibacterial, antifungal activities and almost all research activities are primarily focused in exploring such activities of the compound. The oligomers synthesised from bisaromatic systems by direct arylation seemed to be interesting in the sense that a new technique for the synthesis of new materials with outweighing fluorescence almost covering the entire visible region is really a subject of great interest. Even though lack of proper literature reports on such compounds makes the characterisations a tough job, still the applicability of such systems as optical limiters and the junction like behavior typically called a Schottky junction *ie*, a metal-semiconductor junction obtained from I-V measurements further adds on to the beauty of these oligomers. We have also extended the scope of our studies to the derivatives of these bithiophene cycloalkanones *viz.* pyrazolines and their mechanism of formation was established by theoretical methods. Computational calculations were carried out using B3LYP hybrid functional and the results were obtained in agreement with the experimental data. Novel oligomer and polymer bearing pyrazoline moiety was also synthesised for applications in non-linear optics and PLED's. The conductivity and efficiency of the synthesised compounds, both oligomers and polymer have been successfully accomplished so as to motivate further research in this field. The overall performance of both oligomers and polymer



synthesised in this work generally outweighs all the disadvantages associated with oligomers when compared with polymers.

The thesis incorporates five chapters.

In chapter 1, introduction to the conducting polymers, importance of these polymers in the present era is explained. The advantage of synthesizing thiophene based conducting polymers and oligomers and the various methods available for polymerization are very well stated. A brief introduction to the bisaromatic cycloalkanone systems and their derivatives and possibility of using thiophenes as backbone are explained. Possibilities of exploiting pyrazolines other than any derivatives for carbonyl group modification are well studied in detail. The applicability of organic materials in third order non-linear optical studies and the experimental set-up of Z-scan technique are well presented.

Chapter 2 deals with the synthesis of various bithiophene cycloalkanones systems using four different classes of spacers and their mechanism of formation and regioselectivity are studied. The incorporation of such rigid spacers into the thiophene backbone offers a more planar conformation with diminished steric effect so that maximum delocalization of  $\pi$  electrons can be achieved. Compared with polythiophenes these systems are advantageous in the sense that there are less neighbouring interactions. The HOMO-LUMO levels of selected compounds are also developed by computational methods to calculate the band gap.

Chapter 3 deals with the organic materials *viz* oligomers synthesised by the polymerization of selected bisaromatic compounds by direct

arylation reaction. Two novel materials were synthesised and characterized using  $^1\text{H}$  NMR, Raman, FTIR, UV-Visible, PL, GPC, TGA, DSC, Cyclic voltammetry, Powder XRD and theoretical studies. The third order non-linear optical properties of the synthesised materials revealed their optical limiting nature and Schottky junction characteristics were studied by measuring the I-V characteristics of the material which in turn ensures its conductivity for application in devices. The materials though oligomers are proved to be promising candidates in the field of optoelectronics.

In chapter 4, the structural modification of bithiophene cycloalkanones to pyrazolines are well explained. Six novel pyrazolines were synthesised and characterized out of sixteen reactions performed and the use of computational calculations to account for the unusual behavior of formation of pyrazolines are described in detail. Taking five reactions, ie, three successful and two unsuccessful ones as example, the mechanism of formation of pyrazolines is explored by generating energy profile diagrams using hybrid functional theory. The results were obtained in well agreement with the experimental ones. Moreover, the rate determining step and exothermic behavior obtained by computational studies also confirms well with experimental results.

Chapter 5 focusses on synthesizing a polymer and oligomer from pyrazoline modified bithiophene systems using Stille coupling and direct arylation methods. Band gaps of the synthesised compounds had negligible difference which was established electrochemically, optically and theoretically. The organic materials, proved as

semiconductors, characterized using  $^1\text{H}$  NMR, Raman, FTIR, UV-Visible, PL, GPC, TGA, DSC, Cyclic voltammetry, Powder XRD and theoretical studies. Studies on non-linear optical properties of the compounds reveal the efficiency of oligomer synthesised. Schottky junction characterization of the materials are also discussed here within to prove its applicability for fabricating PLED's.

All the schemes, tables, figures and structural formulae are numbered chapter wise since each chapter forms an individual unit in this thesis. References considered relevant are provided at the end of each chapter.



## List of Abbreviations

Ea	: activation energy
AFM	: atomic force microscopy
E <sub>g</sub>	: band gap
B3LYP	: Becke, 3-parameter, Lee-Yang-Parr
DFT	: density functional theory
DOS	: density of states
DCM	: dichloromethane
DPV	: differential pulse voltammetry
DSC	: differential scanning calorimetry
DMF	: dimethyl formamide
EL	: electroluminescent
FTIR	: Fourier Transform Infrared
FCA	: free carrier absorption
GPC	: gel permeation chromatography
T <sub>g</sub>	: glass transition
HOCO	: highest occupied crystal orbital
HOMO	: highest occupied molecular orbital
ITO	: Indium tin oxide
IR	: infrared
INT	: intermediate
kcal/mol	: kilocalorie per mole
PbBi gallate	: lead bismuth gallate
LED	: light emitting diode
LUCO	: lowest unoccupied crystal orbital
LUMO	: lowest unoccupied molecular orbital
T <sub>m</sub>	: melting temperature
mg	: milligram
mL	: millilitre
mmol	: millimole
<i>Mn</i>	: number average molecular weight
ORTEP	: Oak Ridge Thermal-Ellipsoid Plot Program
OT	: oligothiophene
OLED	: organic light emitting diode
PAT	: polyalkyl thiophene
Poly9BCMU	: poly(dibutyl 4,29-dioxo-5,28-dioxa-3,30-diaza-15,17-dotriacontadiynedioate)

PEDOT:PSS	: poly(3,4-ethylenedioxythiophene)-poly(styrenesulfonate)
PLED	: polymeric light emitting diode
PT's	: polythiophenes
PES	: potential energy surface
RSA	: reverse saturable absorption
SA	: saturable absorption
SCE	: saturated calomel electrode
SEM	: scanning electron microscopy
SCXRD	: single crystal X-ray diffraction
THF	: tetrahydrofuran
TMS	: tetramethylsilane
TGA	: thermogravimetric analysis
Ts	: transition state
UV-Vis	: Ultraviolet-Visible
$M_w$	: weight average molecular weight

## CONTENTS

	<i>Page No.</i>
<b>CHAPTER 1</b>	
<b>Introduction to relevant fundamental aspects</b>	<b>1-51</b>
1.1 <i>Abstract</i>	1
1.2 <i>Conducting Polymers</i>	1
1.2.1 <i>Factors influencing electrical conductivity of polymers</i>	4
1.2.2 <i>Doping</i>	4
1.2.3 <i>Solitons, polarons and Bipolarons as charge carriers</i>	7
1.3 <i>Light emitting polymers</i>	10
1.3.1 <i>LEP device architecture</i>	13
1.3.2 <i>Mechanism of light emission- A detailed study</i>	14
1.4 <i>Polythiophenes as light emitting Materials</i>	17
1.4.1 <i>Effect of structure on optical properties of PT's</i>	20
1.4.2 <i>Synthesis of thiophene based Polymers</i>	21
1.5 <i>Direct arylation</i>	28
1.5.1 <i>Mechanism of direct arylation</i>	29
1.6 <i>Bisarylidene cycloalkanones- An overview</i>	31
1.7 <i>Pyrazolines</i>	33
1.7.1 <i>A glimpse into structural characteristics of</i>	37

	<i>pyrazolines</i>	
1.8	<i>Non-linear optics</i>	39
1.8.1	<i>Second order materials</i>	40
1.8.2	<i>Third order materials</i>	41
1.8.3	<i>Z-scan</i>	43
1.9	<i>Introduction to our project</i>	44
1.10	<i>References</i>	45

## **CHAPTER 2**

### **Synthesis of a few thiophene based molecules, Regioselectivity and their mechanism of Formation 53-82**

2.1	<i>Abstract</i>	53
2.2	<i>Introduction</i>	53
2.3	<i>Results and Discussion</i>	55
2.3.1	<i>Cycloalkanone spacer</i>	55
2.3.2	<i>Heterocyclic ketone spacer</i>	57
2.3.3	<i>Open chain alkanones</i>	57
2.3.4	<i>Fused ring diones</i>	59
2.3.4.1	<i>Synthesis of tetrahydropentalene-2,5(1H, 3H)-dione</i>	59
2.3.4.2	<i>Reaction between tetrahydropentalene-2,5(1H, 3H)-dione and thiophene-2-carboxaldehyde</i>	60
2.3.4.3	<i>Synthesis of (1Z,3E,4Z,6E)-1,3,4,6-tetrakis(thiophen-2-ylmethylene) tetrahydropentalene-2,5(1H,3H)-dione</i>	61
2.3.4.4	<i>Claisen Schmidt condensation of tetrahydropentalene dione with anthraldehyde</i>	63
2.3.4.5	<i>Claisen-Schmidt condensation of tetrahydropenta</i>	64



	<i>lene dione with Pyrene-2-carboxaldehyde</i>	
2.3.4.6	<i>Computational studies</i>	68
2.4	<i>Conclusions</i>	70
2.5	<i>Experimental</i>	71
2.5.1	<i>Synthesis of (2E,4E)-2-((5-bromothiophen-2-yl)methylene)-4-((5-bromothiophen-3-yl)methylene)cyclobutanone</i>	72
2.5.2	<i>Synthesis of (2E,6E)-2,6-bis((5-bromothiophen-2-yl)methylene)-4-(tert-butyl)cyclohexanone</i>	73
2.5.3	<i>Synthesis of (2E,7E)-2,7-bis(thiophen-2-ylmethylene)cycloheptanone</i>	74
2.5.4	<i>Synthesis of (2E, 7E)-2, 7bis((5-bromothiophen-2-yl)methylene) cycloheptanone</i>	74
2.5.5	<i>Synthesis of (3Z,5Z)-3,5-bis((5-bromothiophen-2-yl)methylene) dihydro-2H-thiopyran-4(3H)-one</i>	75
2.5.6	<i>Synthesis of (1E,4E)-1,5-bis(5-bromothiophen-2-yl)-2,4-dimethyl penta-1,4-dien-3-one</i>	76
2.5.7	<i>Synthesis of (E)-4-(5-bromothiophen-2-yl)-1,3-diphenylbut-3-en-2-one</i>	77
2.5.8	<i>Synthesis of (1Z,3E,4Z,6E)-1,3,4,6-tetrakis(thiophen-2-ylmethylene) tetrahydropentalene 2,5(1H,3H)-dione</i>	77
2.5.9	<i>Claisen-Schmidt condensation of tetrahydropentalene dione with Anthraldehyde</i>	78
2.5.10	<i>Claisen-Schmidt condensation of tetrahydropentalene dione with Pyrene-2-carboxaldehyde</i>	79
2.6	<i>References</i>	80

## CHAPTER 3

### **Synthesis, third order non-linear optical properties and Schottky junction characterisation of few yellow light emitting bis(thiophen-2-ylmethylene)cycloalkanone oligomers**

3.1	<i>Abstract</i>	83
3.2	<i>Introduction</i>	83
3.3	<i>Results and Discussion</i>	85
3.3.1	<i><sup>1</sup>H NMR spectra</i>	88
3.3.2	<i>FTIR spectra</i>	89
3.3.3	<i>Powder X-ray diffraction study</i>	90
3.3.4	<i>UV-visible and photoluminescence spectra</i>	91
3.3.5	<i>Scanning electron microscopy</i>	93
3.3.6	<i>Thermal studies</i>	93
3.3.6.1	<i>TGA Analysis</i>	93
3.3.6.2	<i>Differential Scanning Calorimetry</i>	95
3.3.7	<i>Cyclic Voltammetry</i>	95
3.3.8	<i>Computational studies</i>	99
3.3.9	<i>Non-linear optics</i>	101
3.3.10	<i>Measurement of I-V Characteristics</i>	104
3.4	<i>Conclusions</i>	107
3.5	<i>Experimental</i>	108
3.5.1	<i>Synthesis of oligomer (2E,2'E,6E,6'E)-6,6'- ([2,2'-bithiophene]-5,5'-diylbis(methanylylidene )bis(2-((5-methylthiophenyl)methylene)cyclo</i>	109

	<i>hexanone) from (2E,6E)-2,6-bis(thiophen-2-ylmethylene) cyclohex anone and (2E,6E)-2,6-bis((5-bromothiophen-2-yl)methylene)cyclohexanone using direct arylation method</i>	
3.5.2	<i>Synthesis of oligomer (AC2) (2E,6E)-2-((3-methyl-3a1,6-dihydro pyren-1-yl) methyl ene)-6-((3-(5-((E)-(E)-3-((5-methylthiophen-2-yl)methylene)-2-oxocyclohexylidene)methyl)thiophen-2-yl)pyren-1-yl)methylene)cyclohex anone from (2E,6E)-2,6-bis(pyren-2-ylmethylene)cyclohexanone and (2E,6E)-2,6-bis((5-bromothiophen-2-yl)methylene)cyclohex anone by direct arylation</i>	110
3.6	<i>References</i>	111

#### **CHAPTER 4**

	<b>Chemical modification of a few bis(thiophen-2-ylmethylene)cycloalkanones: Synthesis of a few thiophene appended hexahydro-2H-indazole derivatives</b>	<b>115-144</b>
4.1	<i>Abstract</i>	115
4.2	<i>Introduction</i>	115
4.3	<i>Results and Discussion</i>	117
4.3.1	<i>Mechanism of pyrazoline formation</i>	122
4.3.2	<i>The energy profile diagrams</i>	123
4.3.2.1	<i>(E)-2-phenyl-3-(thiophen-2-yl)-7-(thiophen-2-ylmethylene)-3,3a,4, 5,6,7-hexahydro-2H-indazole</i>	123

4.3.2.2	<i>(E)</i> -5-( <i>tert</i> -butyl)-2-phenyl-3-(thiophen-2-yl)-7-(thiophen-2-ylmethylene)-3,3a,4,5,6,7-hexahydro-2H-indazole	125
4.3.2.3	<i>(Z)</i> -2-phenyl-3-(thiophen-2-yl)-7-(thiophen-2-ylmethylene)-2,3,3a,4,6,7hexahydrothiopyrano [4,3- <i>c</i> ]Pyrazole	127
4.3.2.4	Reaction of (2 <i>E</i> ,7 <i>E</i> )-2,7-bis(thiophen-2-ylmethylene)cycloheptanone with phenyl hydrazine	129
4.3.2.5	Reaction of (3 <i>E</i> ,5 <i>E</i> )-3,5-bis(thiophen-2-ylmethylene)dihydro-2H-pyran-4(3 <i>H</i> )-one	130
4.4	Conclusions	134
4.5	Experimental	135
4.5.1	Synthesis of <i>(E)</i> -2-phenyl-3-(thiophen-2-yl)-7-(thiophen-2-ylmethylene)-3,3a,4,5,6,7-hexahydro-2H-indazole from (2 <i>E</i> ,6 <i>E</i> )-2, 6-bis(thiophen-2-ylmethylene)cyclohexanone	135
4.5.2	Synthesis of <i>(E)</i> -5-( <i>tert</i> -butyl)-2-phenyl-3-(thiophen-2-yl)-7-(thiophen-2-ylmethylene)-3,3a,4,5,6,7-hexahydro-2H-indazole from (2 <i>E</i> ,6 <i>E</i> )-2, 6-bis (thiophen-2-yl-methylene) <i>t</i> -butyl cyclohexanone	136
4.5.3	Synthesis of <i>(Z)</i> -2-phenyl-3-(thiophen-2-yl)-7-(thiophen-2-ylmethylene)-2,3,3a,4,6,7-hexahydro thiopyrano[4,3- <i>c</i> ]pyrazolefrom (3 <i>Z</i> ,5 <i>Z</i> )-3,5-bis (thiophen-2-ylmethylene) dihydro-2H-thiopyran-4(3 <i>H</i> )-one	137
4.5.4	Synthesis of <i>(E)</i> -3-(5-bromothiophen-2-yl)-7-((5-bromothiophen-2-yl)methylene)-2-phenyl-3,3a,4,5,6,7-hexahydro-2H-indazole from (2 <i>E</i> ,6 <i>E</i> )-2,6-bis((5-bromothiophen-2-yl)methylene)cyclo	138

	<i>hexanone</i>	
4.5.5	<i>Synthesis of (E)-3-(5-bromothiophen-2-yl)-7-((5-bromothiophen-2-yl)methylene)-5-(tert-butyl)-2-phenyl-3,3a,4,5,6,7-hexahydro-2H-indazole from (2E,6E)-2,6-bis((5-bromothiophen-2-yl)methylene)t-butyl cyclohexanone</i>	139
4.5.6	<i>Synthesis of (Z)-3-(5-bromothiophen-2-yl)-7-((5-bromothiophen-2-yl)methylene)-2-phenyl-2,3,3a,4,6,7-hexahydrothiopyrano[4,3-c]pyrazole from (3Z,5Z)-3,5-bis((5-bromothiophen-2-yl)methylene)dihydro-2H-thiopyran-4(3H)-one</i>	140
4.6	<i>References</i>	141

## **CHAPTER 5**

### **Synthesis and study of third order non-linear optical properties and Schottky junction characteristics of a few thiophene based polymers synthesized through Stille coupling and direct arylation reactions**

5.1	<i>Abstract</i>	145
5.2	<i>Introduction</i>	145
5.3	<i>Results and Discussion</i>	147
5.3.1	<i><sup>1</sup>H NMR Spectra</i>	149
5.3.2	<i>FTIR spectra</i>	149
5.3.3	<i>Theoretical interpretation of influence of chain length on band gap of SC1 and AC3</i>	150
5.3.4	<i>Powder X-ray diffraction</i>	153

5.3.5	<i>UV-Visible and photoluminescence spectra</i>	153
5.3.6	<i>Scanning electron microscopy</i>	156
5.3.7	<i>Thermal Gravimetric Analysis</i>	157
5.3.8	<i>Differential Scanning Calorimetry</i>	158
5.3.9	<i>Atomic Force Microscopy</i>	158
5.3.10	<i>Cyclic Voltammetry</i>	159
5.3.11	<i>Theoretical Methodology</i>	162
5.3.12	<i>Non-linear optics</i>	164
5.3.13	<i>Measurement of I-V characteristics</i>	166
5.4	<i>Conclusions</i>	167
5.5	<i>Experimental</i>	168
5.5.1	<i>Synthesis of Oligomer (E)-3-(5-methylthiophen-2-yl)-7-((5'-(E)-7-((5-methylthiophen-2-yl)methylene)-2-phenyl-3,3a,4,5,6,7-hexahydro-2H-indazol-3-yl)-[2,2'-bithiophen]-5-yl)methylene)-2-phenyl-3,3a,4,5,6,7-hexahydro-2H-indazole (AC3) by direct arylation method</i>	169
5.5.2	<i>Synthesis of polymer (SC1) of (E)-3-(5-bromothiophen-2-yl)-7-((5-bromothiophen-2-yl)methylene)-2-phenyl-3,3a,4,5,6,7-hexahydro-2H-indazole using Stille Coupling</i>	170
5.6	<i>References</i>	171
	<b><i>Summary and Conclusions</i></b>	173-175
	<b><i>List of Publications</i></b>	

## CHAPTER 1

### *Introduction to Relevant Fundamental Aspects*

---

*1.1 Abstract: Introductory ideas related to the present research work are highlighted in this chapter. The chapter begins with a brief historical background of the evolution of polymers, their advancement from insulating materials to the present status with wide range of technological applications. Among various conducting polymers, the advantages of polythiophenes are highlighted and a brief discussion on light emitting polymers with thiophene as backbone is well explained in this chapter. An introduction to bithiophene cycloalkanone systems and their derivatives are explained and the possibility of exploiting pyrazolines and other derivatives of bithiophene cycloalkanones is also introduced. Applicability of organic materials in third order nonlinear optical studies and experimental set-up of Z-scan technique are also presented.*

### **1.2 CONDUCTING POLYMERS**

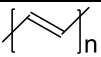
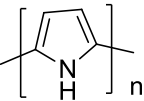
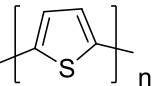
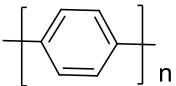
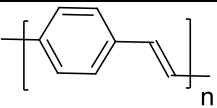
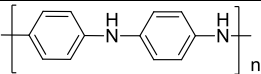
For years, polymers were used as insulating materials since they were considered to be nonconductors of electricity. However, in 1971, Shirakawa created history when he established that acetylene can be polymerized to give a free standing film with variety of interesting mechanical properties. The real reverberation in the field of conducting polymers<sup>1,2</sup> was initiated in 1977 when Alan J Heeger, Alan MacDiarmid and Hideki Shirakawa manifested for the first time that polyacetylene,<sup>3,4</sup> an intrinsically insulating organic conjugated polymer,

shows a substantial increase in electrical conductivity when it was doped with suitable oxidizing or reducing agent. These electron donating or electron accepting reactions which can induce high increase in conductivity is termed as *n*-doping and *p*-doping respectively. They were awarded Nobel Prize in Chemistry in 2000 for the groundbreaking discovery of electrically conducting polymers. The polyacetylene discovery directed the research activity to a wide variety of conducting polymeric systems, viz, polypyrrole (PPY), poly(phenylacetylene) (PPA), poly(*p*-phenylene sulfide) (PPS), poly(*p*-phenylene) (PPP), polythiophene (PTP), polyaniline (PANI), polyisothionaphthalene (PIN) and their derivatives.

For a polymer to be intrinsically conducting a conjugated structure with alternate single and double bonds or conjugated segments coupled with atoms like N or S which can provide *p*-orbitals for a continuous orbital overlap<sup>5,6</sup> is necessary. Thus the second generation polymers are either insulators or poor conductors but on doping they become conducting. Likewise the free movement of electrons is the cause for conductivity in metals, so is the case with polymers where a charge carrier along with an orbital system for the movement of charge carriers is necessary for conduction. Repeating units and conductivities of a few common conjugated polymers are collected in Table 1.1. Due to its simple conjugated structure and outstanding electronic properties, polyacetylene has been widely studied as a prototype for conducting polymers. However, due to the unstable nature of these polymers in air, low solubility and difficulty in synthesis, research advanced in search of new



types of polymers that are essentially conducting. Conducting polymers possess not only the electronic and optical properties of the metals and inorganic semiconductors, but also the flexible mechanics and processability of polymers. The conducting polymers, in addition, also possess a special electrochemical redox activity. Thus it is obvious that conducting polymers including doped conducting polymers and intrinsic semiconducting conjugated polymers will play a key role in the future development of organic optoelectronic and electrochemical devices.

Polymer	Structure	Band gap, eV	Conductivity, S/m
Polyacetylene		1.5	$10^3 - 1.7 \times 10^5$
Polypyrrole		3.1	$10^2 - 7.5 \times 10^3$
Polythiophene		2.0	$10 - 10^3$
Poly(paraphenylene)		3.0	$10 - 10^3$
Poly(paraphenylene vinylene)		2.5	$3 - 5 \times 10^3$
Polyaniline		3.2	30 – 200

**Table 1.1:** Representative conjugated conducting polymers<sup>7-10</sup>.

### **1.2.1 Factors influencing electrical conductivity of polymers.**

Electrical conductivity of polymers depends on many factors.

- 1) Method of synthesis
- 2) Method of processing
- 3) Degree of crystallinity of polymer
- 4) Temperature.

Once the polymer is synthesized, its purification and processing is very important. Even minute concentration of ionic impurities has a drastic influence on its conductivity. Conductivity in general increases with the increase in degree of crystallinity. The redox potential is the main factor which contributes to the chemical stability of the polymer under ambient conditions. For a polymer to be stable in air, its reduction potential should be higher than the reduction potential of oxygen (-0.146V).

### **1.2.2 Doping**

Conductivity of polymers is influenced by doping process and depends on the nature of the dopant, amount of doping etc. Most organic polymers do not have intrinsic charge carriers. Partial oxidation (*p*-doping) of the polymer chain with electron acceptors (e.g., I<sub>2</sub>) or partial reduction (*n*-doping) with electron donors (e.g. Na, K) introduces some charge defects (e.g. polaron,<sup>11</sup> bipolaron, and soliton) which could then be available as charge carriers. The nature of charge transport in polymers is still a matter of controversy; nevertheless, band theory can provide some

information regarding the changes induced by doping in the electronic structure.

According to band theory,<sup>12</sup> the electrons move within discrete energy states called *bands*. The delocalized  $\pi$  electron structure of the conjugated polymers include the band structure of  $\pi$  valence band and  $\pi^*$  conduction band. The highest occupied band is called the valence band where the electrons associated with the band are involved in chemical bonding, are rather localized, and are not free to move through the solid. The lowest unoccupied band is called the conduction band. For a normal basic state of intrinsically conjugated polymers, all valence bands are filled with electrons while conduction band are all empty. The difference between the top of the valence band (highest occupied molecular orbital, HOMO) and bottom of the conduction band (lowest unoccupied molecular orbital, LUMO) *ie*, a forbidden energy region between the valence band and conduction band is called band gap ( $E_g$ ) of the conjugated polymer. Larger the band gap, more the material behaves like an insulator. The  $E_g$  values of most organic polymers are in the range of 0.5-3.0 eV. *ie*, they are organic semiconductors.

$E_g$  values can be measured in numerous ways. From the absorption edge wavelength in the absorption spectrum ( $\lambda_{edge}$ ),  $E_g$  can be calculated using the following equation.

$$E_g = \frac{1240}{\lambda_{edge}} \text{ (eV)}$$

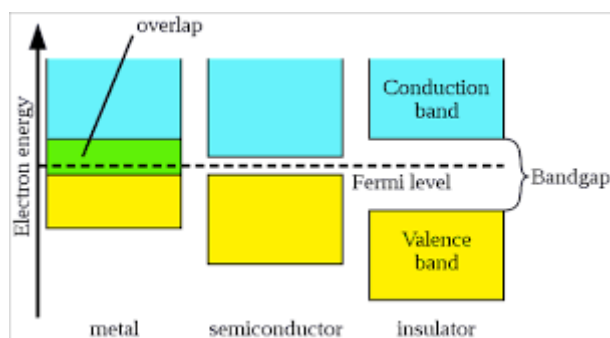
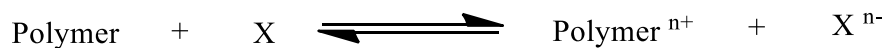


**Figure 1.1:** A schematic representation of energy gaps in a) metal b) semiconductor and c) insulator

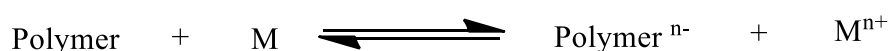
The onset oxidation and onset reduction potential measured by cyclic voltammetry gives information regarding the HOMO and LUMO energy levels of the conjugated polymer. Their difference corresponds to the  $E_g$  values. Electrons must have certain energy to occupy a given band and extra energy should be supplied to move the electron from the valence band to the conduction band. It is important that the bands should be partially filled in order to be electrically conducting – a property shared with metals that are conductors (Figure 1.1 a). The energy bands of insulators are either completely filled or completely empty. (Figure 1.1, b and c).<sup>6, 7, 8</sup>

Conductivity of most common doped conducting polymers is of the order of  $10^{-3}$ - $10^3$  S/cm. The conducting polymers usually have an amorphous structure and in some cases with ordered domains. In conducting polymers, the charge carriers can move easily through the polymer chain, but they have to hop for the transportation within the conjugated polymer chains. Thus charge transportation here is limited by hopping between the conjugated polymer chains.

The doping process can be represented by the following general scheme (Scheme 1.1).



in the case of p-doping process



in case of n-doping process

X = I<sub>2</sub>, ASF<sub>5</sub>,... and M = Na, Li...

**Scheme 1.1: p-doping and n-doping process**

### **1.2.3 Solitons, Polarons and Bipolarons as charge carriers**

It was initially thought that the increase in conductivity of organic conjugated polymers upon doping resulted from the formation of unfilled electronic bands. However with the discovery that the spinless charge carriers was solely responsible for the conductivity in polyacetylene and polyparaphenylene overruled this theory. It has been established that the high conductivities obtained for these polymers on doping are associated with the formation of self-localized excitations such as solitons, polarons and bipolarons.

When an electron is removed from the top of the valence band or added to the bottom of the conduction band, the conduction ( or valence) band ends up being partially filled and a radical anion commonly called polaron<sup>11</sup> is created which carries both spin and charge. Such formation of polaron causes injection of states into the band gap. Formation of a

bipolaron occurs through dimerization of two polarons which in turn is caused due to the addition or removal of a second electron on a chain already having a negative or positive polaron. This results in lowering of total energy. In conjugated polymers having a degenerate ground state, the bipolarons can further lower their energy by dissociating into two spinless solitons at one half of the gap energy. The amount of doping has a significant effect on the population of polarons, bipolarons, and (or) solitons. In case of conjugated polymers having nondegenerate ground state say for example polythiophene, polypyrrole and polyaniline, such formation of solitons do not occur. In these compounds initially polarons are formed on doping which then combine to form spinless bipolarons which act as charge carriers. Thus we can say that these quasi particles formed as a result of interaction between the charges on the chain caused as a result of doping and the molecular structure are the direct consequence of the strong electron-phonon interaction in these quasi-one-dimensional polymers. The electron transportations resulting in the conductivity of polymers can be of three kinds viz.

- a) Intra-Chain
- b) Inter-Chain
- c) Inter domain

Schematic representation for the formation of polaron, bipolaron and soliton in polyacetylene chain after doping is shown in Figure 1.2. Number of these charge carriers formed increases with the level of doping. At very high levels of doping, it is possible that these charge carriers could overlap which results in formation of new intermediate

energy bands or even the overlap of valence band and conduction band. Doping can be of various kinds like chemical doping, electrochemical doping, photodoping, charge injection doping and non-redox doping or secondary doping. Also as already discussed, orientation, purity etc. of a polymer also influences its conductivity to a large extent.

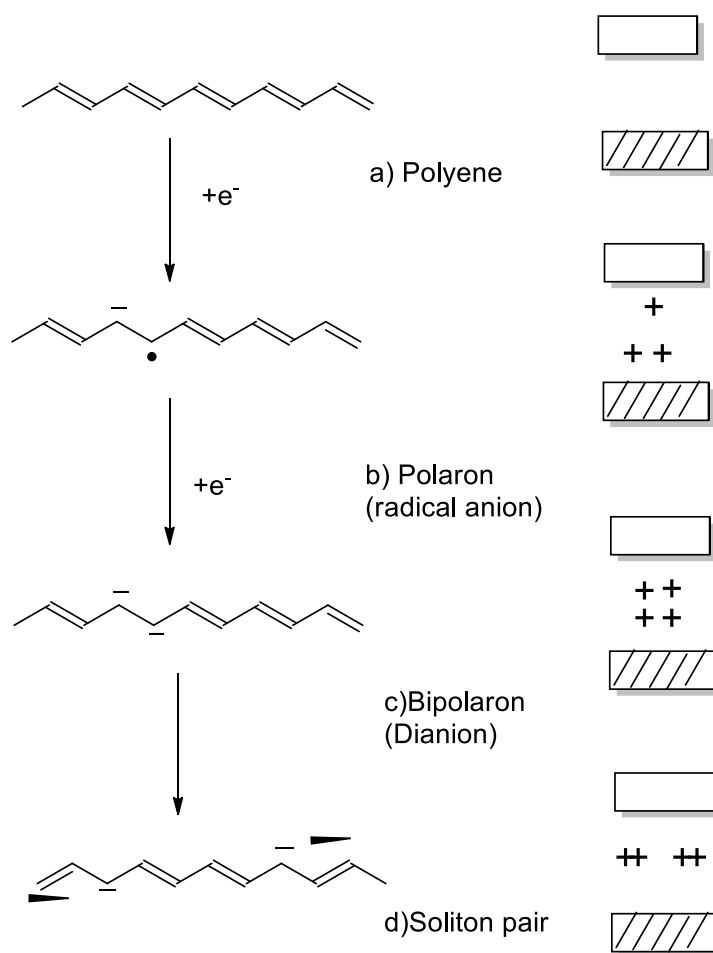


Figure 1.2: A schematic representation for the formation of polaron , bipolaron and soliton pair on a *trans*-polyacetylene chain by doping<sup>6,7</sup>

### **1.3 LIGHT EMITTING POLYMERS**

Light emitting polymers (LEPs)<sup>13</sup> are unique class of organic polymers that glows or emits photons when excited by electricity. They exhibit both electroluminescent and photoluminescent characteristics. The major phenomenon for a light emitting polymer to give off light is “electroluminescence”. Electroluminescence can be defined as a phenomenon by which a material emits light when an electric field or electric current is passed through it. Polymers display or produce light due to the fast decay of excited states and the color emitted depends on the energy difference between those excited states and molecular ground level. Typically a light emitting device<sup>13</sup> encompasses a one or two layer thin film structure not more than 0.1  $\mu\text{m}$  thick, sandwiched between two electrodes. These two electrodes must be dissimilar to achieve optimal device efficiency. In addition, the respective electrode materials should possess Fermi levels or electronic work functions that closely match with the valence and conduction energy levels of the polymer. It is mandatory that one of the electrode should be transparent to the wavelength of light generated. Such devices are called as Polymeric Light Emitting Diodes or PLEDs or OLEDs. LEPs<sup>14, 15</sup> have progressed considerably for the past 10 years and the market potential of LEPs and PLEDs are very high now. Organic LEDs are now comparable with inorganic ones in brightness and efficiency. Also they offer a low cost approach with less complexity in manufacturing process. Some other advantages include:

- a) Improved performance.



- b) They provide all advantages of small-molecule with additional advantages of low power consumption and drive voltages.
- c) Good light generating efficacy.
- d) OLEDs are often smaller, low molecular weight films.
- e) They provide a unique opportunity to explore nature at the interphase between chemistry and physics.
- f) Wide operating temperature range and authentic image quality

The phenomenon of electroluminescence happens in polymers when electrons are sent through the material to fill the electron holes. When a material lacks an electron, a hole is created that carries positive charge. It is possible to create and control the number of electron holes by doping semiconductor materials like silicon and germanium. When an intrinsic semiconductor is doped with trivalent impurity a *p*-junction is created and with pentavalent impurity *n*-junction is created. Doping changes the properties of the material and two separate types of semiconductors are formed within the same crystal. The boundary between the two is called *p-n* junction. LEDs are produced using *p-n* junction. Figure 1.3 shows a typical LED. Only current can pass through this junction and as electrons pass from one crystal to the other they fill the electron holes and emit photon *i.e.*, light. This is the principle behind the working of a semiconductor laser. In 1960's researchers at Dow Chemical Company used doped anthracene to prepare AC-driven electroluminescent cells. This was the first patent on EL devices based on polynuclear hydrocarbons.

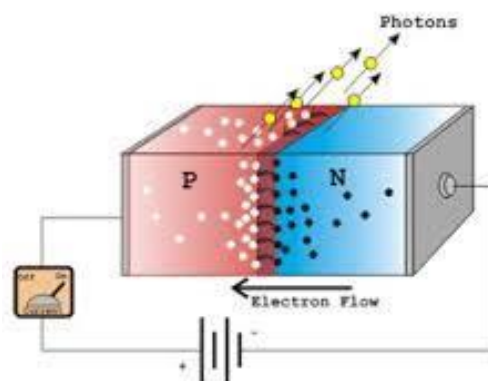


**Figure 1.3: LED *p-n* junction**

With the dawn of electroluminescent polymers, polymeric materials with emission in the range of visible and near infrared have been fabricated. Even devices emitting white light have been generated by appropriate mixing of these electroluminescent materials.

Figure 1.4 shows some examples<sup>15</sup> of electroluminescent polymers.

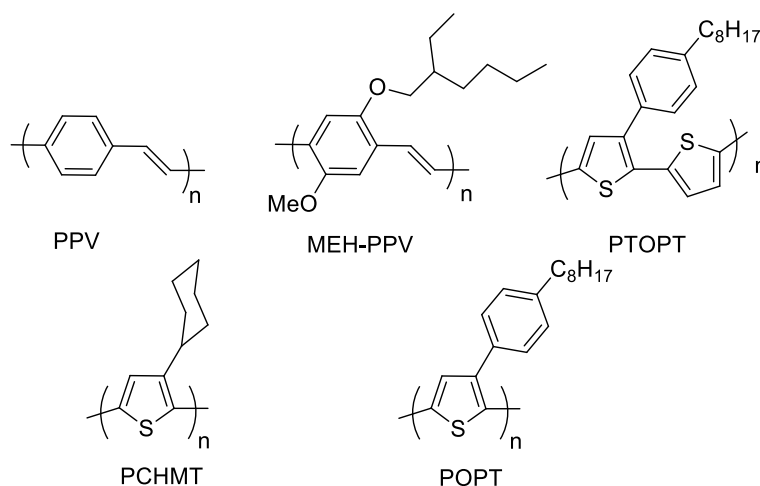


**Figure 1.4: Examples of some electroluminescent polymers**

### 1.3.1 LEP Device Architecture

One of the greatest advantages of an LEP device is their simplicity in architecture and fabrication. A device<sup>13, 15</sup> usually consists of an anode typically Indium Tin Oxide (ITO) on a glass substrate, two thin polymer layers, viz, a polymer hole conducting layer and conjugated polymer emitting layer and a cathode system.<sup>23</sup> The device construction is shown below in Figure 1.5.

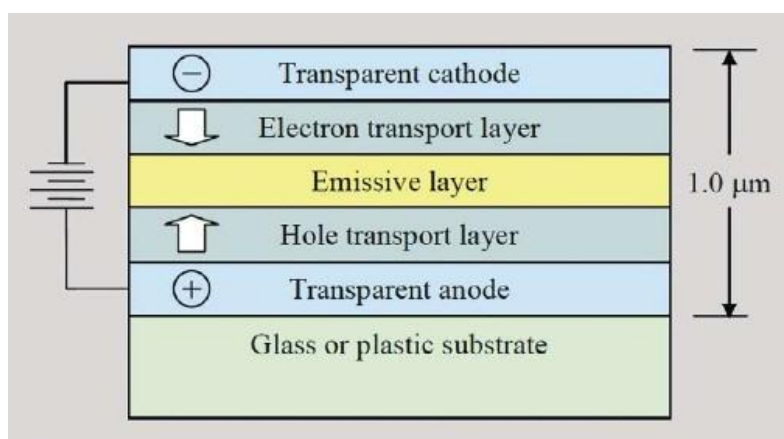


**Figure 1.5: Typical LED device**

The cathode system usually consists of a low work function metal capped usually with aluminum to provide electron injection into to the  $\pi^*$  band of the emitting layer film. It is usually coated by physical vapor deposition method. The hole conduction layer commonly used is poly(3,4-ethylenedioxythiophene)-poly(styrenesulfonate) (PEDOT:PSS). The polymer is usually coated from organic solutions with thickness not more than 750 Å. The whole device should be encapsulated to improve its durability.

Fabrication of PLED<sup>16-18</sup> devices comes in two varieties: a single layer and multiple layer structures. In single layer devices, the efficient injection and transport of both the electrons and holes are hinged upon the emitting material. In addition it should ease the radiative decay of excited molecular states to the ground state. However this method encounters many difficulties owing to the presence of a single matrix layer alone to carry out injection and transport of two charge carriers over a reasonable voltage range. Correspondingly, the drive voltage increases and luminance efficiency deviates from ideality. To overcome these problems, a multiple layer PLED<sup>17-19,24,25</sup> architecture was designed. Here the main motivation is to separate the active layer from ITO and accommodate charge transport specialization for both carriers using different molecular structures.<sup>20-23</sup>

### 1.3.2 Mechanism of light emission—A detailed study

Over the last few decades, organic polymers which emit light on imposition of an electric field have received much attention as materials for optoelectronic devices. Photoluminescence of aromatic organic molecules has enabled their use as electroluminescent materials. For a material to become electroluminescent, the injection of electrons from one electrode and holes from the other, capture of one by the other and the radioactive decay of excited state produced by this recombination are required. In addition to glass substrate, it is possible to fabricate flexible devices by casting polymer films on plastic substrate. Heeger *et al.* prepared a “plastic LED” in which polyaniline film is the anode deposited on Mylar (PET) film. Color tuning can be achieved by varying

the polymer structure since by doing so the energy gap of the  $\pi$ - $\pi^*$  transition which is responsible for the color emitted is changed.

Light emitting devices can operate on DC or AC mode. Electrons are injected from the cathode to the  $\pi^*$  state (conduction band called LUMO-Lowest Unoccupied molecular Orbital) of the polymer and holes are injected from anode to the  $\pi$  state (Valence band called HOMO-Highest Occupied Molecular Orbital). The combination of electrons and holes result in the formation of neutral species called excitons which in accordance with the spin statistics can be singlet or triplet. For fluorescent polymers a maximum quantum efficiency of 25% can only be achieved since there is only one singlet state available for each three triplet states and only singlet states undergo radiative decay. Use of phosphorescent materials can increase the internal quantum efficiency considerably up to 100%.

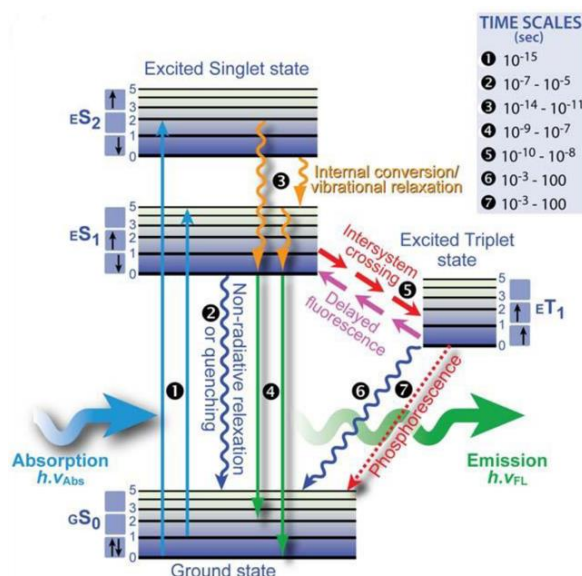


Figure 1.6: General Jablonski diagram

In order to get a real picture on mechanism of light emission it is mandatory to describe the process behind photoluminescence. A typical Jablonski diagram<sup>26, 27</sup> is shown in the Figure 1.6.

Absorption of a photon by a polymer promotes an electron from ground state to upper electronically excited state. The electron at the S<sub>1</sub> level can undergo intramolecular deactivation in several ways which can be radiative or non-radiative.

- a) Fluorescence, the only radiative path, occurs when the electron in singlet excited state S<sub>1</sub> returns to the ground state by emitting photon.
- b) Internal conversion (IC) called radiation less de-excitation occurs when electron occupying higher energy levels relaxes to a lower level.
- c) Intersystem crossing (ISC) where the electron in the first singlet excited state non- radiatively passes to the excited triplet state i.e., S<sub>1</sub>-T<sub>1</sub> and then T<sub>1</sub>-S<sub>0</sub>. A change in spin occurs during this transition i.e. pair of electrons with antiparallel spin is converted into pair of electrons with parallel spin. This process is spin forbidden and takes more time to occur. Emission of photons from triplet states is termed as phosphorescence.

The ratio of radiative to non-radiative process called the internal quantum yield of luminescence depends on the competition between the radiative and non-radiative decays of electron-hole pairs in the polymer layer. The energy of the released photon in radiative process is based on the

difference between the HOMO and LUMO levels called the band gap<sup>28,29</sup> of the polymer.

$$\text{Quantum Efficiency (PL)} = \frac{\text{Number of photons emitted}}{\text{Number of photons absorbed}} \times 100\%$$

$$\text{Quantum Efficiency (EL)} = \frac{\text{Number of photons ejected}}{\text{Number of charge injected}} \times 100\%$$

The ratio between the probability of a singlet exciton radiative decay and PL quantum yield together with the exciton concentration gives the overall quantum efficiency. There is a close relationship between photoluminescence and electroluminescence even though electroluminescence is much more complex, and hence higher the photoluminescence quantum efficiency higher will be the electroluminescence quantum efficiency.

## **1.4 POLYTHIOPHENES AS LIGHT EMITTING**

### **MATERIALS**

Recently, research has extensively intensified in the field of conjugated polymers. Interest in PLEDs is one of the inevitable reasons for this. Polyacetylene was the first conjugated polymer to be established. However, studies have been extended now to a large number of other conjugated light emitting polymers namely, polythiophenes<sup>30-32</sup> (PTs), polycarbazoles, PPV (polyphenylene vinylenes), polyphenylene ethynyls, polyfluorenes<sup>33</sup> etc. The advent in the field of polythiophenes<sup>34</sup> as conjugated polymer began in early 1980s when it was first synthesized from 2,5-dibromothiophene via metal-catalyzed

polycondensation polymerization or via oxidative polymerization of thiophene. Investigations on PTs are of great importance nowadays since they produce yellow-orange color which the other conjugated polymers cannot achieve easily. They serve as materials for electronic and optoelectronic devices since they can be synthesized readily using chemical and electrochemical synthetic methods, functionalization is easier and their electronic properties can be tuned widely. It is possible to reversibly oxidize<sup>35,36</sup> PTs to highly conducting *p* doped form owing to their electron rich nature of the thiophene rings. Unlike the undoped PTs, doped ones are not luminescent. However, partially doped PTs are extensively used in light emitting electrochemical cells. Doping transforms these materials to conducting band covering the entire visible region to deep IR region.

Low molecular weight oligomers having basic thiophene backbone finds interesting applications in field effect transistors.<sup>37-39</sup> A practical reason for this can be the possibility of strong interchain interactions in small molecules which is less likely in polymers. Sulfur can cause heavy atom effects that contribute to non-radiative decay by increased interchain interactions and intersystem crossing. This decreases the photoluminescence efficiency<sup>37,38</sup> in solid state. Usually in accordance with the spin selection rule, transition between two states of different multiplicity is forbidden. But in organic molecules spin orbit coupling can lead to such spin forbidden processes. Since spin orbit coupling arises by the interaction of spin magnetic moment with nuclear magnetic



field and the latter is directly proportional to nuclear charge and atomic number, spin orbit coupling increases with increase in atomic number. Thus organic molecules having atoms of high atomic number are likely to have increased effects of spin forbidden radiative and non-radiative transitions. So is the case with thiophene based polymers. This effect is termed as Heavy-Atom effect<sup>40, 41</sup> which plays an important role in the photophysics<sup>42,43</sup> of PTs. In solution state, the photoluminescence efficiency is found to be considerably higher.

Another interesting feature of polyalkylthiophenes is thermochromism<sup>44-46</sup> that results in the loss of planarity of the polymer backbone to a random coil structure when temperature is increased. This is due to the thermal movement of the polymer side chains which leads to decrease in orbital overlap and conjugation meanwhile increasing the band gap and hypsochromic shift. On cooling the process is reversed. However this property limits its application in LED devices.

It is a noteworthy feature that among the thiophene based  $\pi$ -conjugated systems, oligothiophenes (OT) and polythiophenes (PT) have attracted researchers due to their interesting features and applications. Thiophenes are considered to be the ideal building blocks in transition metal catalyzed cross coupling reactions. Their unique electronic, optical, redox and self-assembling properties makes them promising candidates for organic electronics. OTs are often termed as third generation of organic conjugated materials.

### 1.4.1 Effect of structure on optical properties of PTs

Conjugated polythiophenes have extended  $\pi$  system which imparts interesting optical properties to these materials. Conjugation length depends on the number of coplanar rings. Longer the conjugation length, longer will be the absorption wavelength. As the conjugation length increases, bathochromic shift occurs and the maximum effective conjugation length is called the saturation point of the red shift. Among the PTs synthesized, poly(3-alkylthiophenes) are interesting materials owing to their excellent solubility, electrical conductivity and processability.

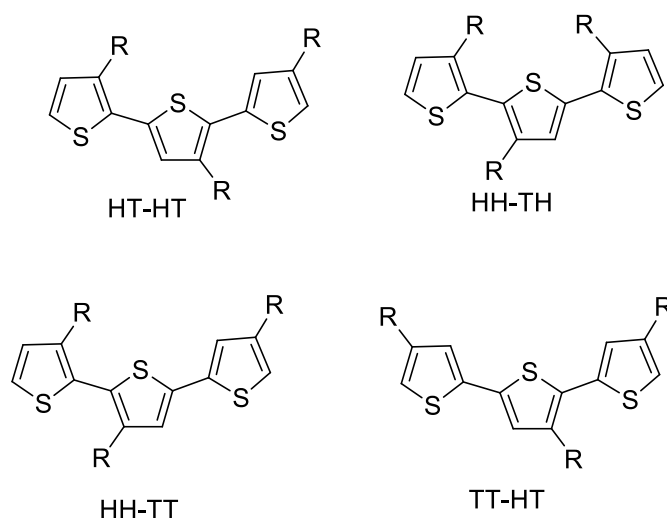


Figure 1.7: Four possible triune formed by coupling of 3-substituted thiophenes

Oligomers of asymmetric 3-substituted thiophenes possess four types of linkages: Head-to-Tail (HT), Head-to-Head (HH),<sup>47-49</sup> Tail-to-Tail (TT) and Tail-to-Head (TH). The latter three cases experiences adverse steric interaction between side chain groups due to which planarity is

compromised. As mentioned above planarity is a very important factor to determine the performance of the resulting material, hence loss of planarity decreases the overall performance of the system. Thus among the four, HT coupling is expected to possess superior properties. Figure 1.7<sup>50,51</sup> shows the four possibilities of coupling in 3-alkylthiophenes.

Mccullough<sup>52</sup> and Reike<sup>53</sup> were the first to report regioselective polymerization at the fifth position of the thiophene ring. The head-to-tail regioregularity was proved by Amou *et al.* where they prepared poly(3-alkylthiophene) via oxidative polymerization of 3-alkylthiophene in presence of FeCl<sub>3</sub>. A few selected examples of polythiophenes are shown in Figure 1.8.<sup>54</sup>

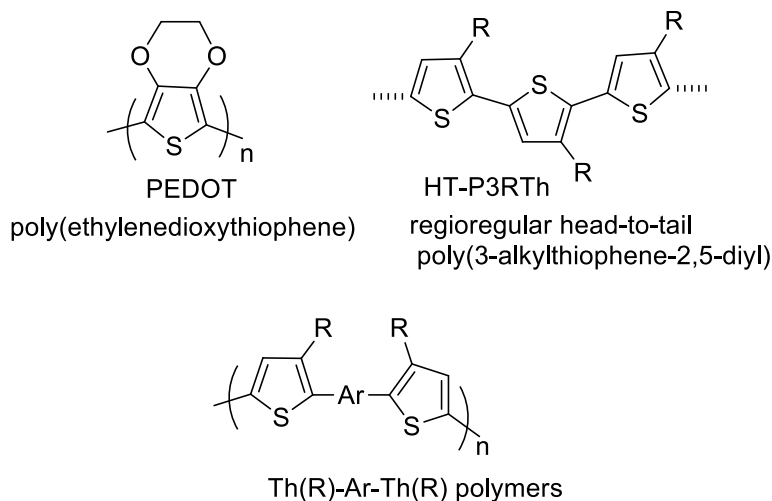
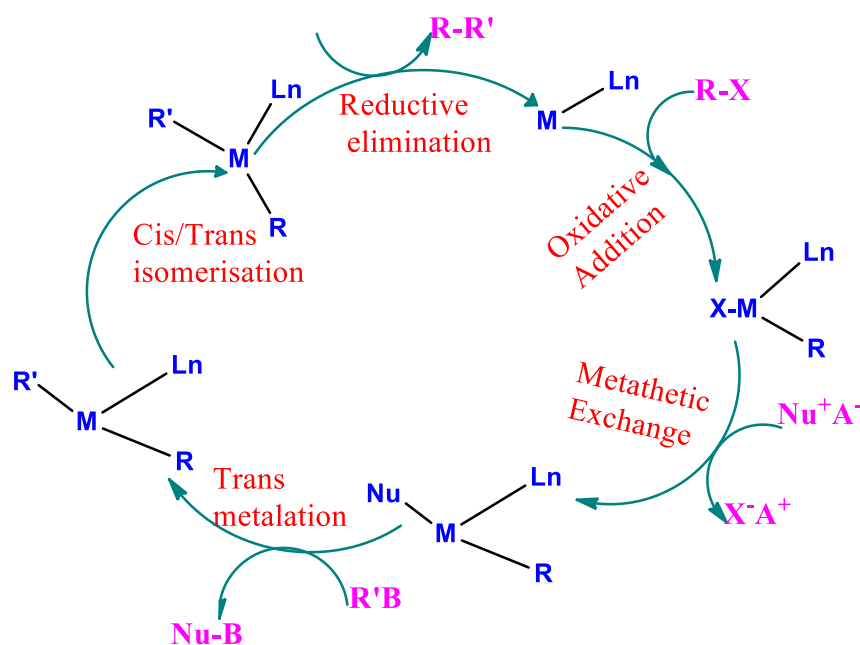


Figure 1.8: Examples of polythiophenes

## 1.4.2 Synthesis of thiophene based polymers

Several methods are available for the preparation of conjugated polymers. Herein, our primary focus is to explain the methods for the

synthesis of thiophene containing conjugated polymers alone and only those are explained below. Oligothiophenes<sup>55,56</sup> and polythiophenes<sup>57-58</sup> can be synthesized either by oxidative homocoupling or by transition metal catalyzed coupling polymerization reactions<sup>55,56</sup> namely McCollough,<sup>59</sup> Stille,<sup>60</sup> Suzuki,<sup>60</sup> Heck,<sup>61-63</sup> Kumada,<sup>64,65</sup> Negishi,<sup>66-68</sup> and Sonogashira<sup>69-71</sup> type coupling reactions. Transition metal catalyzed reactions are widely employed for the synthesis of thiophene based molecules. The general catalytic cycle for transition metal catalyzed reaction is represented below (Figure 1.9).



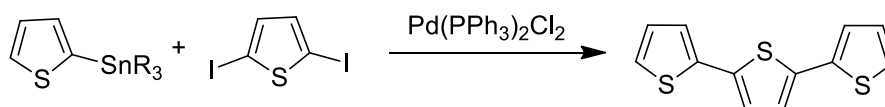
**Figure 1.9: General catalytic cycle**

Here the first step is the oxidative addition of on organohalide to transition metal forming a cis product which being unstable isomerises to a *trans* one. In the second transmetalation step involving tin, copper, zinc etc. an intermediate is formed which after reductive elimination gives the

desired product. The catalyst is regenerated in this reaction. The configuration of the reactants remains the same.

### **Stille reaction<sup>59</sup>**

Stille reaction is the palladium catalyzed coupling reaction involving organotin reagent. This reaction is effectual in the sense that it requires mild reaction conditions, is regioselective and exhibits endurance of many functional groups. No particular protecting groups are required for this reaction due to its tolerance to many functional groups. The solvents that can keep the macromolecules in solution and stabilize the palladium(0) catalyst can produce polymers with high molecular weights. Tin derivatives are fairly stable and are not sensitive to moisture or air. But the toxicity associated with it and the oxidative homocoupling of tin reagents are the only drawbacks associated with Stille reaction. Generally Stille reaction<sup>59</sup> can be depicted as given in the Scheme 1.2 below.

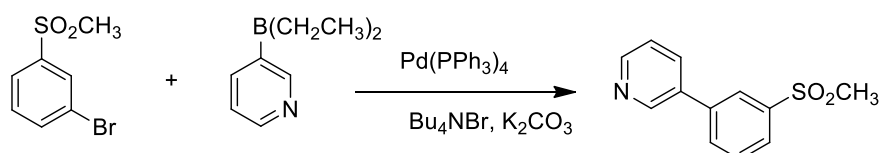


**Scheme 1.2: General Stille reaction**

### **Suzuki coupling reaction<sup>60</sup>**

Suzuki reaction is yet another palladium catalyzed cross-coupling reaction between organoboronic acids and halides. Usually the reaction is carried out in organic solvents like THF and diethyl ether in presence of Pd(0) or Pd(II) catalysts. In addition to aryl halides like bromides and

iodides, triflates and sulfonates are also used. Sulfonates are better option than triflates since they are easy to prepare, less expensive and more stable. The commonly used base for this reaction is  $\text{Na}_2\text{CO}_3$  but with sterically hindered substituents,  $\text{Ba}(\text{OH})_2$ ,  $\text{K}_3\text{PO}_4$  can be used as bases. In some cases, the catalyst  $\text{Pd}(\text{PPh}_3)_4$  can give rise to scrambled products. In such cases bulky phosphine ligand like (*o*-MeOC<sub>6</sub>H<sub>4</sub>)<sub>3</sub>P can be used to avoid side reactions and increase in yield of products. The advantage of this reaction is that it can give excellent yields even with sterically hindered compounds. It is used profusely for the synthesis of alternating copolymers. Disadvantages include saponification of esters and Aldol condensation of carbonyl group. Use of Suzuki coupling to produce a potential central nervous system agent is given below in the scheme 1.3.

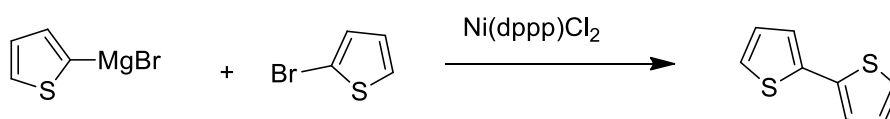


**Scheme 1.3: Suzuki reaction**

### **Kumada Coupling**<sup>64, 65</sup>

Kumada cross coupling reaction is an organic reaction of an aryl or vinyl halide with an aryl, alkyl or vinyl magnesium compounds using nickel or palladium catalyst to give a coupled product. This cross-coupling technique is the most frequent method for the synthesis of various types of thiophenes. Kumada coupling was developed in 1972 and is the first Ni or Pd catalyzed cross coupling reaction for generating carbon-carbon bond. This reaction is of significant importance for the synthesis of

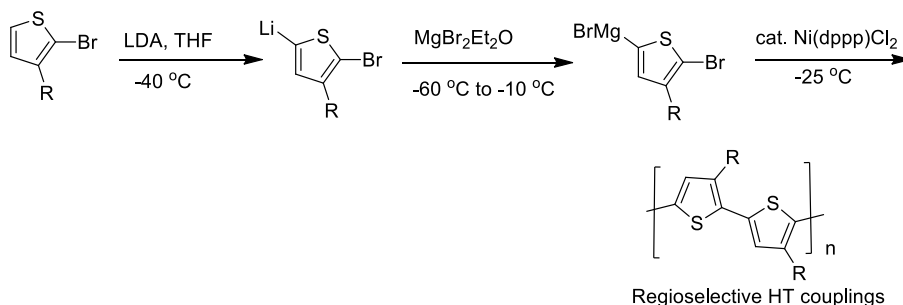
polyalkylthiophenes (PAT) which have applications in light emitting diodes and dye sensitized solar cells. Oligothiophenes can be conveniently prepared by this method. The general Scheme 1.4 for Kumada coupling is given below. The reactivity order for aryl halides increases down the group *i.e.* from fluoride to iodide. Grignard reagents can be prepared either in diethyl ether or THF. Pd catalyst is found to be more selective than Ni catalyst.



**Scheme 1.4: Kumada cross coupling reaction**

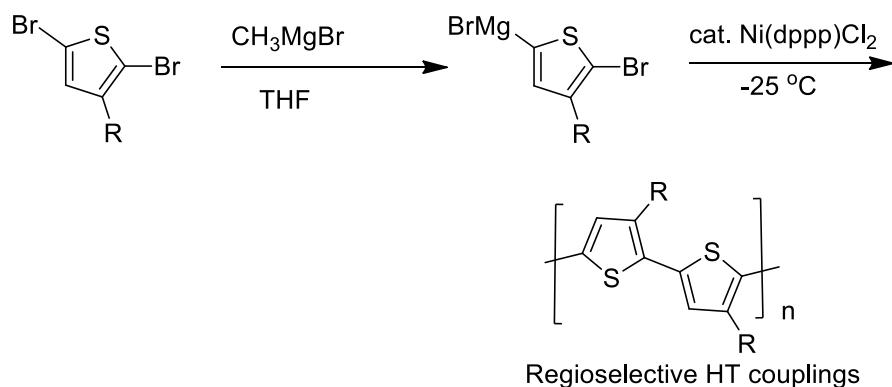
### **McCullough method<sup>52</sup>**

McCullough and Lowe used modified Kumada coupling reaction to prepare regioregular polyalkylthiophenes (PATs) in 1992. The McCullough method is depicted in the scheme 1.5.



**Scheme 1.5: McCullough reaction**

In addition, GRIM (Grignard Metathesis Polymerization) (Scheme 1.6 below) method was also used to prepare PATs. This is also a modified Kumada coupling method which is simpler than the McCollough method. Here 2,5-dibromo-3-alkylthiophene monomer on reaction with Grignard reagent gives 2-bromo-(5-magnesiobromo)-3-alkyl thiophene which undergoes coupling in presence of nickel catalyst to give the product in good yields.



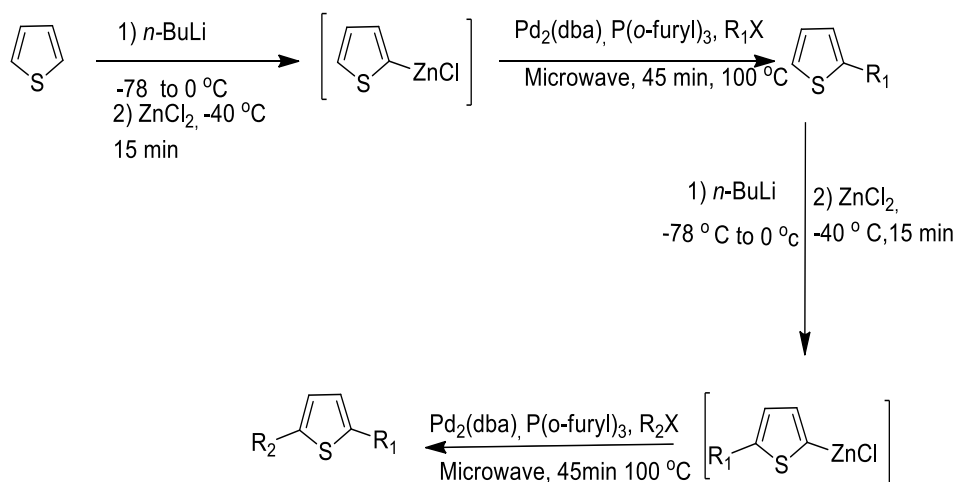
**Scheme 1.6: GRIM metathesis polymerisation**

### Negishi Coupling<sup>66-68</sup>

Negishi coupling is the nickel or palladium catalyzed coupling reaction of organozinc compounds with aryl, benzyl, allyl, vinyl halides or triflates forming C-C bonds in the process. It is a well-known transition metal catalyzed coupling reaction in which Pd(0) catalyst generally and sometimes nickel is used. This is because nickel may sometimes cause the decay in stereospecificity whereas no such problems occur with palladium. It was used for the synthesis of unsymmetrical biaryls, however the scope is not restricted to biaryls alone. Monica *et al.* utilized



Negishi coupling for the synthesis of thiophene based lignans that had Leishmanicidal<sup>67, 68</sup> effects. The reaction is shown in Scheme 1.7 below.

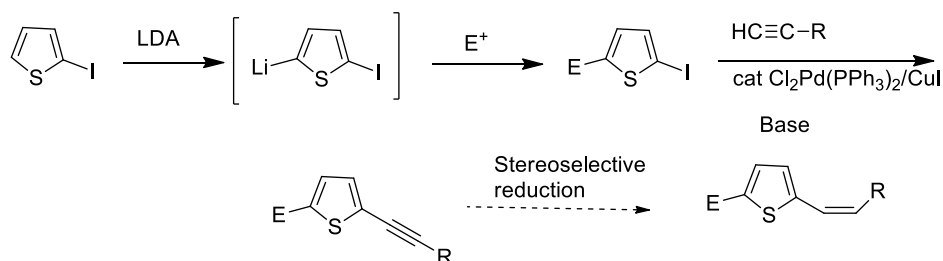


Scheme 1.7: Synthesis of biarylthiophene using Negishi coupling

### Sonogashira coupling reaction<sup>69-71</sup>

The coupling of aryl/vinyl halides with terminal alkynes in the presence of Pd(II)/Cu(I) catalyst system is called Sonogashira reaction. This coupling reaction is one of the most useful, powerful and advantageous method in synthetic organic chemistry due to the possibility for the straightforward construction of  $sp^2$ - $sp$  carbon-carbon bonds. A homogeneous phase is usually selected to carry out the Sonogashira coupling reaction. However Choudhary *et al.* and Djakovitch *et al.* have reported this coupling reaction in heterogeneous phase. In Sonogashira reactions, copper iodide was used as a co-catalyst and this was an extremely helpful approach and offered a new method to synthesize

conjugated alkynes and enynes at room temperatures. However this copper co-catalyst also suffers drawbacks since when exposed to air there is a possibility of homocoupling instead of undergoing coupling with vinyl or aryl halides. Thus instead of copper, zinc, tin, boron etc. have also been tried out. Paulo *et al.* have synthesized 2,5-disubstituted acetylinic thiophenes from 2-iodo-5-lithiothiophene by electrophilic trapping followed by Sonogashira coupling<sup>71</sup> as shown in the Scheme 1.8 below.



**Scheme 1.8: Synthesis of disubstituted acetylinic thiophenes using Sonogashira coupling reaction**

## 1.5 DIRECT ARYLATION<sup>72</sup>

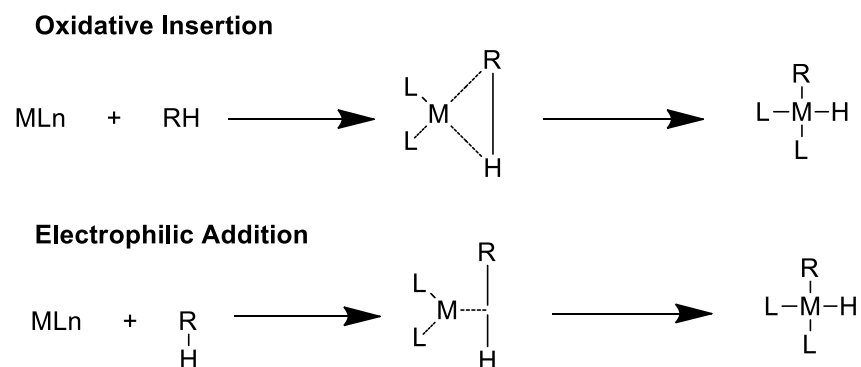
Typically, reactions like Heck coupling cannot be applied for aryl-aryl bond forming processes. Though Suzuki and Stille coupling provide convenient route for biaryl synthesis,<sup>72</sup> involvement of organoboranes and toxic organostannanes as reactants make them less desirable. Direct arylation strategy has emerged as an alternative to well-established C-C bond forming reactions discussed earlier. In organic compounds, C-H bond<sup>73</sup> is the most pervasive. Coupling reactions involving these can create numerous transformations and miracles. However this is not an

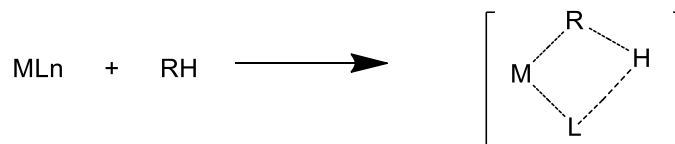
easy process owing to their immanent unreactivity. The direct arylation technique is efficient and advantageous over the other methods because of its:

- Environmentally friendly nature
- Less number of synthetic steps
- Easy availability of cheap precursors
- High yield ability

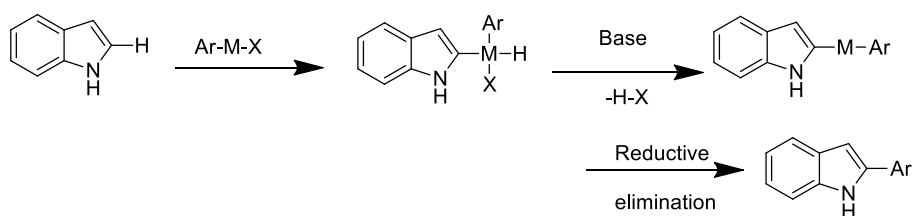
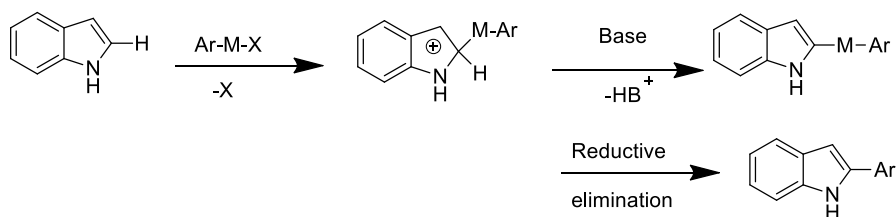
### 1.5.1 Mechanism of direct arylation

The exact mechanism of direct arylation reaction is still a matter of controversy, and a large number of generalizations and experimentations are still going on in this matter. C-H activation<sup>73-75</sup> is thought to be a key step in the mechanism which in turn proceeds through any of several mechanisms like oxidative insertion into the alkyl halide bond, electrophilic attack or  $\sigma$  bond metathesis. This in turn also depends on the nature of metal and the coordinated C-H bond and the type of coordinated ligands. A possible mechanism for direct arylation strategy is presented in Scheme 1.9.



**$\sigma$  Bond metathesis****Scheme 1.9: Mechanism of C-H bond activation**

Thus the mechanism of direct arylation can either be an oxidative insertion or electrophilic attack as shown in the scheme 1.10.<sup>76</sup>

**C-H activation****Electrophilic substitution****Scheme 1.10: Possible pathways in C-H activation**

The successive loss of ligands after the insertion of metal into the alkyl-halide bond is expected to occur but beyond that the mechanism again becomes unclear. Various eminent scientists have proposed different mechanisms but not any of them has yet been established fully. The electrophilic substitution mechanism as shown in the scheme<sup>76</sup> is yet

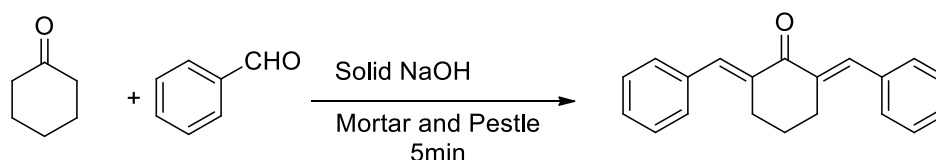
another substitute to the above said mechanism which includes the attack of the aryl palladium(II) species followed by reductive elimination forming biaryl compound. Various literature reports show the second mechanism to be the dominating one. Catalytic coupling reactions which are often very mild are involved for aryl-aryl and heteroaryl bond forming processes. Plausible pathways for C-H activation are presented in Scheme 1.10.

## **1.6 BISARYLIDINECYCLOALKANONES : AN**

### **OVERVIEW**

Studies on various bisaromatic systems have considerably progressed over last few decades. The aromatic groups may be naphthalene, anthracene, benzene, thiophene, pyrene etc. which act as donors in these systems. These aromatic donors are connected via a rigid 1,4-dien-3-one linker to the cycloalkanone acceptor moiety resulting in the formation of a very versatile photoactive molecule- bisarylidinecycloalkanone.<sup>77</sup> As these systems have interesting biological activities extensive research work is being carried out in this field especially in Bisbenzylidene systems. These materials act as precursors to various natural products. The biological activities<sup>78-81</sup> include antitubercular, antibacterial, antifungal, anticancer activities, drug resistance reversal, cytotoxicity etc. In addition, these compounds are effective photosensitive materials, can act as fluorescent probes and exhibit two-photon absorption properties. Typically the bisaromatic cycloalkanones are synthesized in the presence of a solvent *viz.* ethanol. Rahman *et al.*<sup>77</sup> have synthesized  $\alpha,\alpha'$ -(bis

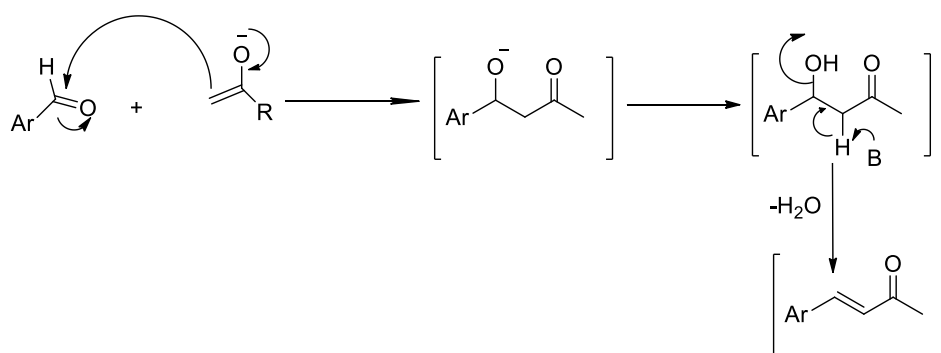
substituted benzylidene)cycloalkanones using a solvent free technique, *i.e.* by simple grinding method.



**Scheme 1.11: Synthesis of Bisbenzylidene cycloalkanone**

Recently, studies on heterocyclic ring systems namely thiophene with cycloalkanone as spacers has been exploited. Incorporation of such rigid cycloalkanone spacers into the thiophene backbone offers a planar conformation to the system as a whole with diminished steric effects so that a maximum delocalization of  $\pi$  electrons can be achieved. Consequently, compared to polythiophenes such a system will have less neighboring interactions offering good stability to the system. Synthesis of these compounds is achieved via Claisen-Schmidt condensation.<sup>82-84</sup> Claisen-Schmidt reaction is the condensation of aromatic aldehydes (or between ketones and aldehydes lacking  $\alpha$ -hydrogen) with aliphatic or mixed alkyl aryl ketones in the presence of a relatively strong base<sup>85</sup> to form  $\beta$ -hydroxy carbonyl compounds that undergoes subsequent dehydration to give  $\alpha,\beta$ -unsaturated ketones. A large number of elegant synthesis reactions employ Claisen-Schmidt reaction as a key step which clearly demonstrates the importance of this reaction in synthetic organic chemistry. Claisen-Schmidt condensation can also be catalysed by acid. The first step involves the nucleophilic addition of enol or enolate ion derived from methyl ketone to the carbonyl-carbon of the aromatic

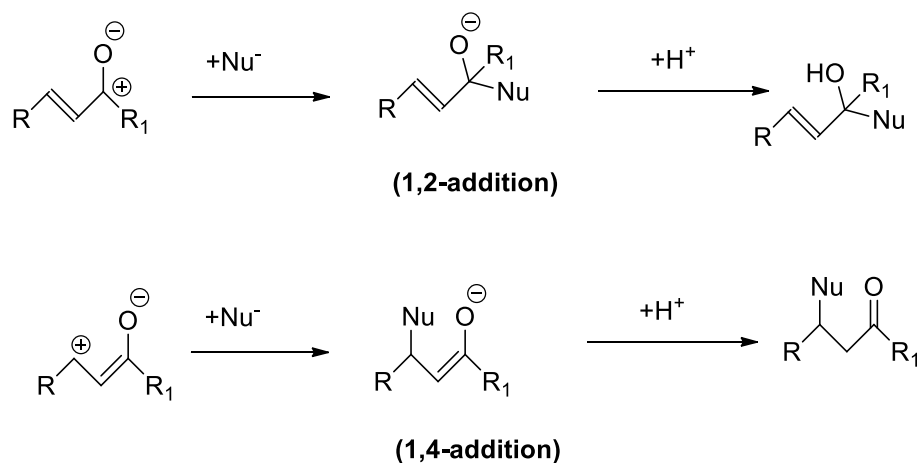
aldehyde i.e. a typical aldol type condensation. Dehydration of the hydroxyketone to form the conjugated unsaturated carbonyl compound occurs spontaneously. Normally Claisen–Schmidt reactions prefer the formation of a *trans* double bond. The general Scheme 1.12<sup>82</sup> is represented below.



**Scheme 1.12: Mechanism of Claisen-Schmidt condensation reaction**

## 1.7 PYRAZOLINES

The  $\alpha,\beta$ -unsaturated ketones find interesting applications in synthetic organic chemistry partially because they act as precursors to natural products and partially since they can be used for the synthesis of certain classes of nitrogen containing heterocycles. These ketones as such have two electrophilic reaction centers which is the responsible feature to undergo such reactions. The electron density is delocalized in the  $\text{>C=C<}$  C=O system making these compounds suitable to react as ambident electrophiles. Addition of nucleophiles to these compounds can take place either via attack of the carbonyl group (1,2-addition) or via  $\beta$ -carbon (1,4-addition), 1,4-addition being preferable (Scheme 1.13).



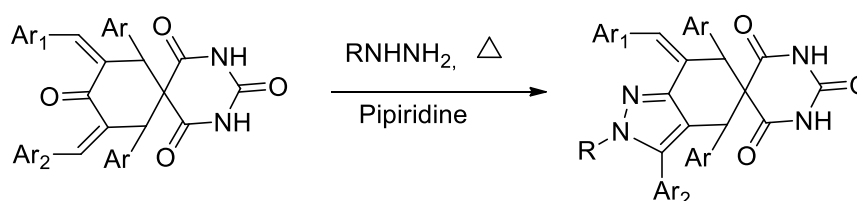
**Scheme 1.13: Pathways for 1,2- and 1,4-additions**

Perturbation theory can explain the reactivity of 1,2- and 1,4- additions. Accordance with this theory, considering the electronic structure of the enone fragment, 1,2-addition is controlled by charge and 1,4-addition is controlled by orbital. Decreasing the HOMO energy and localization of charge at the nucleophilic group favors 1,2-addition while increasing the HOMO energy and charge delocalization causes orbital control of 1,4-addition.

The well-known synthetic route<sup>86</sup> to five membered nitrogen containing heterocycles is the condensation of  $\alpha,\beta$ -unsaturated ketones with 1,2-binucleophiles like hydrazines, hydroxylamines or their derivatives. Synthesis of pyrazolines is carried out in a number of ways. Reactions carried out under acidic conditions<sup>87-91</sup> are expected to produce good yields. Rate of the reaction can be accelerated using microwave

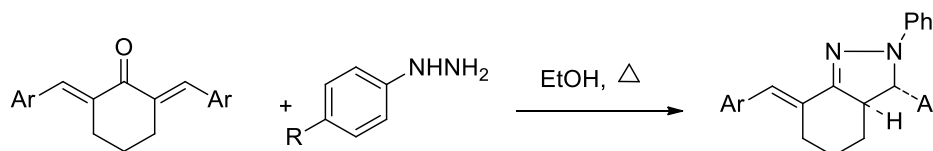


accelerated procedures even without the presence of solvents. Sterically hindered substituents are usually subjected to this reaction by using piperidine as base and ethanol as solvent. The rigid structure of  $\alpha,\beta$ -unsaturated ketone requires stronger reaction conditions like the one said above rather than the acid conditions. Reaction scheme<sup>92</sup> is given below (Scheme 1.14).



**Scheme 1.14: Reaction of sterically hindered type ketones**

Gella *et al*<sup>93</sup> described the direction of reaction of bisaromatic cycloalkanones with hydrazones. It was proved that the reaction with phenylhydrazines and semicarbazides gives *trans* product whereas 4-nitrophenylhydrazines, thiosemicarbazides etc. gave *cis* products (Scheme 1.15).

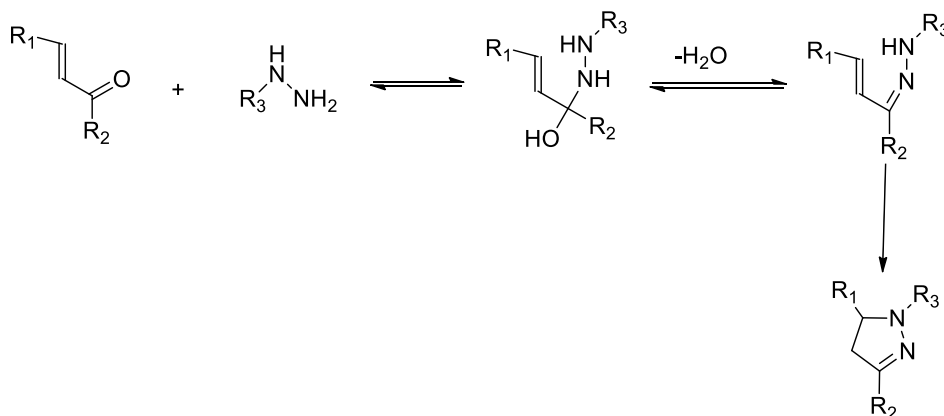


**Scheme 1.15: Reaction yielding *trans* product**

Stereoselective synthesis of both *trans* and *cis* isomer is possible. When the reaction is carried out in presence of pyridine or piperidine under

boiling conditions trans isomer is formed, whereas the reaction in ethanol with catalytic amounts of hydrochloric acid yields cis isomer.

The mechanism of pyrazoline formation<sup>94,95</sup> can be described in three stages. The first stage is the addition of the more nucleophilic  $\beta$ -nitrogen atom of phenylhydrazine to the carbon of the carbonyl group on the unsaturated ketone forming an intermediate. The next step, consisting of dehydration of adduct is the rate-determining stage, while subsequent cyclization occurs instantaneously resulting in the formation of the product. Scheme 1.16 shows the mechanism of formation of pyrazolines.



**Scheme 1.16: Mechanism of formation of pyrazoline**

A clear picture of the mechanism (as in scheme above) and kinetics of the reaction of the chalcones with phenyl hydrazine i.e. the pyrazoline formation was carried out by polarographic studies.<sup>96</sup>



$\pi$  electron density are higher for the *N*-phenyl substituent in the para position than in the phenyl in the position-3 of pyrazoline in the case of Ph-N-N-CH<sub>2</sub>  $\pi$  system thus motivating the pyrazolines unsubstituted in position 3. Even if the ortho-para position  $\pi$  electron density is greater than on C-3, the boundary electron density has a maximum value exactly at position-3. The features of electronic structure of pyrazolines have a great influence on their chemical properties. Thus various reactions like formylation, sulfonation, nitration, azocoupling etc. occurs at para or ortho positions. But in contrast to this, the electrophilic reactions for 3-unsubstituted pyrazolines like bromination, chlorination, nitrations occurs at position 3. This may be due to predominance of orbital control over charge control. The scheme below shows that in the first case where the position 3 is substituted the substitution normally prefers at the para position of the *N*-phenyl ring. But when the position-3 is unsubstituted there is a possibility for the formation of product with electrophilic substitution at the third position along with a mixture as given in Scheme 1.17<sup>98, 99</sup>. Generally, the pyrazolines unsubstituted at 1-and 3- positions are highly unstable compounds that decompose in presence of air.

Recently, pyrazolines have attracted many researchers owing to their immense biological and synthetic applications. These are important class of pharmacophores.<sup>100-103</sup> These substances are important components for the synthesis of various biologically active compounds possessing tranquilizing, antidepressant, anticonvulsant, anti-inflammatory effects. In addition, their bright green fluorescence makes them important compounds for optoelectronic devices. Pyrazolines and their derivatives

have been used in manufacture of green light emitting diodes, fluorophores, luminophores etc.

## **1.8 NONLINEAR OPTICS**

Pioneering efforts of Bloembergen and Schawlow on non-linear optics<sup>104</sup> during the 1960's earned them Nobel Prize in 1981. In free space, light travels in a linear manner and the non-linearity is caused by the medium through which light travels. For a linear medium, the relation between polarization density and electric field is given by the equation

$$\rho = \epsilon_0 \chi \epsilon$$

A linear medium is characterized by a linear relation between  $\rho$  and  $\epsilon$  whereas a non-linear relation occurs between  $\rho$  and  $\epsilon$  occurs in a non-linear medium (Figure 1.8).

For an optical field applied, the polarization density  $P(t)$  can be expressed as a power series of expansion of electric field as given below:

$$P(t) = \chi^{(1)}E(t) + \chi^{(2)}E^2(t) + \chi^{(3)}E^3(t) + \dots$$

$\chi^{(1)}$  is the linear electric susceptibility,  $\chi^{(2)}$  is the second order susceptibility and  $\chi^{(3)}$  is the third order susceptibility.

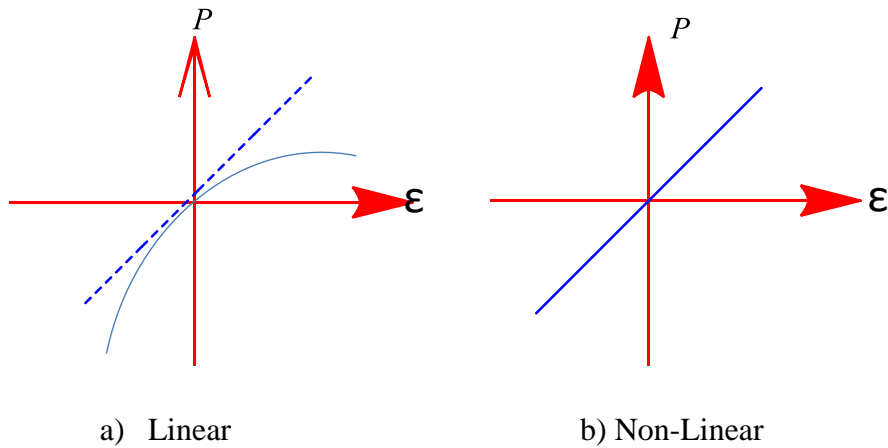


Figure 1.8: Relation between  $p$  and  $\epsilon$  in a) linear and b) non-linear medium

### 1.8.1 Second order materials

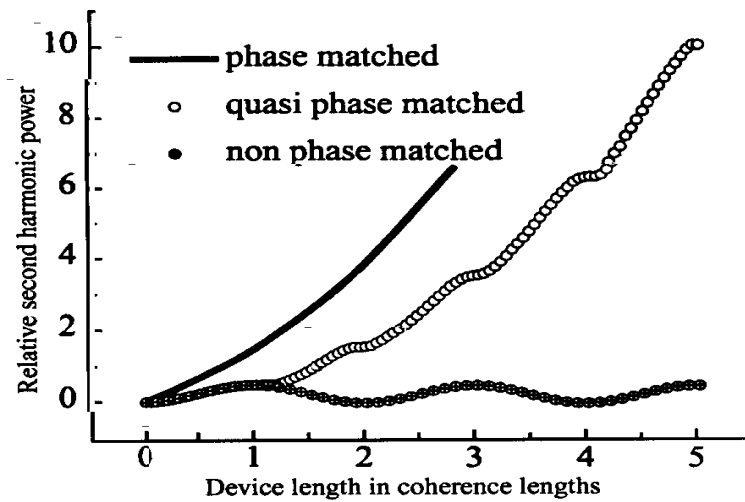


Figure 1.9: The signal amplitude obtained for phase matched, quasi phase matched and non-phase matched versus device length in coherence lengths<sup>105</sup>

The materials which show second order susceptibility are second order materials. This category typically contains non centrosymmetric molecules or those crystals which lack a center of inversion. There is no much selection of crystals in this regard which limits their application. In addition, a phase matching condition like birefringence instead of dispersion or quasi phase matching is required (Figure 1.9). Crystals like silver Gallium arsenide, lithium iodate, lithium niobate, potassium dihydrogen phosphate etc. are some second order materials.

### **1.8.2 Third Order Materials**

Likewise second order materials response leads to second harmonic generation, third order materials response leads to third harmonic generation and two-photon absorption. The intensity dependent refractive index is the major criteria of third order materials because this factor determines the optical switching behavior of materials. The intensity and refractive index can be related by the equation:

$$\eta = \eta_0 + \eta_2 I$$

I is the intensity of laser beam and  $\eta_2$  is the refractive index coefficient (intensity dependent).

Boyd equation <sup>105</sup> relates this quantity to Non-linear susceptibility by the relation

$$\eta_2 = \frac{12\pi^2 \chi^3}{\eta_0^2}$$

Semiconductors often exhibit good susceptibility of the order of  $10^{-13}$ - $10^{-10}$  esu. Susceptibility for a given material depends largely on the photon energy and band gap energy of semiconductor. Depending on whether photon energy is comparable or greater or lesser than band gap energy linear or non-linear behavior is observed. Organic compounds are reported to have larger non linearity typically due to the conjugated structure which allows delocalization of electrons. Polydiacetylene has third order susceptibility of the order of  $10^{-10}$  esu.

Material	$\chi^3$ (esu)
<i>Crystals</i>	
Al <sub>2</sub> O <sub>3</sub>	$2.2 \times 10^{-14}$
Diamond	$1.8 \times 10^{-13}$
GaAs	$1.0 \times 10^{-10}$
Ge	$4.0 \times 10^{-11}$
<i>Glasses</i>	
As <sub>2</sub> S <sub>3</sub>	$2.9 \times 10^{-11}$
Pb Bi gallate	$1.6 \times 10^{-12}$
<i>Polymers</i>	
PTS	$3 \times 10^{-12}$
9BCMU	$1.9 \times 10^{-10}$

**Table 1.2: Third order Non-linear susceptibilities of various compounds**



Table 1.2 shows the third order non-linear susceptibilities of various materials. From the figure it is evident that large number of third order materials finds applications in Non-linear optics. Only those materials having large susceptibility ranges can be chosen for non-linear optics. Also the material should be stable under all conditions, resistant to laser damage, and transmits at all wavelengths of interests. Usually for small values of  $\epsilon$  non linearity is not observed.

### 1.8.3 Z-scan

Z-scan<sup>106,107</sup> is a flexible technique by which the non-linear optical characteristics of compounds can be explored. Here typically lasers of high intensity are required as excitation sources. Z-scan set up is shown in the figure 1.10.

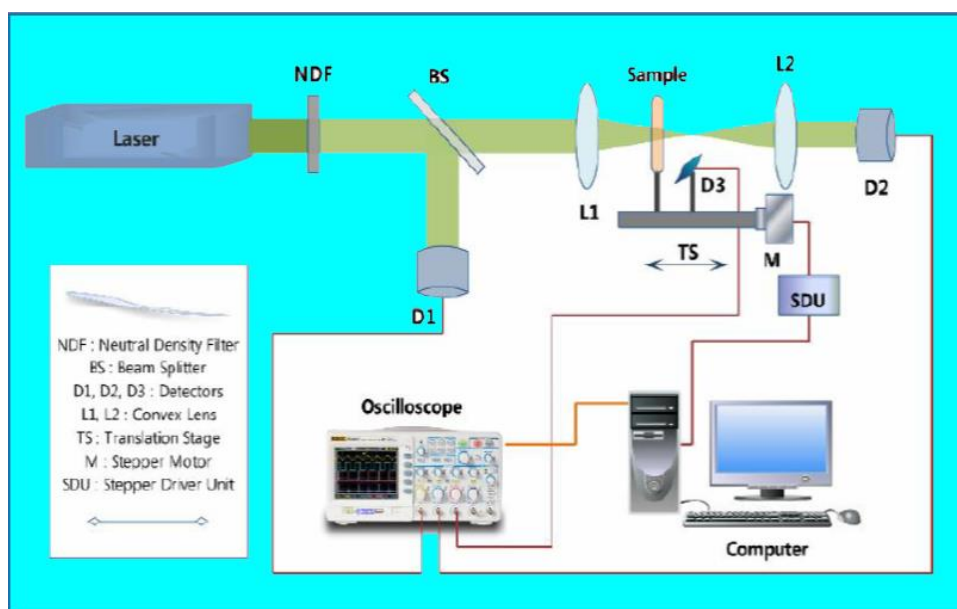


Figure 1.10: Z-scan set up<sup>106</sup>

During the experiment<sup>106</sup> the focal point is fixed as  $z = 0$  and the sample can be propagated along the direction of laser beam with the help of a motor. The intensity of the laser beam and the number of photons will be highest at this center point and symmetrically decreases to either side. The Z-scan technique can be either closed aperture, in which some kind of aperture is placed to prevent some light from reaching the detector or open aperture in which no aperture is placed so as to allow the entire light to reach the detector.

## **1.9 INTRODUCTION TO OUR PROJECT**

The present work mainly focusses on the synthesis of various bithiophene cycloalkanone systems with a view to effectively utilize these systems for conversion into more useful materials employing polymerization techniques. Thiophene based polymers and oligomers have received much attraction nowadays in optoelectronic devices, and studies based on oligomers and polymers derived from bithiophene cycloalkanones is probably considered to be a novel approach. We have also extended our studies to synthesis of derivatives of bithiophene systems by modifying the keto group with some other structural entities *viz.*, pyrazolines. The third order non-linear optical properties and conductivity of the synthesised materials were also studied to ensure its application in devices.

## **1.10 REFERENCES**

1. Shirakawa, H.; Lewis, E. J.; Mac Diarmid, A. G.; Chiang, C. K.; Heeger, A. J. *J. Chem. Soc. Chem. Commun.* **1977**, 578.
2. Bhakshi, A. K.; Bhalla, G. *J. Sci. Ind. Res.* **2004**, *63*, 715.
3. Chiang, C. K.; Finchee, C. R.; Park, Y. W.; Heeger, A. J.; Lewis, E. J.; Gan, S. C.; Mac Diarmid, A. G. *Phys Rev Lett.* **1977**, *39*, 1098.
4. Chiang, C. K.; Drug, M.A.; Gan, S. C.; Heeger, A. J.; Lewis, E. J.; Mac Diarmid, A. G.; Park, Y. W.; Shirakawa, H. *J. Am. Chem. Soc.* **1978**, *100*, 1013.
5. Chien, J. C. W.; Wenk, G. E.; Karasz, F. E.; Hirsch, J. A. *Macromolecules* **1981**, *14*, 479.
6. Dai, L. *J. Macromol. Sci., Rev. Macromol. Chem. Phys. C.* **1999**, *39*, 273.
7. Dai, L. *J. Phys. Chem.* **1992**, *96*, 6469.
8. Dai, L.; Huang, S.; Lu, J.; Mau, A. W. H.; Zhang, F. *ACS Polym. Prepr.* **1998**, *39*, 171.
9. Dai, L.; White, J. W. *Polymer* **1991**, *32*, 2120.
10. Dai, L.; Winkler, B.; Dong, L.; Tong, L.; Mau, A. W. H. *Adv. Mater.* **2001**, *13*, 915.
11. Bredas, J. L.; Street, G. B. *Acc. Chem. Res.* **1985**, *18*, 309.
12. Harrison, W. A. *J. Poly. Sci.* **1974**, *12*, 11.
13. Bernius, M. T.; Inbasekaran, M.; O'Brien, J.; Wu, W. *Adv. Mater.* **2000**, *12*, 23.
14. Tada, K.; Sonoda, T.; Yokota, Y.; Kobashi, K.; Yoshino, K. *J. Appl. Phys.* **1998**, *84(10)*, 5635.
15. Faraggi, E. Z.; Davidov, D.; Cohen, G.; Noah, S.; Golosovsky,

- M.; Avny, Y.; Neumann, R.; Lewis, A. *Synth. Met.* **1997**, *85(1-3)*, 1187.
16. Akcelrud, L. *Polym. Sci.* **2003**, *28*, 873.
  17. Hamberg, I.; Granqvist, C. *J. Appl. Phys.* **1986**, *60*, R20.
  18. Kobayashi, H.; Ishida, T.; Nakato, Y.; Tsubomura, H. *J. Appl. Phys.* **1991**, *69*, 1736.
  19. Tahar, R.; Ban, T.; Ohya, Y.; Takahashi, Y. *J. Appl. Phys.* **1998**, *83*, 2631.
  20. Osada, T.; Kugler, T.; Broms, P.; Salaneck, R.; Daik, W. F. *J. Appl. Phys.* **1998**, *96*, 77.
  21. Kim, J.; Granstrom, R.; Friend, N.; Johansson, W.; Salaneck, R.; Daik, W. F. *J. Appl. Phys.* **1998**, *84*, 6859.
  22. Milliron, D.; Hill, I.; Shen, C.; Kahn, A.; Schwartz, J. *J. Appl. Phys.* **2000**, *87*, 572.
  23. Scott, J.; Kaufmann, J.; Brock, P.; Dipietro, R.; Salem, J.; Goitia, J. *J. Appl. Phys.* **1996**, *79*, 2745.
  24. Heeks, H. K.; Burroughes, A. H.; Towns, C.; Cina, S.; Baynes, N.; Athanassopoulou, N.; Carter, J. C.; Miyashita, S. *Nature* **1990**, *347*, 539-541.
  25. Burroughes, H.; Bradley, D. D. C.; Brown, A. R.; Marks, R. N.; Mackay, K.; Friend, R. H.; Burns, P. L.; Holmes, A. B. *Nature* **1990**, *347*, 539.
  26. Braun, D.; Heeger, A. *J. Appl. Phys. Lett.* **1991**, *58*, 1982.
  27. Deng, X. *Int. J. Mol. Sci.* **2011**, *12*, 1575.
  28. Vidya, G. *Ph.D Thesis*, CUSAT, **2012**.
  29. Ishikawa Ankerhold, H. C.; Ankerhold, R.; Drummen, G. P. C. *Molecules* **2012**, *17*, 4047.
  30. Ohmori, Y.; Uchida, M.; Muro, K.; Yoshino, K. *Jpn. J. Appl.*

- Phys.* **1991**, 30, L1938.
31. Ohmori, Y.; Morishita, C.; Uchida, M.; Yoshino, K. *Jpn. J. Appl. Phys.* **1992**, 31, L568.
  32. Braun, D.; Gustaffson, G.; Macbranch, D.; Heeger, A. *J. Appl. Phys.* **1992**, 72, 164.
  33. Grem, G.; Leditsky, G.; Ullrich, B.; Leising, G. *Adv. Mater.* **1992**, 4, 36.
  34. Yamamoto, T. *NPG Asia Mater.* **2010**, 2, 54.
  35. Roncali, J. *J. Mater. Chem.* **1999**, 9, 1875.
  36. Theander, M.; Inganas, O.; Mammo, W.; Olinga, T.; Svensson, M.; Andersson, M. *J. Phys. Chem. B.* **1999**, 103, 7771.
  37. Greenham, N. C.; Samuel, I. D. W.; Hayes, G. R.; Philips, R. T.; Kessener, Y. A. R. R.; Moratti, S.C.; Holmes, A. B.; Friend, R. H.; *Chem. Phys. Lett.* **1995**, 241, 89.
  38. Chen, F.; Mehta, P. G.; Takiff, L.; McCullough, R. D. *J. Mater. Chem.* **1996**, 6, 1763.
  39. Garnier, F. *Acc. Chem. Res.* **1999**, 32, 209.
  40. Saadeh, H.; Goodson, T.; Yu, L. *Macromolecules* **1997**, 30, 4608.
  41. Kraabel, B.; Moses, D.; Heeger, A. J. *J. Chem. Phys.* **1995**, 103, 5102.
  42. Belijonne, D.; Shuai, Z.; Pourtois, G.; Bredas, J. L. *J. Phys. Chem. A.* **2000**, 105, 3899.
  43. Rughooputh, S. D D.; Hotta, S.; Heeger, A. J.; Wudl, F. *J. Polym. Sci., Part B: Polym. Phys.* **1987**, 25, 1071.
  44. Inganas, O.; Salaneck, W. R.; Osterholm, J. E.; Laakso, J. *Synth. Met.* **1988**, 22, 395.
  45. Inganas, O.; Gustafson, G.; Salaneck, W.R. *Synth. Met.* **1989**, 28, C377.

46. Inganas, O.; Gustafson, G. *Synth. Met.* **1990**, *37*, 195.
47. Amou, S.; Haba, O.; Shirato, K.; Hayakawa, T.; Ueda, M.; Takeuchi, K.; Asai, M. *J. Polym. Sci., Part A: Polym. Chem.* **1999**, *37*, 1943.
48. Andersson, M. R.; Selse, D.; Berggren, M.; Jarvinen, H.; Hjertberg, T.; Inganas, O.; Wennerstrom, O.; Osterholm, J. E. *Macromolecules* **1994**, *27*, 6503.
49. Souto Maior, R. M.; Hinkelmann, K.; Eckert, H.; Wudl, F. *Macromolecules* **1990**, *23*, 1268.
50. McCullough, R. D.; Lowe, R. D. *J. Chem. Soc., Chem. Commun.* **1992**, 70.
51. McCullough, R. D.; Lowe, R. D.; Jayaraman, M.; Anderson, D. L. *J. Org. Chem.* **1993**, *58*, 904.
52. McCullough, R. D. *Adv. Mater.* **1998**, *10*, 93.
53. Chen, T.-A.; Rieke, R. D. *Synth. Met.* **1993**, *60*, 175
54. Peripichka, I. F.; Peripichka, D. F.; Meng, H.; Wudl, F. *Adv. Mater.* **2005**, *17*, 2281.
55. Barbarella, G.; Favaretto, L.; Zanelli, A.; Gigli, G.; Mazzeo, M.; Anni, M.; Bongini, A. *Adv. Funct. Mater.* **2005**, *15*, 664.
56. Peripichka, I. I.; Peripichka, I. F.; Bryce, M. R.; Palsson, L. O. *Chem. Commun.* **2005**, 3397.
57. Ramey, M. B.; Hiller, J.A.; Rubner, M. F.; Tan, C.; Schanze, K. S.; Reynolds, J.R. *Macromolecules* **2005**, *38*, 234.
58. Wu, C. G.; Lin, Y. C.; Wu, C. E.; Huang, P. H. *Polymer* **2005**, *46*, 3748.
59. McCullough, R. D.; Ewbank, P. C.; Loewe, R. S. *J. Am. Chem. Soc.* **1997**, *119*, 633.
60. Guillerez, S.; Bidan G. *Synth. Met.* **1998**, *93*, 123.

61. Li, Y.; Vamvounis, G.; Yu, J.; Holdcroft, S. *Macromolecules* **2001**, *34*, 3130.
62. Andersson, M. R.; Thomas, O.; Mammo, W.; Svensson, M.; Theander, M.; Inganäs, O. *J. Mater. Chem.* **1999**, *9*, 1933.
63. Andersson, M. R.; Berggren, M.; Inganäs, O.; Gustafsson, G.; Gusatafsson-Carlberg, J. C.; Selse, D.; Hjertberg, T.; Wennerstrom, O. *Macromolecules* **1995**, *28*, 7525.
64. Tamao, K.; Sumitani, K.; Kumada, M. *J. Am. Chem. Soc.* **1972**, *94*, 4374.
65. Heravi, M. M.; Hajiabbasi, P. *Monatsh Chem.* **2012**, *143*, 1575.
66. King, A. O.; Okukado, N.; Negishi, E. *J. Chem. Soc., Chem. Commun.* **1977**, 683, 684.
67. Amaral, M. Z. F. J.; Callejon, D. R.; Riul, T. B.; Baruffi, M. D.; Toledo, F. D.; Lopes, N. P.; Clososki, G. C. *J. Braz. Chem. Soc.* **2014**, *25*, 1907-1913.
68. Brendle, J. J.; Outlaw, A.; Kumar, A.; Boykin, D. W.; Patrick, D. A.; Tidwell, R. R.; Werbovetz, K, A. *Antimicrob. Agents Chemother.* **2002**, *46*, 797.
69. Chinchilla, R.; Nájera, C. *Chem. Rev.* **2007**, *107*, 874.
70. Liang B.; Dai, M.; Chen J.; Yang, Z. *J. Org. Chem.* **2005**, *70*, 391.
71. Sonogashira, K.; Tohda, Y.; Hagihara, N. *Tetrahedron Lett.* **1975**, *50*, 4467.
72. Miura, M.; Nomera, M. *Curr. Chem.* **2002**, *219*, 211.
73. Labinger, J. A.; Bercaw, J. E. *Nature* **2002**, *417*, 507.
74. Glover, B.; Harvey, K. A.; Liu, B.; Sharp, M. J.; Tymoschenko, M. F. *Org. Lett.* **2003**, *5*, 301.
75. Grigg, R.; Sridharan, V.; Stevenson, P.; Sukirthalingam, S.;

- Worakun, T. *Tetrahedron* **1990**, *46*, 4003.
76. Park, C. H.; Ryabova, V.; Seregin, I. V.; Sromek, A. W.; Gevorgyan, V. *Org. Lett.* **2004**, *6*, 1159.
77. Motiur Rahman, A. F. M.; Jeong, B. S.; Kim, D. H.; Park, J. K.; Lee, E. S.; Jahng, Y. *Tetrahedron* **2007**, *63*, 2426.
78. Robinson, T. P.; Ehlers, T.; Hubbard, R. B.; Bai, X.; Arbiser, J. L.; Goldsmith, D. J.; Bowena, J. P. *Boiorg. Chem. Med. Lett.* **2003**, *13*, 115.
79. Dinkova-Kostova, A. T.; Abeygunawardana, C.; Talalay, P. *J. Med. Chem.* **1998**, *41*, 5287.
80. Dimmock, J. R.; Padmanilayam, M. P.; Zello, G. A.; Nienaber, K. H.; Allen, T. M.; Santos, C. L.; De Clereq, E.; Balzarini, J.; Manavathu, E. K.; Stables, J. P. *Eur. J. Med. Chem.* **2003**, *38*, 169.
81. Piantadosi, C.; Hall, I. H.; Irvine, J. L.; Carlson, G. L. *J. Med. Chem.* **1973**, *16*, 770.
82. Motiur Rahman, A. F. M.; Ali, R.; Jahng, Y.; Kadi, A. A. *Molecules* **2012**, *17*, 571-583.
83. Nielsen, A. T.; Houlihan, W. J. *Organic Reactions. In The Aldol Condensation*; Adams, R., Blatt, A.H., Boekelheide, V., Cairns, T. L., Cram, D. J., House, H. O. *J. Am. Chem. Soc.* **1998**, *120*, 231.
84. Gall, E.L.; Texier-Boullet, F.; Hamelin, J. *Synth. Commun.* **1999**, *29*, 3651.
85. Singh, N.; Pandey, J.; Yadav, A.; Chaturvedi, V.; Bhatnagar, S.; Gaikwad, A. N.; Sinha, S. K.; Kumar, A.; Shukla, P. K.; Tripathi, R. P. *Eur. J. Med. Chem.* **2009**, *44*, 1705.
86. Levai, R. J. *Heterocyclic Chem.* **2002**, *39*, 1.
87. Von Auwers, K.; Muller, K. *Chem. Ber.* **1908**, *41*, 4230.
88. Von Auwers, K.; Muller, K. *Chem. Ber.* **1908**, *42*, 4411.
89. Von Auwers, K.; Kreuder, A. *Chem. Ber.* **1925**, *58*, 1974.



90. Kishner, N. *J. Phys. Chem.* **1913**, *45*, 949.
91. Raiford, L. C.; Entrikin, J. B. *J. Am. Chem. Soc.* **1933**, *55*, 1125.
92. Behera, R. K.; Behera, A. K.; Pradhan, R.; Pati, A.; Patra, M. *Synth. Commun.* **2006**, *36*, 3729.
93. Gella, I. M.; Yaya, A. R.; Orlov, V. D. *Karkov University Bulletin* **2001**, *30*, 103.
94. Suchchar, S. P.; Singh, A. K. *J. Indian Chem. Soc.* **1985**, *62*, 142.
95. Ferres, H.; Hamdam, M. S.; Jackson, W. R. *J. Chem. Soc. B.* **1971**, 1892.
96. Bezuglyi, V. D.; Kotok, L. A.; Shimanskaya, N. P.; Bondarenko, V. E. *Zh. Obsch. Khim.* **1969**, *39*, 2167.
97. Orlov, V. D.; Aziz, M. A.; Savran, A. T.; Asoka, P. K. D. *Khim. Geterotsikl. Soedin.* **1984**, 965.
98. Bouchet, P.; Elguero, J.; Jacquier, R. *Bull. Soc. Chim. Fr.* **1967**, *95*, 4716.
99. Duffin, G. F.; Kendall, J. D. *J. Am. Chem. Soc.* **1954**, 408.
100. Bilgin, A. A.; Palaska, E.; Sunal, R.; Guemuesel, D. *Pharmazie.* **1994**, *49*, 67.
101. Abbady, M. A.; Hebbachy, R. *Indian J. Chem. Sect. B.* **1993**, *32*, 1119.
102. Attia, A.; Michael, M. *Acta Chim. Hung.*, **1983**, *114*, 337.
103. Descacq, P.; Nuhlich, F.; Varache-Beranger, V.; Capdepuy, V.; Devaux, D. *Eur. J. Med. Chem. Chim. Ther.* **1990**, *25*, 285.
104. Bloembergen, N. *Phys. Rev.*, **1964**, *133*, A1493.
105. Boyd, R. W. *J. Mod. Opt.* **1999**, *46*, 367.
106. Anand, P. B. *Ph. D Thesis*, CUSAT, **2015**.
107. Boyd, R. W.; Sipe, J. E. *J. Opt. Soc. Am.* **1994**, *11*, 297.



## CHAPTER 2

### *Synthesis of a few thiophene based molecules, regioselectivity and mechanism of their formation*

---

#### 2.1 Abstract

*In this chapter, we describe the synthesis of a few novel bithiophene monomers having different spacers viz cycloalkanones, heterocyclic ketones, open chain alkanones and fused ring diones. Different alkanone spacers have been effectively utilized to study the mechanism and regioselectivity of Claisen-Schmidt condensation reaction. Structures of the synthesized compounds were confirmed on the basis of spectral and analytical data.*

---

#### 2.2 Introduction

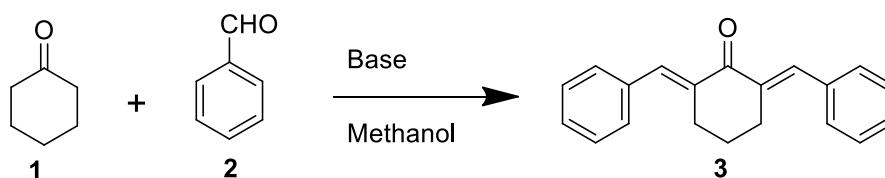
Bisaromatic cycloalkanones<sup>1,2</sup> are typical donor-acceptor systems with aromatic group acting as the donor and cycloalkanone moiety as the acceptor. The aromatic group can be benzene, thiophene, naphthalene, anthracene, flourene, etc. Several reports are available on the synthesis of bisbenzylidene cycloalkanones. Being precursors to natural products, their biological applications<sup>1-3,6</sup> have been thoroughly investigated. These compounds are well known for their antitubercular, antifungal, antibacterial and even antitumor<sup>3</sup> activities. However, it appears that polymerization reactions of bisarylidene cycloalkanones remain unexplored. Thiophenes are widely explored nowadays owing to their potential importance in electronic and optoelectronic devices. Thiophenes

are highly electron rich compounds and hence, compared with benzene,  $\pi$ -electron density is much higher with thiophenes. In addition, steric effects are less with these compounds. Alkskas *et al* have reported the synthesis of polyketones of bithiophene cycloalkanone<sup>3-6</sup> system by Friedel-Crafts polycondensation reaction with terephthaloyl dichloride using CS<sub>2</sub> as solvent. Here too similar to the benzylidene compound, thiophene derivatives showed good antimicrobial activities against *Streptococcus pyogenes*, *Staphylococcus aureus* and *Escherichia coli*. No further reports on the synthesis of such bithiophene cycloalkanone monomers or their corresponding polymers are available.

In the present work, we have investigated the synthesis of various bithiophene systems using different alkanone spacers. We have effectively employed four classes of cyclic ketone spacers in our study *viz.* cycloalkanones, heterocyclic ketones,<sup>7,8</sup> open chain alkanones and fused ring diones. To the best of our knowledge, no reactions are reported with bis(thiophen-2-ylmethylene) alkanone systems having open chain ketones or fused ring diones as spacers. We have accounted for the plausible regioselectivity and mechanism of formation of bis(thiophen-2-ylmethylene)alkanone products. It was inferred that steric effect plays a crucial role on the stereochemistry of product. The compounds were synthesized using typical Claisen Schmidt<sup>9,10</sup> condensation reaction using KOH as base and methanol as solvent. Structure of all new compounds was confirmed on the basis of spectral and analytical data. Due to the intense color of fused ring dione products, we also carried out preliminary photophysical studies on these compounds.

## 2.3 Results and discussion

We utilized Claisen-Schmidt condensation reaction for the synthesis of bithiophene alkanone systems. Typical reaction scheme is given below:

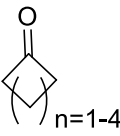
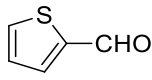
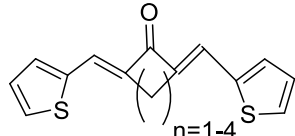
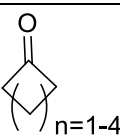
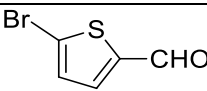
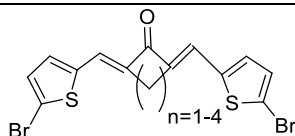
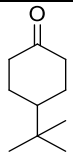
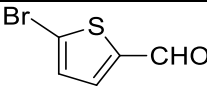
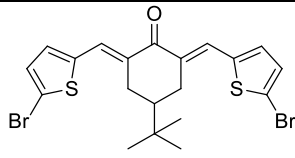


**Scheme 2.1**  
Synthesis of bis benzylidene systems

Using a reported procedure, we synthesized several novel bromo derivatives of bisaromatic systems where the aromatic group is thiophene.

### 2.3.1 Cycloalkanone spacer

The first class of spacers effectively used for our study is the cycloalkanone spacers. We used five cycloalkanones *viz.* cyclobutanone, cyclopentanone, cyclohexanone, 4-(*t*-butyl)cyclohexanone and cycloheptanone. We examined Claisen-Schmidt condensation reaction between thiophene-2-carboxaldehyde and 5-bromothiophene-2-carboxaldehyde with these cycloalkanones in the presence of KOH in methanol solvent. Reaction time varied with substrates. Structure of cycloalkanones and thiophene-2-carboxaldehydes employed and the bithiophene products are collected in Table 2.1.

Entry	Cycloalkanone	Aldehyde	Reaction time	Product
1.			6-8 h	
2.			10-12 h	
3.			10 h	

**Table 2.1: Structures of products synthesised from cycloalkanones**

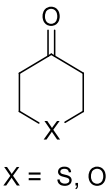
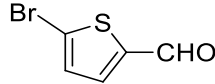
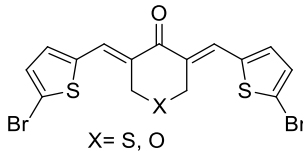
(*2E,7E*)-2,7-Bis(thiophen-2-ylmethylene)cycloheptanone (**8**) yielded beautiful yellow crystals which were subjected to Single Crystal X-ray diffraction analysis.<sup>11</sup> ORTEP diagram for **8** is given in Figure 2.1.



**Figure 2.1: ORTEP plot of compound 8**

### 2.3.2 Heterocyclic ketone spacers

The second type of spacer used is the heterocyclic alkanones. We selected tetrahydrothiopyranone and tetrahydropyranone for our study.

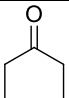
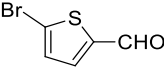
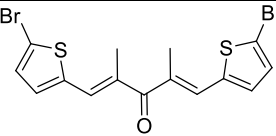
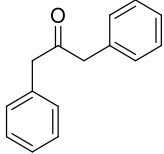
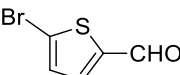
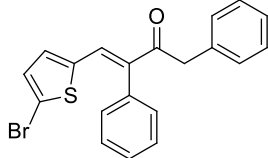
Entry	Cycloalkanone	Aldehyde	Reaction time	Product
1.	 X = S, O		10-12 h	 X = S, O

**Table 2.2: Structures of product synthesized from heterocyclic ketones**

We effectively synthesized the bromo derivative of bithiophene system using tetrahydrothiopyranone which is also a novel compound. Structure of heterocyclic ketones and thiophene-2-carboxaldehydes employed and the bithiophene products are collected in Table 2.2.

### 2.3.3 Open chain alkanones

The third type of compound selected was open chain ketones such as 3-pentanone and dibenzylacetone. The closed systems are highly rigid systems, so in order to increase the solubility of these compounds we opted for open chain alkanones. As expected, the reaction with 3-pentanone, in contrast to all the other reactions was a time consuming one. Structure of open chain alkanones and thiophene-2-carboxaldehydes employed and the products are collected in Table 2.3.

Entry	Cycloalkanone	Aldehyde	Reaction time	Product
1.			10 hrs	
2.			6-8 hrs	

**Table 2.3: Structures of products synthesised from open chain alkanones**

Bisthiophenes **13** and **14** gave diffraction quality yellow crystals. We carried our SCXRD analysis to confirm their structure.<sup>12</sup> ORTEP diagram of **13** (Figure 2.2) and **15** (Figure 2.3) are given above.



**Figure 2.2: ORTEP plot of compound 13**



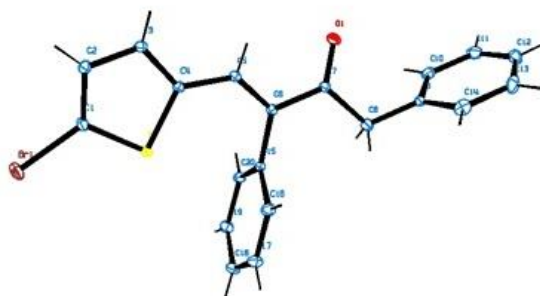


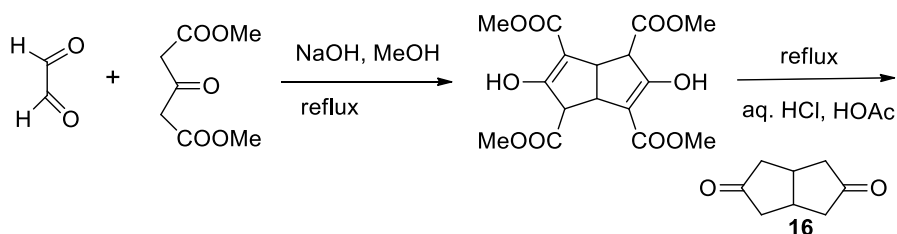
Figure 2.3: ORTEP plot of compound 15

### 2.3.4 Fused ring diones

After successful synthesis of several bithiophenes having different alkanone spacers, we extended bithiophene synthesis to other fused cyclic diketones such as tetrahydropentalene-2,5-(1*H*,3*H*)-dione . Claisen-Schmidt condensation on bicyclic diones is probably a novel route. We have successfully employed tetrahydropentalene dione for condensation which was synthesised in the lab using the Weiss-Cook procedure<sup>13</sup>. Strategy adopted by us is presented hereunder.

#### 2.3.4.1 Synthesis of tetrahydropentalene-2,5(1*H*,3*H*)-dione (16)

The compound was prepared using Weiss-Cook procedure from literature.



Scheme 2.2: Synthesis of tetrahydropentalene dione 16

### 2.3.4.2 Reaction between tetrahydropentalene-2,5(1*H*,3*H*)-dione and thiophene-2-carboxaldehyde

Tetrahydropentalene-2,5(1*H*,3*H*)-dione (**16**) has four active methylene centers for Claisen-Schmidt condensation. Generally, Claisen-Schmidt condensation yields product with *E*-geometry. Our own findings, as evidenced by the SCXRD data on **8**, **13**, and **15**, are also in agreement with this proposal. However, it is likely that steric constraints can alter the geometry of Claisen-Schmidt condensations. Consequently, seven geometrical isomers are expected in the reaction between **16** and suitable aldehydes. Structure of all the possible products is pictorially represented in Chart 2.1. Based on  $^1\text{H}$  and  $^{13}\text{C}$  NMR data's, it is possible to differentiate between these isomers.

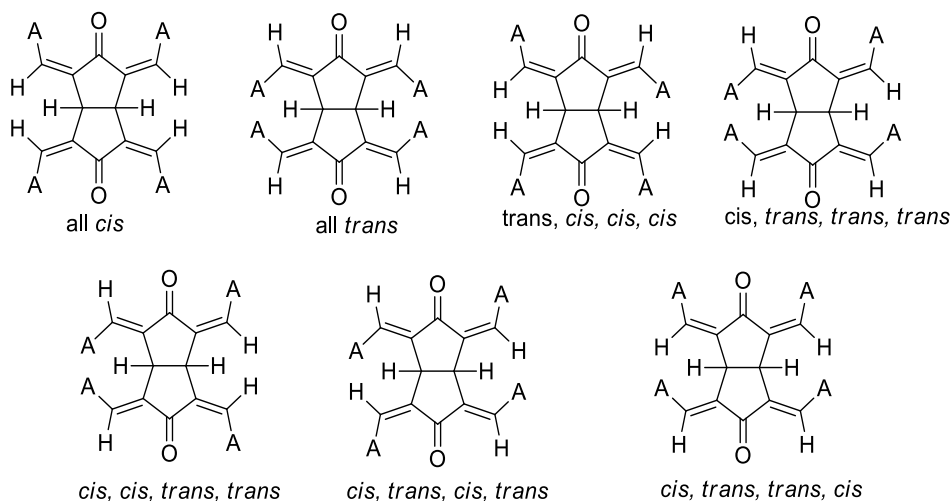
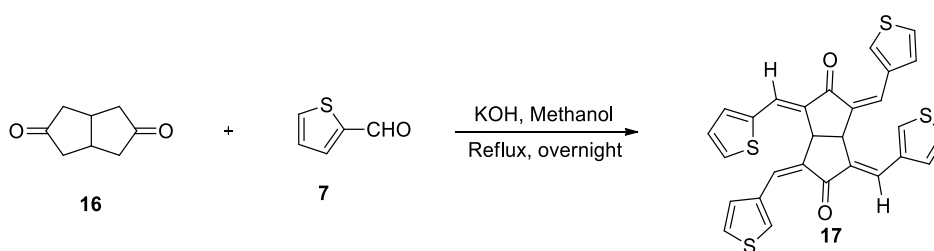


Chart 2.1 : Structures of possible products

### 2.3.4.3 Synthesis of (1*Z*,3*E*,4*Z*,6*E*)-1,3,4,6-tetrakis(thiophen-2-ylmethylenetetrahydropentalene-2,5(1*H*,3*H*)-dione (17)

Tetrahydropentalene dione (**16**) was subjected to condensation with thiophene-2-carboxaldehyde and the scheme is shown below.



**Scheme 2.3: Synthesis of 17 from tetrahydropentalene dione**

Here all the four  $\alpha$ -positions underwent condensation reaction with thiophene carboxaldehyde forming a tetrasubstituted compound. Structure of the product was identified as the *cis,trans,cis,trans*-isomer on the basis of spectral data. In the  $^1\text{H}$  NMR spectrum (Figure 2.4), the two vinylic protons appeared as two distinct singlets ( $\delta$  6.94 and 7.97 suggesting *cis* and *trans* geometry) whereas the two methine protons appeared as a singlet at  $\delta$  4.74. Based on this data, we conclude that the molecule possesses neither plane nor centre of symmetry. A  $C_2$  axis of symmetry is present that renders the two methine protons and the two carbonyl carbons chemical shift equivalent. NMR data is consistent with assignment of 1*Z*,3*E*,4*Z*,6*E*-configuration for **17**. Double bonds generated at 3- and 6-positions possess the expected *E*-geometry while the double bonds generated at 1- and 4-positions possess *Z*-geometry.

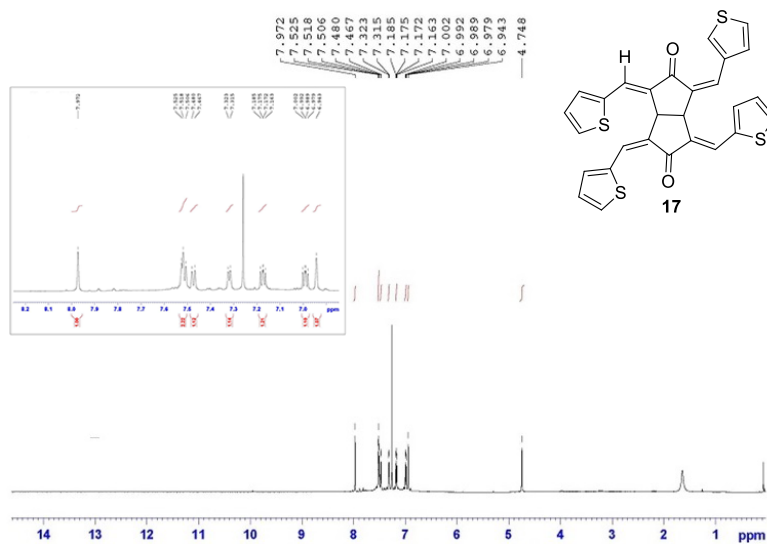


Figure 2.4:  $^1\text{H}$  NMR spectrum of compound 17

The structure was further confirmed from  $^{13}\text{C}$  NMR spectra given in figure 2.5 below.

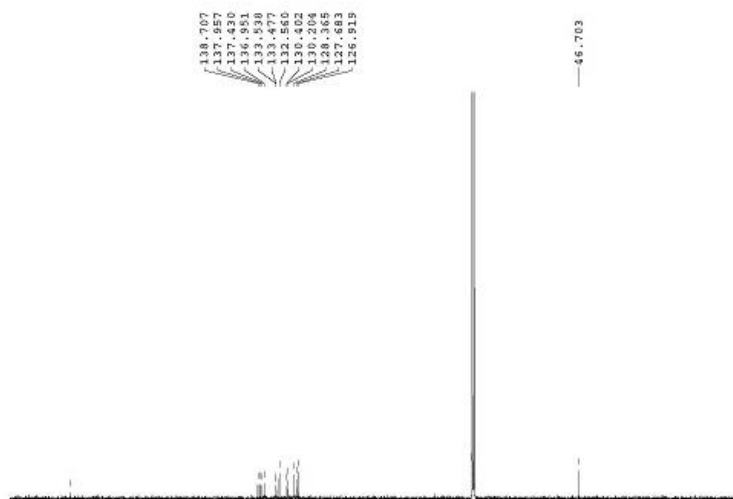
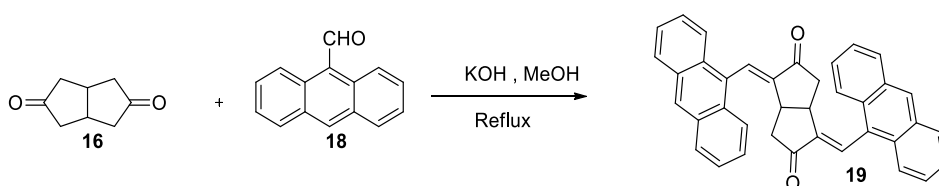


Figure 2.5:  $^{13}\text{C}$  NMR spectrum of compound 17

In order to account for the mechanism and regioselectivity of this reaction, we carried out the reaction using two bulky aldehydes viz, anthraldehyde and pyrene-2-carboxaldehyde. Bisanthracylidene cycloalkanones have been widely exploited due to their intramolecular energy transfer process. Bisanthracenes<sup>14</sup> are interesting compounds with varying photochemistry. Pyrene is one of the most widely used neutral fluorescent probes. They are highly conjugated molecules that are used to make dyes and dye precursors. Its derivatives are valuable molecular probes via fluorescence spectroscopy. Their fluorescence emission spectrum being very sensitive to solvent polarity, they are widely used as probe to determine solvent environments. In this context we have chosen anthracene and pyrene compounds owing to their bulky nature which enables us to study the regioselectivity of this reaction and hence propose a suitable mechanism for the formation of product.

#### **2.3.4.4 Claisen Schmidt condensation of tetrahydropentalene dione (16) with anthraldehyde**



**Scheme 2.4: Synthesis of 19 from tetrahydropentalene dione**

From the spectral data, we could clearly identify the formation of a bisanthracene product. Geometry of the double bond was assigned *E*-configuration based on literature precedence.<sup>15-20.</sup>

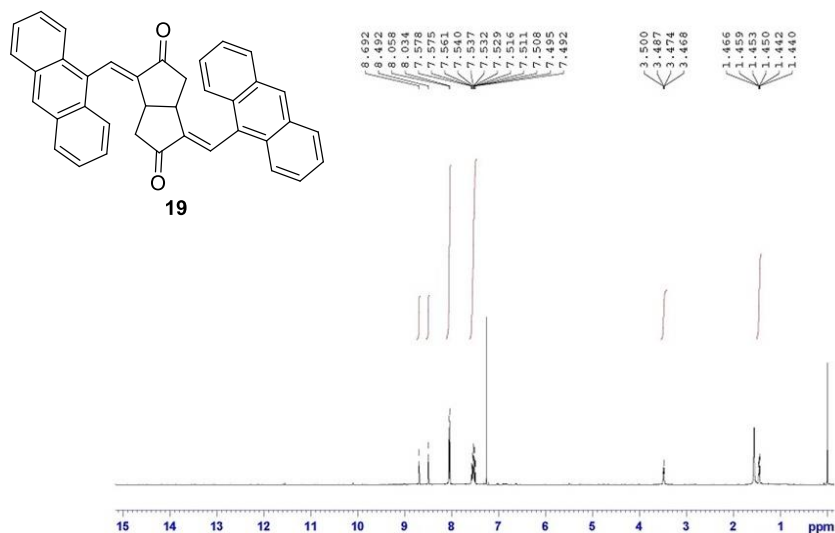
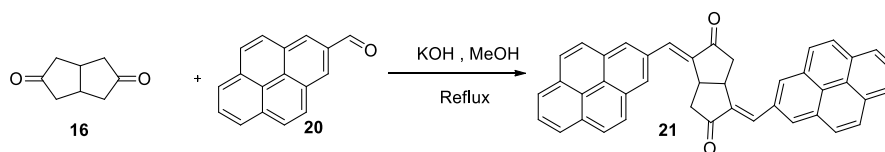


Figure 2.6: <sup>1</sup>H NMR spectrum of compound 19

### 2.3.4.5 Claisen-Schmidt condensation of tetrahydropentalene dione with Pyrene-2-carboxaldehyde



Scheme 2.5: Synthesis of 21 from tetrahydropentalene dione

The spectral data of the compound revealed the formation of a bispyrene product as in the case with anthracene. In both cases owing to steric effect of the bulky anthracene and pyrene groups, the reaction resulted in the formation of biscompounds.

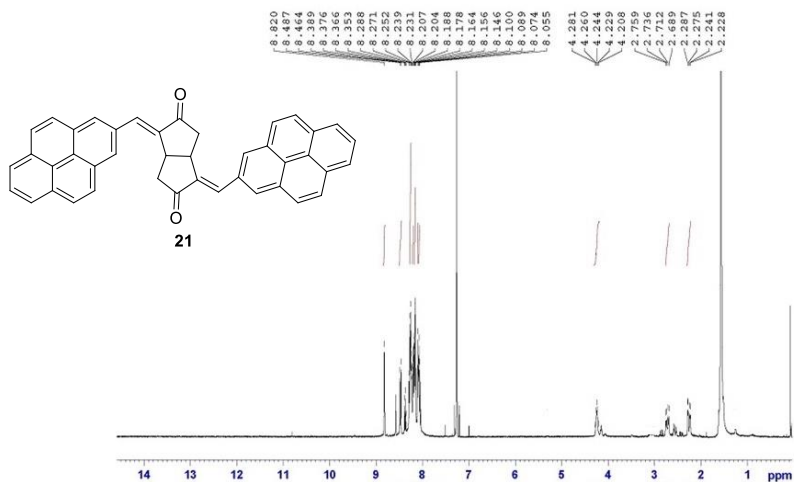
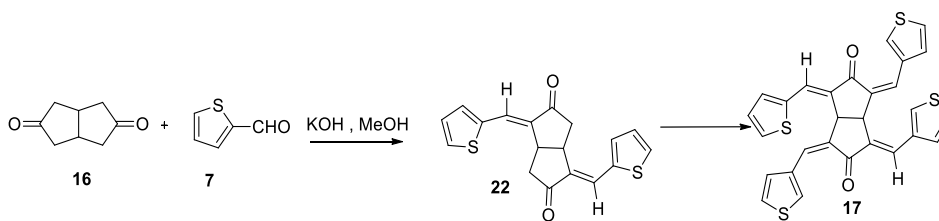


Figure 2.7:  $^1\text{H}$  NMR spectrum of compound 21

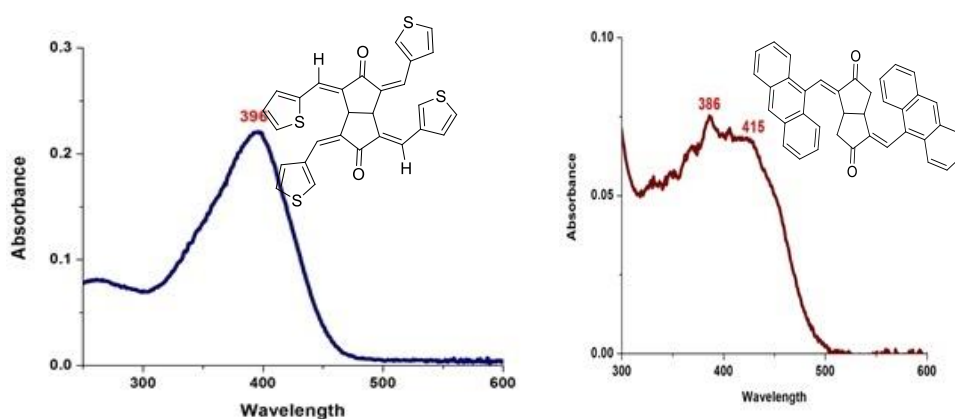
Thus, we propose the following mechanism involving 1:2 adduct to account for the unusual geometry exhibited by **17**. Initial Claisen-Schmidt condensation at 1 and 4 (or 3 and 6) position follows typical pattern leading to the corresponding *E*-isomers. With bulky aldehydes such anthraldehyde and pyrene carboxaldehyde, further condensation is restricted by steric factors.



Scheme 2.6: Mechanism of formation of compound 17

Based on the results obtained with bulky aldehydes, we propose **22** as a possible intermediate in the generation of **17**. Initial Claisen-Schmidt condensation leading to **22** proceeds with the expected geometry. However, stereochemical outcome of subsequent condensations are controlled by steric factors. Adverse steric crowding present in all trans isomer is avoided in the *cis,trans,cis,trans*-isomer **17**. In summary, the reaction occurs by trans addition of thiophene-2-carboxaldehyde to tetrahydropentalene-2,5(1*H*,3*H*)-dione followed by a *cis* addition owing to steric effects. In case of bulky aldehydes such as anthracene-9-carboxaldehyde and pyrene-2-carboxaldehyde, irrespective of geometry, steric crowding limits Claisen-Schmidt condensation to 1 and 4 positions of the dione **16**.

Absorption spectra of **17**, **19** and **21** are given in Figure 2.8. Compounds **17**, **19** and **21** gave  $\lambda_{\max}$  around 396, 415 and 440nm respectively.





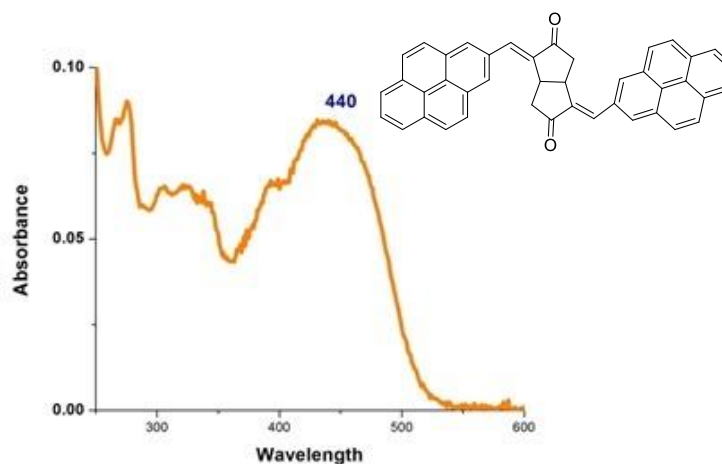


**Figure 2.8: UV-Visible spectra of 17, 19 and 21**

It is also evident that the absorption spectra of **19** and **21** are dominated by anthracene and pyrene absorption respectively. Upon excitation at 365 nm, **19** and **21** gave intense yellow emission in solution.

Pyrenes typically exhibit solvatochromism. Compound **21**, as expected, exhibited solvatochromism (Figure 2.9 and Table 2.4). In case of **21**,  $\lambda_{\text{max}}$  values were in the range of 440nm, 432nm, 428nm and 412nm in DCM,  $\text{CHCl}_3$ , Toluene and THF respectively. The lowest  $\lambda_{\text{max}}$  values were obtained with THF as solvent. The UV-Visible spectra in DCM and chloroform were found to be nearly identical with a small shift in  $\lambda_{\text{max}}$  values alone whereas toluene and THF spectra were different with respect to former ones with considerable shift in  $\lambda_{\text{max}}$  values.

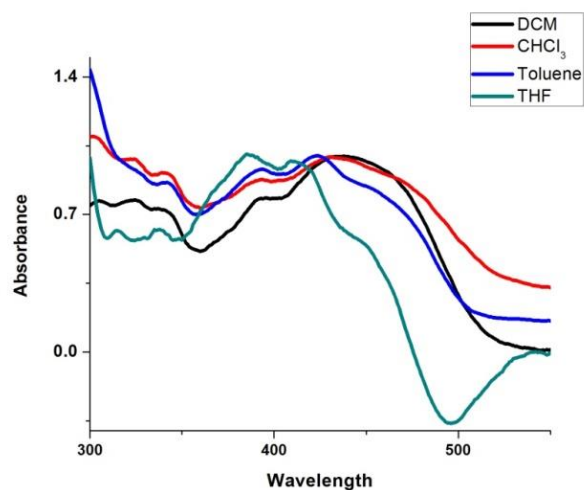


Figure 2.9: UV-Visible spectra of 21 in different solvents

Solvent	Methylene chloride	Chloroform	Toluene	Tetrahydrofuran
$\lambda_{\max}$ (nm)	440	432	428	412

Table 2.4:  $\lambda_{\max}$  values of 21 in different solvents

Compounds **17** and **19**, on the other hand, exhibited only negligible solvatochromism.

#### 2.3.4.6 Computational Studies

Since **17**, **19** and **21** exhibited strong absorption characteristics, the HOMO and LUMO of these compounds were determined using B3LYP/6-31G (d, p) theory.<sup>26</sup> The density functional theory using hybrid functional is an excellent route to determine the energy level diagram of compounds which in turn gives an idea regarding the band gap of the monomers. The HOMO and LUMO orbitals are

given below in Figure 2.10. The energy profile diagram is also shown below (Figure 2.11).

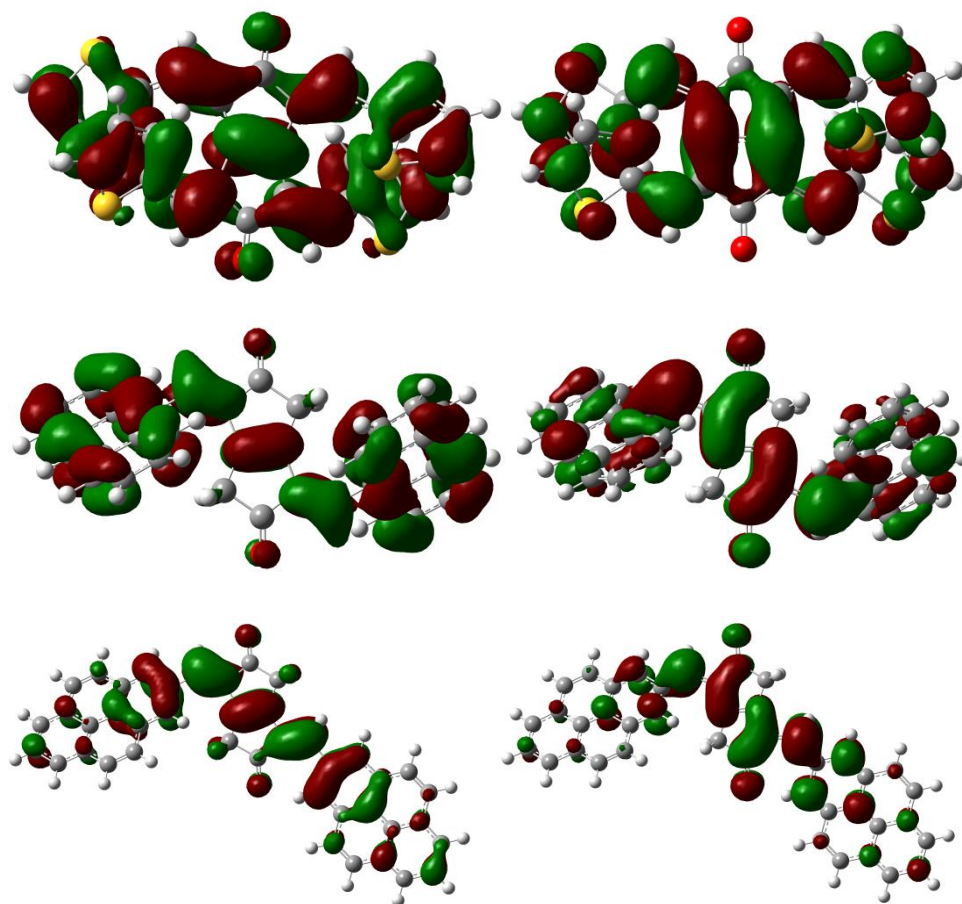


**Figure 2.10: HOMO and LUMO of compounds 17, 19 and 21**

Figure 2.11 clearly depicts that the band gap is largest for **21** and smallest for **17**.

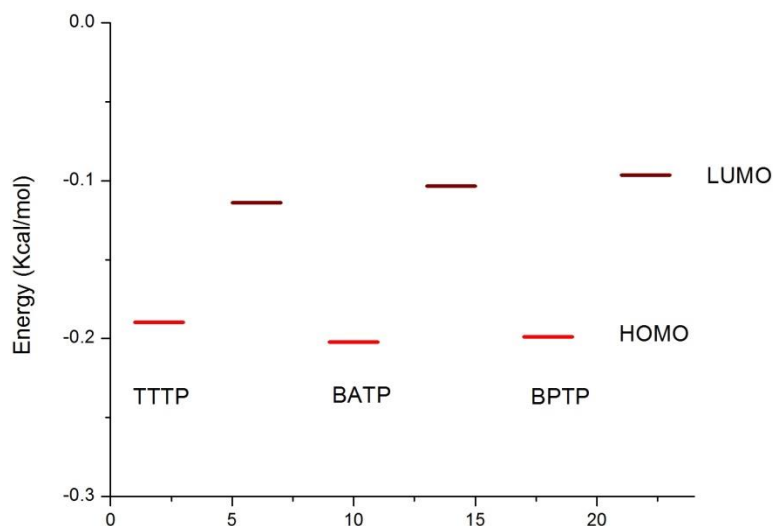


**Figure 2.11: Energy profile diagram of 17, 19 and 21**

The results are shown in the Table 2.5 below. Compounds **17**, **19** and **21** have band gaps of the order 2.07, 2.69 and 2.79 respectively.

	<b>HOMO</b>	<b>LUMO</b>	<b>Energy Gap</b>
<b>TTTP (17)</b>	-5.16	-3.09	2.07
<b>BATP (19)</b>	-5.51	-2.82	2.69
<b>BPTP (21)</b>	-5.41	-2.62	2.79

**Table 2.5: Band gaps of 17, 19 and 21**

## 2.4 CONCLUSIONS

We successfully synthesized 10 novel bithiophene systems with different spacers. There are only few reports on the synthesis of similar systems since majority of literature reports are confined with benzylidene

systems. We employed four classes of spacers *viz.* cycloalkanones, heterocyclic ketones, open chain ketones and fused ring diones, the latter two classes probably being novel systems. We accounted for the mechanism and regioselectivity of the reaction with fused ring systems by comparison with bulky ring substituents like anthracene and pyrene. From the geometry of the anthracene and pyrene product formed, it is evident that both the reactions favored the formation of *E* isomer in their disubstituted product. Further substitution is restricted in case of anthracene and pyrene due to its bulky nature whereas thiophene favours a tetrasubstituted product with (*E, E*) and (*Z, Z*) geometry. The structures of all the compounds were confirmed on the basis of spectral and analytical data. SCXRD analysis was also carried out on samples that gave diffraction quality crystals. We have also established solvatochromism of a compound synthesized by us.

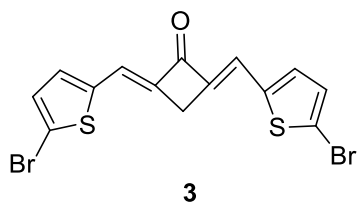
## **2.5 EXPERIMENTAL**

All reactions were carried out using oven dried glasswares. All experiments were done with distilled and dried solvents by using standard protocols. All starting materials were purchased from either *Sigma-Aldrich* or *Spectrochem Chemicals* and were used without further purification. Separation and purification of compounds were achieved by a combination of chromatographic and crystallization techniques. Infra-red spectra were recorded using *JASCO 4100* and *ABB Bomem (MB Series)* FT-IR spectrometers. <sup>1</sup>H and <sup>13</sup>C NMR spectra were recorded at 400 MHz on a *Bruker Avance III* FT-NMR spectrometer with

tetramethylsilane (TMS) as internal standard. Chemical shifts ( $\delta$ ) are reported in parts per million (ppm) downfield of TMS. Single crystal X-ray diffraction studies were performed on a Bruker Kappa Apex II instrument. UV-visible absorption spectra were recorded using Thermo Evolution Model 201 UV-Vis spectrometer in suitable solvents. Melting points are uncorrected and were determined on a Neolab melting point apparatus. Here, we have provided the spectral data of novel compounds only.

### 2.5.1 Synthesis of (2*E*,4*E*)-2-((5-bromothiophen-2-yl)methylene)-4-((5-bromothiophen-3-yl)methylene)cyclobutanone (3)

To a mixture of cyclobutanone (**1**, 0.2 g, 3.2 mmol) and 5-bromothiophene-2-carboxaldehyde (**2**, 1.2 g, 6.4 mmol) in methanol (25 mL) taken in 100 mL flask, potassium hydroxide pellets (0.4 g, 6.4 mmol) were added and the reaction mixture was stirred at room temperature overnight whilst a yellow-orange product separated out and the precipitate was collected by vacuum filtration. The crude product was washed several times with ice cold 1 mL portions of ethanol.

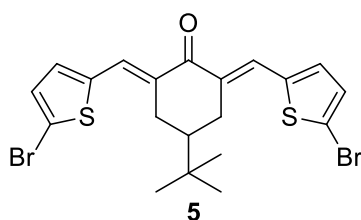


*Characterization data:* Yield: 87%, m.p: 130 °C; IR (KBr) 3442, 2923, 1732, 1620, 1413, 1324, 1099, 964, 793, 615, 504, 450  $\text{cm}^{-1}$ ;  $^1\text{H}$  NMR ( $\text{CDCl}_3$ )  $\delta$  7.53 (s, 1H), 7.51-7.44 (m, 1H), 7.15-7.13 (m, 1H), 3.64-3.63 (t, 1H);  $^{13}\text{C}$  NMR ( $\text{CDCl}_3$ )  $\delta$  187.0, 145.2, 142.9, 136.4, 131.4, 118.9, 20.9; MS  $m/z$  415 ( $M^+$ ). Anal. Calcd for

C<sub>14</sub>H<sub>8</sub>Br<sub>2</sub>S<sub>2</sub>O: C: 40.10, H: 1.73, S: 15.35. Found: C: 40.41, H: 1.94, S: 15.41.

### 2.5.2 Synthesis of (2*E*,6*E*)-2,6-bis((5-bromothiophen-2-yl)methylene)-4-(*tert*-butyl)cyclohexanone (5)

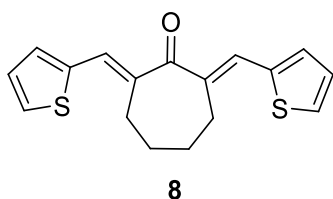
To a mixture of 4-(*tert*-butyl)cyclohexanone (**4**, 0.9 g, 2.2 mmol) and 5-bromothiophene-2-carboxaldehyde (**2**, 0.7 g, 4.4 mmol) in methanol (25 mL) taken in 100 mL flask, potassium hydroxide pellets (0.2 g, 4.4 mmol) were added and the reaction mixture was stirred at room temperature for 6 h whilst a pale yellow product separated out and the precipitate was collected by vacuum filtration. The crude product was washed several times with ice cold ethanol.



*Characterization data:* Yield: 85%; m.p: 152 °C; IR (KBr) 3431, 3067, 2957, 2861, 1596, 1493, 1443, 1369, 1221, 1109, 1044, 965, 890, 837, 793, 692, 568 cm<sup>-1</sup>; <sup>1</sup>H NMR (CDCl<sub>3</sub>) δ 7.75-7.74 (d, 2H), 7.04 (s, 4H), 3.04-2.99 (m, 2H), 2.28-2.20 (m, 2H), 1.60-1.52 (m, 2H), 1.01 (s, 9H). <sup>13</sup>C NMR (CDCl<sub>3</sub>) δ 189.0, 139.5, 132.9, 129.8, 127.6, 60.1, 33.0, 28.1, 21.7; MS *m/z* 499 (*M*<sup>+</sup>). Anal. Calcd for C<sub>20</sub>H<sub>20</sub>Br<sub>2</sub>S<sub>2</sub>O: C: 47.90, H: 3.95, S: 12.79. Found: C: 48.01, H: 4.03, S: 12.82.

### 2.5.3 Synthesis of (2*E*,7*E*)-2,7-bis(thiophen-2-ylmethylene)cycloheptanone (8)

To a mixture of cycloheptanone (6, 0.5 g, 4.4 mmol) and thiophene-2-carboxaldehyde (7, 1.0 g, 8.7 mmol) in methanol (25 mL) taken in 100 mL flask, potassium hydroxide pellets (0.5 g, 8.7 mmol) were added and the reaction mixture was stirred at room temperature overnight whilst a pale yellow product separated out and the precipitate was collected by vacuum filtration. The crude product was washed several times with ice cold ethanol. Recrystallization from xylene gave diffraction quality crystals.



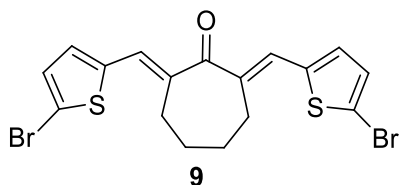
*Characterization data:* Yield: 98%; m.p: 144 °C; IR (KBr) 2906, 1598, 1401, 1297  $\text{cm}^{-1}$ ;  $^1\text{H}$  NMR ( $\text{CDCl}_3$ )  $\delta$  7.58 (d, 1H), 7.46 (d, 1H), 7.31(t, 1H), 7.10 (s, 1H), 2.80 (t, 2H), 1.95 (m, 2H);  $^{13}\text{C}$  NMR ( $\text{CDCl}_3$ )  $\delta$  187.3, 141.4, 137.8, 129.0, 128.3, 28.3, 27.1. MS  $m/z$  300 ( $M^+$ ). Anal. Calcd for  $\text{C}_{17}\text{H}_{16}\text{S}_2\text{O}$ : C: 67.37, H: 45.01, S: 21.05. Found: C: 67.96, H: 45.37, S: 21.35.

### 2.5.4 Synthesis of (2*E*, 7*E*)-2, 7-bis((5-bromothiophen-2yl)methylene) cycloheptanone (9)

To a mixture of cycloheptanone (6, 0.5 g, 4.4 mmol) and 5-bromothiophene-2-carboxaldehyde (2, 1.0 g, 8.8 mmol) in methanol (25 mL) taken in 100 mL flask, potassium hydroxide pellets (0.5 g , 8.8 mmol) were added and the reaction mixture was stirred at room temperature overnight whilst a pale yellow product separated out and the



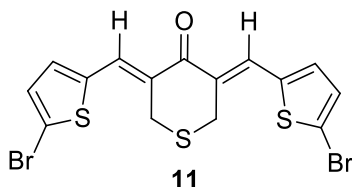
precipitate was collected by vacuum filtration. The crude product was washed several times with ice cold ethanol.



*Characterization data:* Yield 96%; m.p: 124 °C; IR (KBr) 3420, 3067, 2930, 2853, 1773, 1654, 1607, 1582, 1456, 1326, 1263, 968, 941, 877, 811 cm<sup>-1</sup>; <sup>1</sup>H NMR (CDCl<sub>3</sub>) δ 7.36 (s, 1H), 7.19 (s, 1H), 7.00-6.96 (m, 1H), 2.63 (t, 2H), 1.84 (m, 2H); <sup>13</sup>C NMR (CDCl<sub>3</sub>) δ 197.5, 140.5, 138.1, 132.4, 128.4, 116.4, 77.3, 77.0, 76.8, 28.2, 25.9. MS *m/z* 457(*M*<sup>+</sup>). Anal. Calcd. for C<sub>17</sub>H<sub>14</sub>Br<sub>2</sub>S<sub>2</sub>O C: 44.36, H: 2.97, S: 14.00. Found: C: 44.56, H: 3.08, S: 14.00.

### 2.5.5 Synthesis of (3Z,5Z)-3,5-bis((5-bromothiophen-2-yl)methylene)dihydro-2H-thiopyran-4(3H)-one (11)

To a mixture of tetrahydrothiopyranone (**10**, 0.46 g, 4.4 mmol) and 5-bromo thiophene-2-carboxaldehyde (**2**, 1.0 g, 8.8 mmol) in methanol (25 mL) taken in 100 mL flask, potassium hydroxide pellets (0.5 g, 8.8 mmol) were added and the reaction mixture was stirred at room temperature overnight whilst a yellow product separated out and the precipitate was collected by vacuum filtration. The crude product was washed several times with ice cold ethanol.

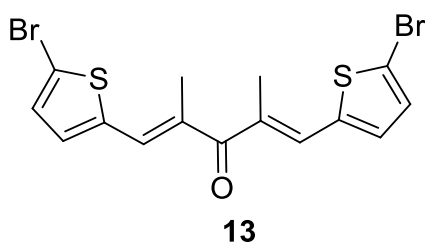


*Characterization data:* Yield: 60%; m.p: 158 °C; IR (KBr) 3825, 3708, 3448, 1651, 1586, 1560, 1502, 1416, 1312, 1256, 1225, 1182, 953, 862, 736 cm<sup>-1</sup>; <sup>1</sup>H NMR (CDCl<sub>3</sub>) δ 7.72 (s, 1H), 7.19-7.04 (d, 2H), 3.81 (s, 2H), 2.10 (s, 2H);

$^{13}\text{C}$  NMR ( $\text{CDCl}_3$ )  $\delta$  186.0, 139.9, 133.7, 130.8, 130.2, 129.0, 118.1, 77.3, 77.0, 76.8, 30.9, 29.7; MS  $m/z$  461 ( $M^+$ ).  
Anal. Calcd for  $\text{C}_{15}\text{H}_{10}\text{Br}_2\text{S}_3$ : C: 38.97, H: 2.15, S: 20.79. Found: C: 38.98, H: 2.18, S: 20.81.

### 2.5.6 Synthesis of (1*E*,4*E*)-1,5-bis(5-bromothiophen-2-yl)-2,4-dimethyl penta-1,4-dien-3-one (13)

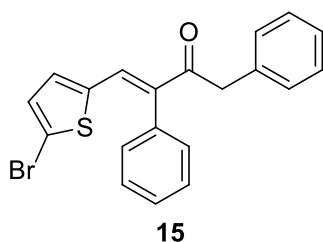
To a mixture of 3-pentanone (**12**, 0.50 g, 1.2 mmol) and 5-bromothiophene-2-carboxaldehyde (**2**, 2.2 g, 2.4 mmol) in methanol (25 mL), potassium hydroxide pellets (0.2 g, 2.4 mmol) was added and the reaction mixture was stirred at room temperature overnight whilst a yellow product separated out. The crude product was washed several times with ice cold ethanol. Recrystallization from chloroform gave good quality crystals.



Characterization data: Yield: 85%. m.p: 128°C; IR (KBr,  $\text{cm}^{-1}$ ) 1680, 3061;  $^1\text{H}$  NMR ( $\text{CDCl}_3$ )  $\delta$  7.18-7.17 (s, 1H), 7.08-7.07 (d, 1H), 6.97-6.96 (d, 1H), 2.20 (s, 3H);  $^{13}\text{C}$  NMR ( $\text{CDCl}_3$ )  $\delta$  200.0, 140.8, 133.8, 131.4, 131.3, 130.2, 116.7, 15.5. MS:  $m/z$  431 ( $M^+$ ); Anal. Calcd. for  $\text{C}_{15}\text{H}_{12}\text{Br}_2\text{S}_2\text{O}$ : C: 41.69, H: 2.80, Br: 36.98, S: 14.84; found: C: 41.59, H: 2.78, Br: 36.90, S: 14.74.

### 2.5.7 Synthesis of (*E*)-4-(5-bromothiophen-2-yl)-1,3-diphenylbut-3-en-2-one (**15**)

To a mixture of dibenzylketone (**14**, 1.0 g, 4.7 mmol) and 5-bromothiophene-2-carboxaldehyde (**2**, 1.8 g, 9.5 mmol) in methanol (25 mL), potassium hydroxide pellets (0.6 g, 9.5 mmol) was added and the reaction mixture was stirred at room temperature overnight whilst a yellow product separated out, and washed with cold ethanol and recrystallized from  $\text{CHCl}_3$ .

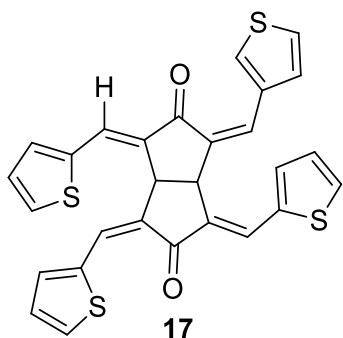


*Characterization data:* Yield: 90%; m.p: 110 °C; IR (KBr):- 3080, 1627  $\text{cm}^{-1}$ ;  $^1\text{H}$  NMR ( $\text{CDCl}_3$ )  $\delta$  7.80 (s, 1H), 7.51-7.48 (m, 1H), 7.47 (m, 1H), 7.23-7.20 (m, 2H), 7.15-7.14 (m, 2H), 7.13-7.12 (m, 2H), 7.04-7.02 (m, 2H), 6.97-6.96 (d, 1H), 6.90-6.89 (d, 1H), 3.78 (s, 2H);  $^{13}\text{C}$  NMR ( $\text{CDCl}_3$ )  $\delta$  197.3, 140.5, 137.2, 135.6, 134.4, 134.3, 132.0, 129.9, 129.7, 129.6, 129.4, 129.2, 129.0, 128.4, 126.7, 119.3, 46.8. MS:  $m/z$  383 ( $M^+$ ); Anal. Calcd for  $\text{C}_{20}\text{H}_{15}\text{BrOS}$ : C: 62.67, H: 3.94, Br: 20.85, S: 8.37; found: C: 62.57, H: 3.92, Br: 20.77, S: 8.27.

### 2.5.8 Synthesis of (1*Z*,3*E*,4*Z*,6*E*)-1,3,4-tris(thiophen-2-ylmethylene)-6-(thiophen-3-ylmethylene) tetrahydropentalene-2,5(1*H*,3*H*)-dione (**17**)

To a mixture of tetrahydropentalene dione (**16**, 0.1 g, 1 mmol) and thiophene-2-carboxaldehyde (**7**, 0.23 g, 2 mmol) in methanol (25 mL) taken in 100 mL flask, potassium hydroxide pellets (0.3 g, 2 mmol) were

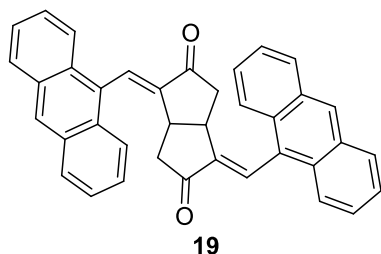
added and the reaction mixture was stirred at room temperature overnight minutes whilst a greenish brown precipitate separated out. The crude product (1*Z*,3*E*,4*Z*,6*E*)-1,3,4-tris(thiophen-2-ylmethylene)-6-(thiophen-3-ylmethylene) tetra hydro pentalene-2,5(1*H*,3*H*)-dione was washed several times with ice cold ethanol.



*Characterization data:* Yield: 72%; m.p: 208 °C (dc); IR (KBr) 3056, 3009, 2948, 2841, 1656, 1600, 1576, 1511, 1263 cm<sup>-1</sup>; <sup>1</sup>H NMR (CDCl<sub>3</sub>):- 7.97 (s, 2H), 7.52-7.31 (m, 4H), 7.48-7.46 (d, 2H), 7.32-7.31 (d, 2H), 6.94 (s, 2H), 7.18-7.16 (dd, 2H, 5.2 and 4Hz), 7.00-6.97 (dd, 2H, 5.2 and 4Hz), 4.74 (s, 2H). <sup>13</sup>C NMR (CDCl<sub>3</sub>) δ 192.5, 138.7, 137.9, 137.4, 136.9, 133.5, 133.4, 132.5, 130.4, 130.2, 128.3, 127.6, 126.9, 46.7. MS: *m/z* 514 (*M*<sup>+</sup>). Anal. Calcd. for C<sub>28</sub>H<sub>18</sub>O<sub>2</sub>S<sub>4</sub>: C: 65.24, H: 3.41, S: 24.76. Found: C: 65.27, H: 3.46, S: 24.86.

### 2.5.9 Claisen-Schmidt condensation of tetrahydropentalene dione with Anthraldehyde (19).

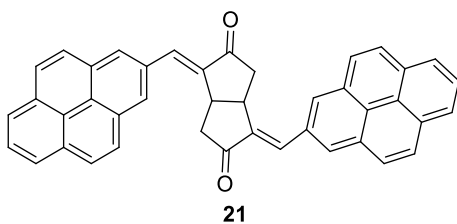
To a mixture of tetrahydropentalene dione (**16**, 0.1 g, 1 mmol) and anthraldehyde (**18**, 0.60 g, 4 mmol) in methanol (25 mL) taken in 100 mL flask, potassium hydroxide pellets (0.17 g, 4 mmol) were added and the reaction mixture was stirred at room temperature overnight minutes whilst an orange-red precipitate separated out. The crude product was washed several times with ice cold ethanol.



*Characterization data:* Yield: 62%, m.p: 160 °C (d.c); IR (KBr): 3047, 2853, 1632, 1406, 1276, 886  $\text{cm}^{-1}$ ;  $^1\text{H}$  NMR ( $\text{CDCl}_3$ ): 1.46-1.44 (m, 2H), 3.50-3.46 (m, 1H), 7.57-7.49 (m, 4H), 8.05-8.03 (m, 4H), 8.49 (s, 1H), 8.69 (s, 1H);  $^{13}\text{C}$  NMR ( $\text{CDCl}_3$ ): 196.1, 146.1, 135.1, 131.2, 129.1, 128.8, 128.4, 126.6, 125.5, 125.3, 41.6, 38.5. MS:  $m/z$  514 ( $\text{M}^+$ ). Anal. Calcd. for  $\text{C}_{38}\text{H}_{26}\text{O}_2$ : C: 88.60., H: 5.03. Found C: 88.69, H: 5.09.

### 2.5.10 Claisen-Schmidt condensation of tetrahydropentalene dione with Pyrene-2-carboxaldehyde (21).

To a mixture of tetrahydropentalene dione (**16**, 0.1 g, 1 mmol) and pyrene-2-carboxaldehyde (**20**, 0.60g , 4 mmol) in methanol (25 mL) taken in 100 mL flask, potassium hydroxide pellets (0.17g, 4 mmol) were added and the reaction mixture was stirred at room temperature overnight whilst red precipitate separated out. The crude product was washed several times with ice cold ethanol.



*Characterization data:* Yield: 50%; m.p: 180 °C; IR (KBr): 3042, 1658, 1592, 645  $\text{cm}^{-1}$ ;  $^1\text{H}$  NMR ( $\text{CDCl}_3$ ):  $\delta$  8.75 (s, 2H), 8.41-8.39 (m, 2H), 8.21-8.16 (m, 2H), 8.13-8.10 (m, 3H), 8.09-8.07 (m, 4H), 8.03-8.01 (m, 4H), 8.00-7.98 (m, 4H), 4.18-4.15 (m, 2H), 2.69-2.61 (m, 2H), 2.21-2.15 (m, 2H);  $^{13}\text{C}$  NMR ( $\text{CDCl}_3$ ): 202.0, 145.3, 132.7, 130.9, 129.4, 127.3, 126.6, 125.1, 123.5, 121.8, 40.3, 34.3; MS:  $m/z$  562 ( $\text{M}^+$ ). Anal. Calcd. for  $\text{C}_{42}\text{H}_{26}\text{O}_2$ : C: 89.60, H: 5.49. Found C: 89.66, H: 5.66.

## 2.6 REFERENCES

- 1) Zhao, C. Y.; Liu, J. Y.; Wang, Y.; Zhao, X. J.; Yuan, B.; Yue, M. M. *Synth. Commun.* **2014**, *44*, 827.
- 2) Sun, Y. F.; Wang, Z. Y.; Zhao, X.; Zheng, Z. B.; Li, J. K.; Wu, R. T.; Cui, Y. P. *Dyes and Pigments* **2010**, *86*, 96.
- 3) Alkskas, A. I.; Alhubgeb, A. M.; Azamc, F. *Chinese J. Polym. Sci.* **2013**, *31*, 471.
- 4) Rahman, A.; Ahmed, M.; Ali, H. M. *Designed Monomers and Polymers.* **2013**, *16(4)*, 377.
- 5) Abaee, S. M.; Mojtahedi, M. M.; Zahdi, M. M.; Mesbah, A.W.; Ghandchi, N. M. *Phosphorus, Sulfur and Silicon.* **2007**, *182*, 2891.
- 6) Burroughes, J. H.; Bradley, D. D. C.; Brown, A. R.; Marks, R. N.; Mackay, K.; Friend, R.H.; Burns, P. L.; Holmes, A. B. *Nature* **1990**, *347*, 539.
- 7) Balaji, M.; Bharad, J.; Ubale, M.; Sonwane, B.; Shingare, M. *Elixir Appl. Chem.* **2012**, *42*, 6320.
- 8) Mojtahedi, M. M.; Abaee, M. S.; Samianifard, M.; Shamloo, A. *Scientia Iranica C.* **2014**, *21(3)*, 719.
- 9) Claisen, L.; Claparede, A. *Ber.* **1881**, *14*, 2460.
- 10) Schmidt, J. G. *Ber.* **1881**, *14*, 1459.
- 11) Nithya, C.; Sithambaresan, M.; Prathapan, S.; Prathapachandra Kurup, M. R. *Acta Cryst.* **2014**, *E70*, o722.
- 12) Nithya, C.; Sithambaresan, M.; Prathapachandra Kurup, M. R. *Acta Cryst.* **2016**, *E72*, 199.
- 13) Bertz, S.H.; Cook, J. M.; Gawish, A.; Weiss, U. *Org. Synth.* **1990**, *7*, 50.
- 14) Becker, H. D.; Anderson, K. *J. Org. Chem.* **1983**, *48*, 4542.
- 15) Gisha, G. Ph.D. Thesis, CUSAT, 2010.

- 16) Bayomi, S. M.; Hassan, M.; Kashef, A. E.; Ashmawy, M. B.; Nasr, M. N. A.; Sherbeny, M.A.; Radria, F. A. *Med. Chem. Res.* **2012**, 1147.
- 17) Wayne, W.; Adkins, H. *J. Am. Chem. Soc.* **1940**, 62, 3401.
- 18) Marvel, C. C.; King, W. B. *Org. Syn.* **1944**, 1, 252.
- 19) Stiles, M.; Wolf, D.; Hudson, G. V. *J. Am. Chem. Soc.* **1959**, 81, 628.
- 20) Hu, Z. P.; Lou, C. L.; Wang, J.; Chen, C. X.; Yan, M. *J. Org. Chem.* **2011**, 76, 3797.
- 21) Saeed, A. M.; Kahedi, M.; Mohammed, M.; Soudabeh, F.; Nafisih, G.; Mehdi, F.; Behnam, C. *J. Braz. Chem. Soc.* **2009**, 20, 1895.
- 22) Abaee, S. M.; Mojtahedi, M. M.; Zahdi. *Synlett* **2005**, 17, 2317.
- 23) Abdolkarim, Z.; Maria, A.; Alireza, H.; Zarc, M.; Riza, A.; Vahid, K. *C. R. Chim.* **2013**, 16(4), 380.
- 24) Vatsadze, S. Z.; Manaenkova, M. A.; Sviridenkova, N. V.; Zyk, N. V.; Krut'ko, D. P.; Churakov, A. V.; Antipin, M. Yu.; Howard, J. A. K.; Lang, H. *Russ. Chem. Bull.* **2006**, 55(7), 1184.
- 25) Fatmah, A. O.; Hassan, A. M.; Ghahda, H.; Messery, E.; Shahenda, M.; Hussein, E. L. *Eur. J. Med. Chem.* **2012**, 47, 65.
- 26) Kulik, H.J.; Cococcioni, M.; Scherlis, D. A.; Marzari, N. *Phys Rev Lett.* **2006**, 97, 103001.





## CHAPTER 3

### *Synthesis, third order non-linear optical properties and Schottky junction characterisation of few yellow light emitting bis(thiophen-2-ylmethylene)cycloalkane oligomers*

---

#### 3.1 Abstract

*This chapter describes the synthesis of two novel yellow-orange light emitting oligomers of bis(thiophen-2-ylmethylene)cyclohexanone using direct arylation method which is probably a new concept of polymerization of bithiophene systems. The structures of oligomers were confirmed on the basis of <sup>1</sup>H NMR spectral data and these oligomers were examined by FTIR, UV-Vis spectroscopy, Powder XRD, SEM, TGA and DSC analysis. The compounds showed a semi-crystalline nature and good thermal stability suitable for device applications. Third order non-linear optical studies were performed using Z-scan technique which proved the applicability of these materials as optical limiters as well as optical switches. Current-voltage characteristics clearly confirm the Schottky junction like behavior making these materials suitable for fabrication of PLEDs.*

---

#### 3.2 INTRODUCTION

Direct arylation<sup>1-4</sup> has emerged as a new methodology which can be considered as one of the most versatile and efficient carbon-carbon bond forming processes in organic chemistry. Direct arylation involves catalytic dehydrohalogenative cross-coupling reactions of arenes or heteroarene compounds. For decades, C-H bonds<sup>5-8</sup> were considered to

be inert and the discovery of carrying out reactions by activating these C-H bonds with suitable metal catalyst unfolded the path to various mesmerizing chemical transformations which in turn also led to the formation of new C-C bonds. This is extremely advantageous strategy due to decreased number of steps involved and reduced wastage from organometallic reagents.

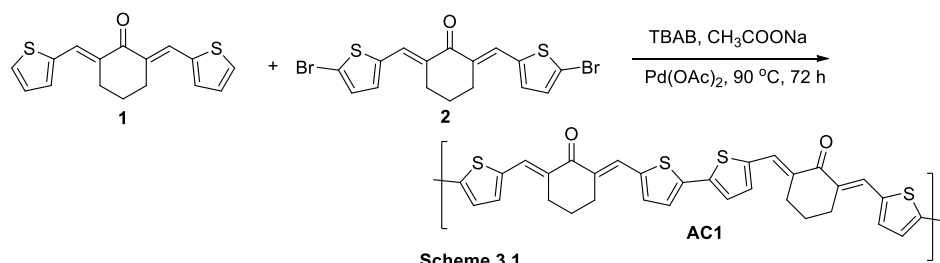
Fujinami<sup>4</sup> and coworkers successfully employed direct arylation for the synthesis of thiophene and bithiophene based alternating copolymers. The major advantage of direct arylation method compared with other coupling reactions like Stille reaction is the non-toxicity associated with the reagents used. Thiophenes being highly electron rich in nature, thiophene based oligomers and polymers<sup>9-14</sup> received much attention due to their extensive delocalization which makes them suitable for application in optoelectronic devices. The  $\pi$  conjugated structures of these materials also makes them suitable in non-linear optical studies.<sup>15-22</sup> Several studies<sup>23</sup> on the nonlinear optical properties of oligomers, polymers and dendrimers have been carried out but few or no studies have been performed on oligomers from bis(thiophen-2-ylmethylene)cycloalkanones. Our findings on non-linear optical properties of a few novel bis(thiophen-2-ylmethylene)cycloalkanone based oligomers is presented in this chapter. These materials had intense orange-yellow emission and good optical limiting behavior. In addition the materials exhibited a slight flipping between saturable absorption and reverse saturable absorption making them suitable for optical switches<sup>24</sup>

as well. The current-voltage characteristics with Ag/oligomer/Au configuration showed a junction like behavior with steep increase in current which is characteristic for fabrication of PLED's. We have also used computational studies to calculate the energy levels and DOS spectrum of the synthesized materials which in turn gives information regarding the HOMO and LUMO necessary to calculate the band gap.

### **3.3 RESULTS AND DISCUSSION**

Using direct arylation technique, we successfully synthesized two oligomers: 1) a bis(thiophen-2-ylmethylene)cyclohexanone oligomer and 2) a copolymer of bis(thiophen-2-ylmethylene)cyclohexanone and bis(pyrene-2-ylmethylene)cyclohexanone. Generally for such type of polyketones reported in literature typical Friedel-Crafts polymerization technique has been adopted. In the present investigation, we employed direct arylation as a new method for synthesis. Though the materials formed are oligomers having limited number of thiophene units in the backbone, they possess interesting properties. Both the monomers were synthesized using Claisen-Schmidt condensation reaction as described in section 2.4.1 in Chapter 2 of this thesis.

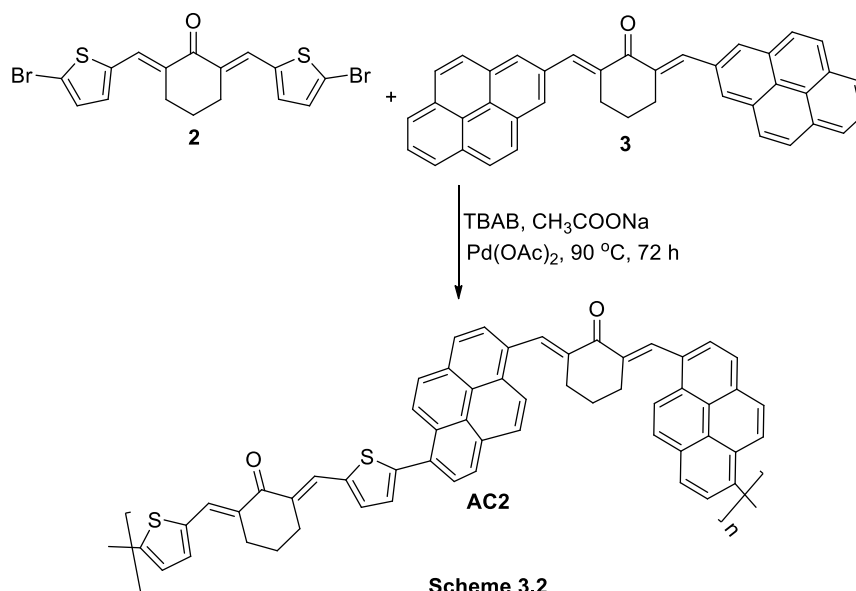
Direct arylation reaction between bis(thiophen-2-ylmethylene)cyclohexanones **1** and **2** gave (2*E*,2'*E*,6*E*,6'*E*)-6,6'-([2,2'-bithiophene]-5,5'-diylbis(methanylylidene))bis(2-((5-methylthiophen-2yl)methylene)cyclohexanone) oligomer **AC1** in moderate yields (Scheme 3.1).



Synthesis of oligomer AC1

In continuation, we performed direct arylation reaction between bis(thiophen-2-ylmethylene)cyclohexanone (**2**) and bis(pyrene-2-ylmethylene)cyclohexanone (**3**) to assemble (2*E*,6*E*)-2-((4-methylpyren-2-yl)methylene)-6-((4-(5-((*E*)-((*E*)-3-((5-methylthiophen-2-yl)methylene)-2-oxocyclohexylidene)methyl)thiophen-2-yl)pyren-2-yl)methylene)cyclohexanone to generate oligomer **AC2** incorporating regularly spaced thiophene and pyrene residues in low yields (Scheme 3.2).

Oligomers **AC1** and **AC2** were purified by sequential Soxhlet extraction using methanol, hexane and chloroform as solvents. Methanol extraction is performed to remove the catalyst and any excess reagent present. Subsequent extraction with hexane removes low molecular weight impurities. Final extraction with chloroform separates insoluble fractions with comparatively high molecular weight. We collected the chloroform extract for further investigations. The oligomer was separated by pouring the chloroform extract into ice-cold methanol. The orange-red material obtained was soluble in common solvents such as methylene chloride,  $\text{CHCl}_3$ , THF and toluene.



The molecular weights of the compounds were analyzed by Gel Permeation Chromatographic (GPC) analysis. THF was used as solvent for both the materials. The weight average molecular weight ( $M_w$ ) and number average molecular weight ( $M_n$ ) of **AC1** are 1919 g/mol and 1794 g/mol respectively and that of **AC2** are 2178 g/mol and 1614 g/mol respectively. Polydispersity indices (PDIs) of the oligomer **AC1** and **AC2** were 1.07 and 1.35 respectively. PDI value suggests that the repeating units are arranged in uniform fashion for both cases. The PDI value of **AC2** is higher compared with that for **AC1** presumably due the rigidity and bulkiness of pyrene units present.

### 3.3.1 <sup>1</sup>H NMR spectra

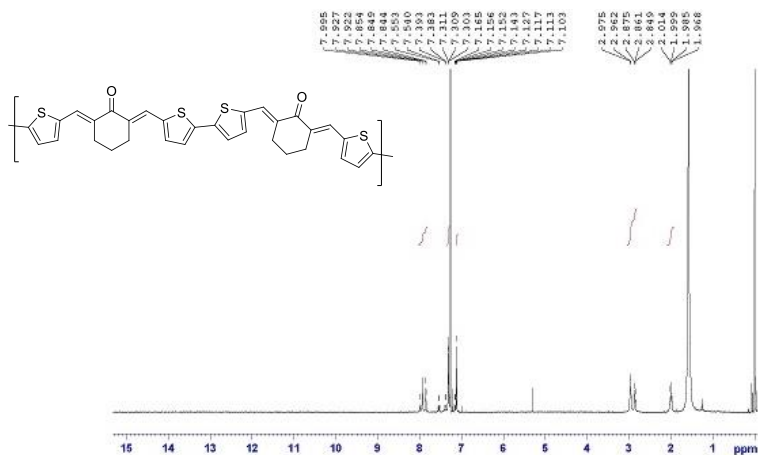


Figure 3.1: <sup>1</sup>H NMR spectrum of AC1

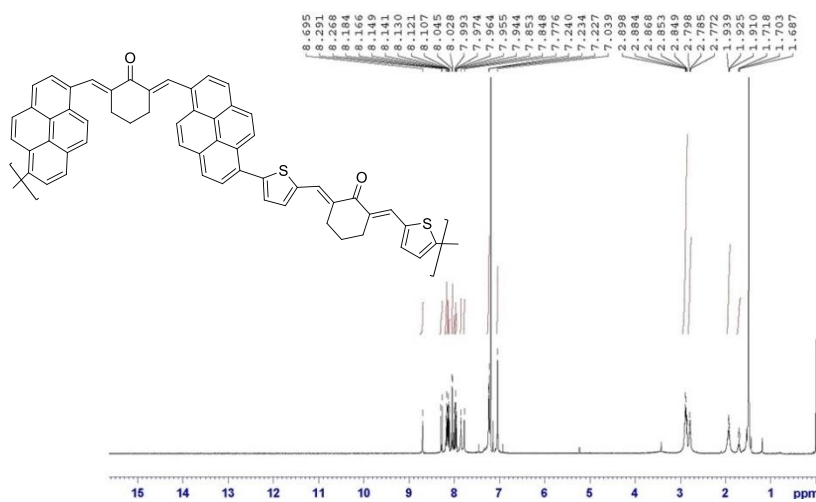


Figure 3.2: <sup>1</sup>H NMR spectrum of AC2

Structures of the oligomers were confirmed by <sup>1</sup>H NMR spectra. <sup>1</sup>H NMR spectra of AC1 and AC2 are shown in the Figures 3.1 and 3.2. <sup>1</sup>H NMR spectrum of AC1 clearly indicates high symmetry of the

synthesized oligomer. The vinylic proton peak appears around  $\delta$  7.93 as a singlet. The aliphatic protons appear as multiplets around  $\delta$  2.97-2.84 and  $\delta$  2.01-1.96 where the first one is a four proton multiplet and the second one is a two proton multiplet which corresponds to a single cyclohexanone unit due to the symmetry properties of the molecule.

Oligomer **AC2** lacks the symmetry associated with **AC1** and this is reflected in its  $^1\text{H}$  NMR spectrum. Both vinylic and methylene protons of the cyclohexanone ring residue appear as multiple peaks. The chemical shift distinct vinylic protons here, for example, appear around  $\delta$  8.69 and  $\delta$  7.03 as singlets.

### **3.3.2 FTIR Spectra**

In the IR spectra, peaks around  $1643\text{ cm}^{-1}$  and  $1648\text{ cm}^{-1}$  for **AC1** and **AC2** indicates C=O stretching of cycloalkanones and the characteristic C=C- IR band for **AC1** and **AC2** appears at  $1598\text{ cm}^{-1}$  and  $1586\text{ cm}^{-1}$  respectively.  $\alpha,\beta$ -unsaturated ketones usually gives such low intensity sharp peaks characteristic of C=O group. The aromatic -C-H bonds shows in plane and out of plane bending vibrations in the region of  $800\text{-}1150\text{ cm}^{-1}$  for **AC1** and **AC2**. From IR spectra it is clear that the carbonyl groups remained intact during polymerization process.

The IR spectrum of **AC1** and **AC2** is shown below.

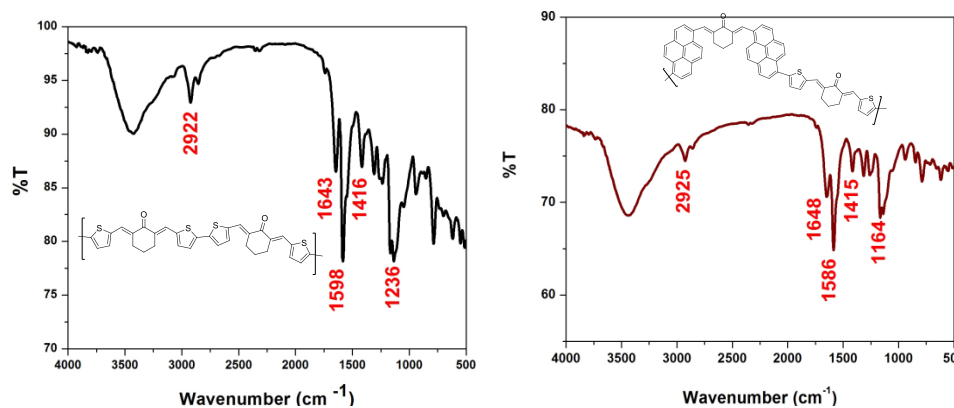
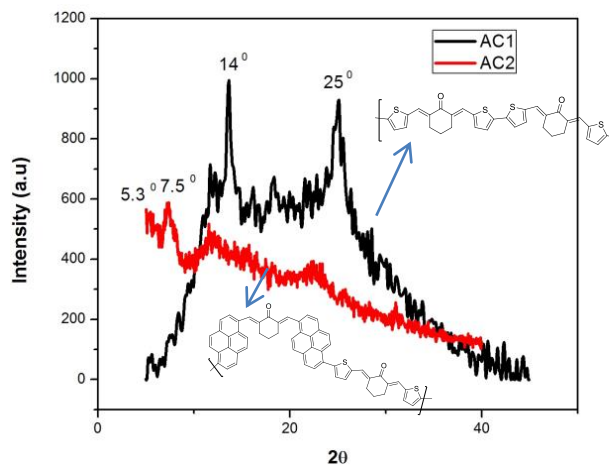


Figure 3.3: FTIR spectra of AC1 and AC2

### 3.3.3 Powder X-ray diffraction study

Powder X-ray diffraction (XRD) was used to investigate the crystalline nature and molecular organization of the oligomers. The XRD patterns of obtained materials **AC1** and **AC2** are shown in **Figure 3.4**. From the powder XRD spectra, sharp diffraction peaks for **AC1** make it evident that they have a highly crystalline nature which in turn reveals the ordered arrangement of the molecular chains. The material **AC1** shows two sharp peaks at  $2\theta$  values  $14^\circ$  and  $25^\circ$ . For **AC2**, the peaks at  $2\theta$  values  $5.3^\circ$  and  $7.5^\circ$  is sharp whereas the rest of the peaks are seen to be broad. The presence of sharp peak can be ascribed to the presence of ordered arrangements of chains in the oligomers which in turn contribute towards crystallinity of the material, whereas the broad peak typically arises from diffraction from the amorphous halo region of oligomers.





**Figure 3.4: Powder X ray spectra of AC1 and AC2**

From the figure, it can be clearly seen that **AC1** has more crystalline nature than **AC2** which can be explained due to the high symmetrical structure of **AC1**. The lower packing of unsymmetrical repeating units in **AC2** gives an amorphous character to the substance. Moreover, presence of bulky rings in the chain backbone of **AC2** can be considered the main reason for its amorphous nature. However, it also has a slight crystalline nature owing to the presence of carbonyl polar group and C=C bonds which brings about a well-defined order in the chain. Thus it can be concluded that the new materials synthesized show a semi-crystalline nature.

### 3.3.4 UV-Visible and Photoluminescence Spectra

UV-Vis absorption spectra and PL spectra provide information on the electronic structures of the synthesized compounds. The compounds **AC1**

and **AC2** gave characteristic absorption peaks at 485 and 465 nm respectively (Figure 3.5). This absorption peak can be attributed to  $\pi-\pi^*$  transition. The major emission peak of these compounds appears at 563 and 557 nm respectively, which are in the UV-Visible region.

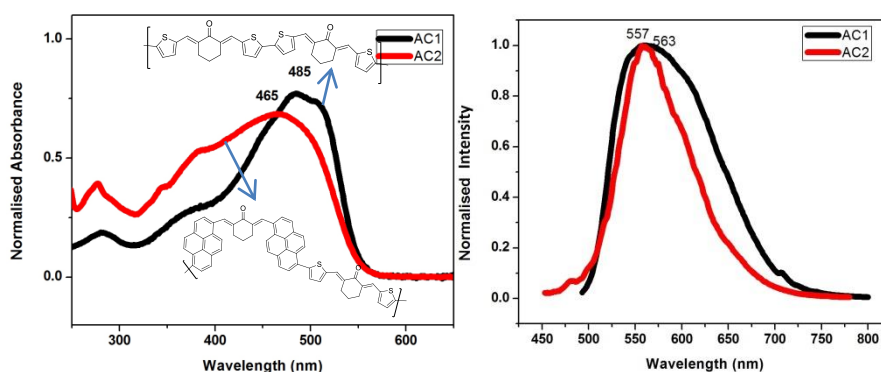


**Figure: 3.5: UV-Visible and PL spectra of AC1 and AC2**

Oligomers **AC1** and **AC2** exhibited intense luminescence.



**Figure 3.6: Luminescence of AC1 and AC2**

Oligomer **AC1** emits in the yellow-orange region whereas **AC2** emit light in yellow region of the electromagnetic spectra.

### 3.3.5 Scanning Electron Microscopy

Scanning Electron Microscopy gives the surface resolution of the samples in micrometer realm. It gives an idea regarding morphological arrangement and shape of the particle. The figure 3.7 shows the SEM images of the powdered samples. **AC1** has a flake like morphology with no particular shape and **AC2** has globular structures in between irregularly shaped particles. In general, both the samples have a more or less irregular arrangement.

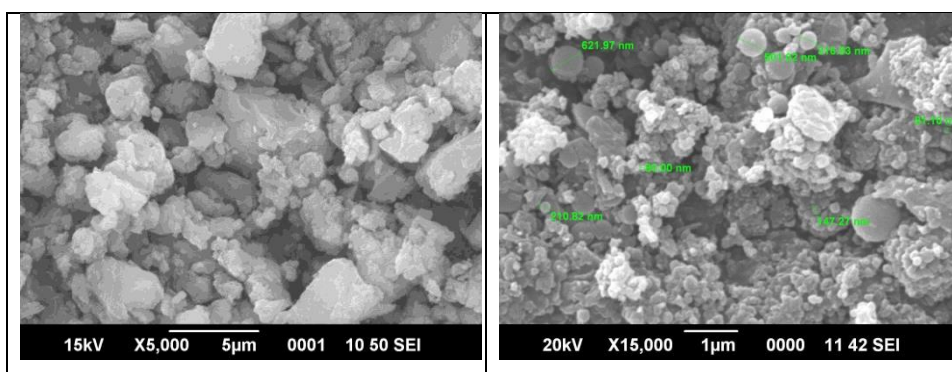


**Figure 3.7: SEM images of AC1 and AC2**

### 3.3.6 Thermal Studies

#### 3.3.6.1 TGA analysis

The Thermal Gravimetric analysis is a thermal method in which the physical or chemical changes in the sample are measured as a function of temperature. On heating, a sample can undergo various changes which may be vaporization, adsorption, absorption, sublimation etc. The TGA curves of **AC1** and **AC2** are shown below.

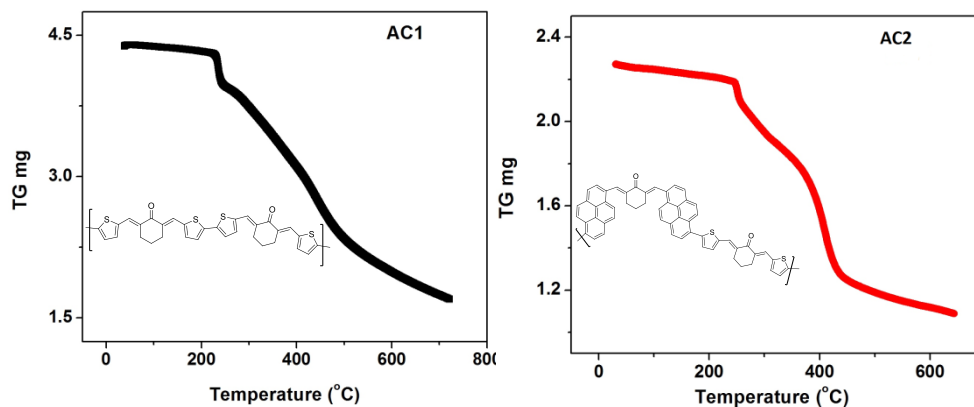


**Figure 3.8: TGA curves of AC1 and AC2**

Here both the samples show two rapid mass losses. Table 3.1 shows the percentage weight losses of both the samples.

OLIGOMER	PERCENTAGE WEIGHT LOSS	
	200 °C	400 °C
AC1	11%	40.4%
AC2	6.95%	43%

**Table 3.1: Percentage weight losses of AC1 and AC2**

Initially a small percentage weight loss in the range of 6% for **AC1** and 11% for **AC2** can be ascribed due to the loss of moisture or solvents which might have trapped inside. This occurs in the temperature range of around 200 °C. The next percentage weight loss in the temperature range of 441 °C is 40.4% for **AC1** and 43% for **AC2** at 416 °C. A possible explanation for the second stage weight loss can be either breakage of bonds or pyrolytic oxidation of -C=C- bonds. Thus, both the compounds

exhibited two stages of decomposition with charring at the end. They can be considered to be thermally stable up to 400 °C which is almost comparable with the polyketones<sup>25</sup> reported.

### **3.3.6.2 Differential Scanning Calorimetry**

DSC is yet another thermal technique in which the temperature and heat flow due to various physical or chemical changes in the sample is measured as a function of temperature. The glass transition temperature ( $T_g$ ) and melting temperatures ( $T_m$ ) can be conveniently measured from DSC. We have performed DSC analysis to find out the glass transition temperature of the synthesized compounds.

<b>Oligomer</b>	<b><math>T_g</math> (°C)</b>	<b><math>T_m</math> (°C)</b>
<b>AC1</b>	<b>42.2 °C</b>	<b>230 °C</b>
<b>AC2</b>	<b>44.8 °C</b>	<b>220 °C</b>

**Table 3.2:  $T_g$  and  $T_m$  values of AC1 and AC2**

The  $T_g$  values of **AC1** and **AC2** were found to be 42.20 °C and 44.85 °C respectively. For **AC1**,  $T_m$  was in the range of 230 °C and for **AC2**,  $T_m$  was around 220 °C. This is in agreement with the TGA results obtained.

### **3.3.7 Cyclic Voltammetry**

Cyclic voltammetry is an electrochemical method in which current produced is measured as a function of applied voltage. In the present

context, we have employed a three electrode system which consists of a Standard Calomel Electrode (SCE) (Ag/AgCl electrode), working electrode and a counter electrode. The counter electrode used is a Pt wire and platinum disc is the working electrode. Tetra-*n*-butylammonium hexafluorophosphate was used as the supporting electrolyte. Measurements were done using a BAS CV50W voltammetric analyzer. Ferrocene was the external standard selected for our study. The potential of Ag/AgCl electrode under vacuum level were calibrated using Ferrocene/Ferrocenium redox system and was obtained as 4.8 eV. CV of ferrocene/Ferrocenium shows two peaks with oxidation and reduction potentials 0.36V and 0.55V and the arithmetic average of these potential versus Ag/ AgCl gives the  $E_{\text{foc}}$  value calculated to be 0.46.

The Cyclic Voltammograms of **AC1** and **AC2** are given below.

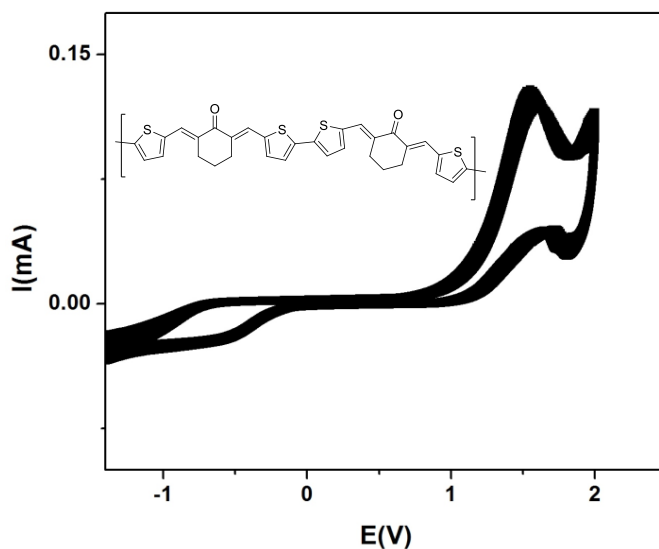
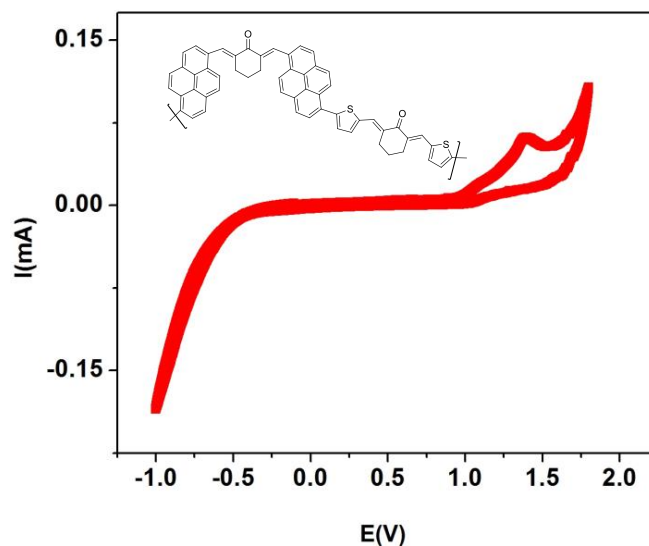


Figure 3.9: Cyclic Voltammogram of AC1



**Figure 3.10: Cyclic voltammogram of AC2**

Thus, now by using the equation below, we can calculate the  $E_{\text{HOMO}}$  and  $E_{\text{LUMO}}$  which in turn gives the band gaps of the synthesised compounds.

$$\text{HOMO} = -(E_{\text{ox-on}} - E_{\text{foc}}) - 4.8 \text{ eV}$$

$$\text{LUMO} = -(E_{\text{red-on}} - E_{\text{foc}}) - 4.8 \text{ eV}$$

The electrochemical band gap can hence be calculated using the equation

$$E_g^{\text{EC}} = E_{\text{HOMO}} - E_{\text{LUMO}}$$

For compound **AC2**, differential pulse voltammetry (DPV) was used to obtain the reduction peak since it was difficult to interpret this part from the CV curve. The DPV curve for the reduction part is shown in the Figure 3.11 below.

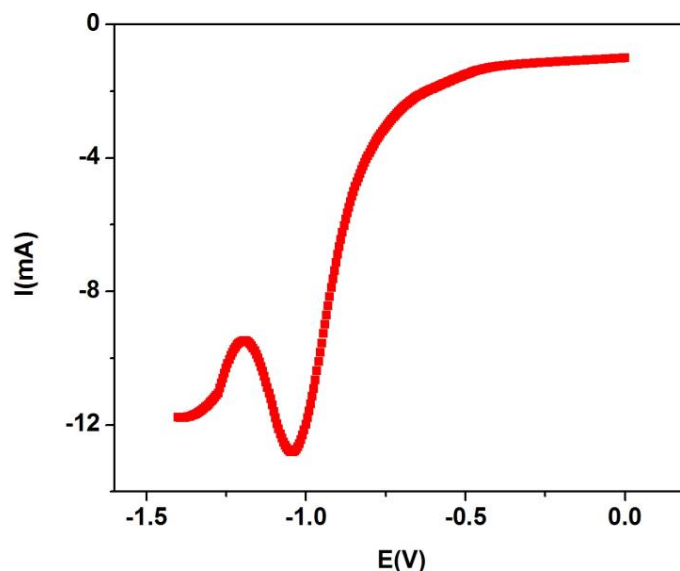


**Figure 3.11: Differential Pulse Voltammogram of AC2**

DPV is a much more sensitive technique, in which the current is measured at two points for each pulse, first one being the measurement just before the application of pulse and the second one at the end of the pulse. Graph is plotted by determining the difference between the current measurements at these points versus the potential. The HOMO, LUMO and electrochemical band gap ( $E_g^{EC}$ ) are displayed in the table 3.3 below.

Compound	$E_{ox,on}(V)$	$E_{re,on}(V)$	HOMO (eV)	LUMO (eV)	$E_g^{EC}(eV)$
<b>AC1</b>	1.50	-0.63	-5.84	-3.71	2.13
<b>AC2</b>	1.38	-1.04	-5.72	-3.30	2.42

**Table 3.3: Electrochemical data's of AC1 and AC2**



### **3.3.8 Computational Studies**

The energy levels and density of states of **AC1** and **AC2** were calculated using Density Functional Theory. DFT was performed using G09 suites of codes<sup>26</sup>. Here, the minimum energy structure of the molecule is arrived at by performing geometry optimization and this is followed by frequency calculation at the optimized geometry. Various other thermodynamic quantities are also calculated. We opted for B3LYP/6-31G (d) theory to calculate the geometry and energy levels. B3LYP is a hybrid functional which stands for Becke, 3-parameter, Lee-Yang-Parr. Hybrid functional modification to DFT was introduced by Axel Becke in 1993. B3LYP/6-31G has been proved to be a reliable and accurate method for such calculations. The stationary points are characterized by frequency calculation. Energy levels and density of states of **AC1** and **AC2** are shown in Figure.3.12.

DOS spectrum gives an idea regarding the number of states available at different energies. It also gives an idea about the number of occupied orbitals and virtual orbitals in the molecule which in turn reveals the HOMO and LUMO levels present. Larger the number of substitution in the molecule, additional energy levels is created which are closely spaced. The HOMO of **AC1** and **AC2** occurs at -5.34 and -5.28 respectively and LUMO occurs at -2.96 and -2.66 respectively. The difference between the HOMO and LUMO gives the band gap of the compound. The band gaps are calculated to be 2.38 and 2.62 for **AC1** and **AC2**.

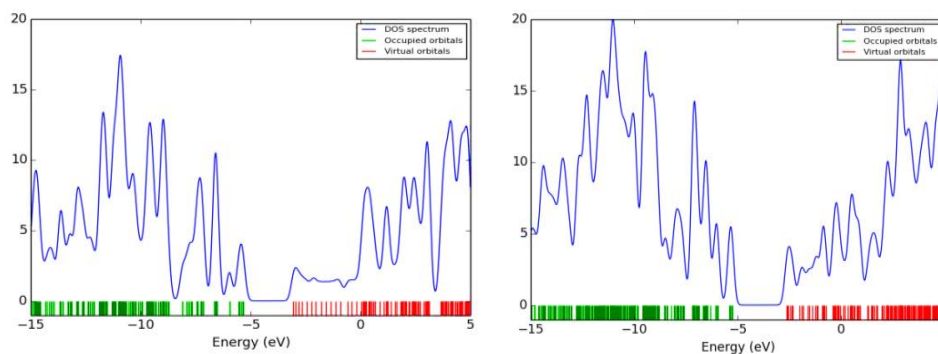


**Figure 3.12: Energy levels and DOS spectra of AC1 and AC2**

In addition to theoretical band gap, it is possible to calculate the optical band gap from UV spectra. The equation for calculation is given below.

$$E_g = \frac{1242}{\lambda} \text{ eV}$$

Here  $\lambda$  represents wavelength.

Oligomer	HOMO	LUMO	$E_g^{\text{DFT}}$ (eV)	$E_g^{\text{UV}}$ (eV)	$E_g^{\text{Ec}}$ (eV)
AC1	-5.34	-2.96	2.38	2.26	2.24
AC2	-5.28	-2.86	2.62	2.22	2.42

**Table 3.4: Comparison of Band gaps of AC1 and AC2 from DFT and UV spectra**

The Table 3.4 below shows the theoretical and optical band gap calculated. A slight variation is shown in the band gaps due to the differences in measurement in gaseous state and solution state.

### **3.3.9 Non-Linear Optics**

The non-linear optical properties of the compounds were determined by Z-scan technique using laser light of second harmonic output (532nm) of a Q switched Nd:Yag laser (Minilite, Continuum). Z-scan set up is given in the Introduction chapter section 1.7.3.

In the present experiment, laser beam is focused by means of a plano-convex lens of 10cm focal length and the sample mounted can be moved along the propagation direction of focused laser beam by means of a motor. The input laser beam and the sample transmittance are measured by pyroelectric probes, and their ratio corresponds to the percentage of transmittance. Laser pulse of 50  $\mu$ J energy is used in our case. Successive laser pulses are given at regular intervals in such a way that the sample has enough time for thermal relaxation.

When laser light focusses on the sample the electrons gets excited to higher energy levels. If the rate of de-excitation is less compared with the rate of excitation, the molecular ground energy level gets depleted and this is indicated by a peak in the curve. This peak corresponds to Saturable Absorption (SA). At this intensity, the transmittance will increase. On the other hand, when the intensity of laser beam is increased sufficient for the molecules in the excited state to get excited to higher energy levels by absorbing the energy, Free Carrier absorption (FCA)<sup>27</sup> comes into play due to which transmittance decreases and a valley is indicated in the curve. This is called Reverse Saturable Absorption (RSA). It is possible to plot the input laser fluence versus the sample transmission from the open aperture Z scan curves. Open aperture Z scan curves for the samples **AC1** and **AC2** is given below in the figure 3.13.

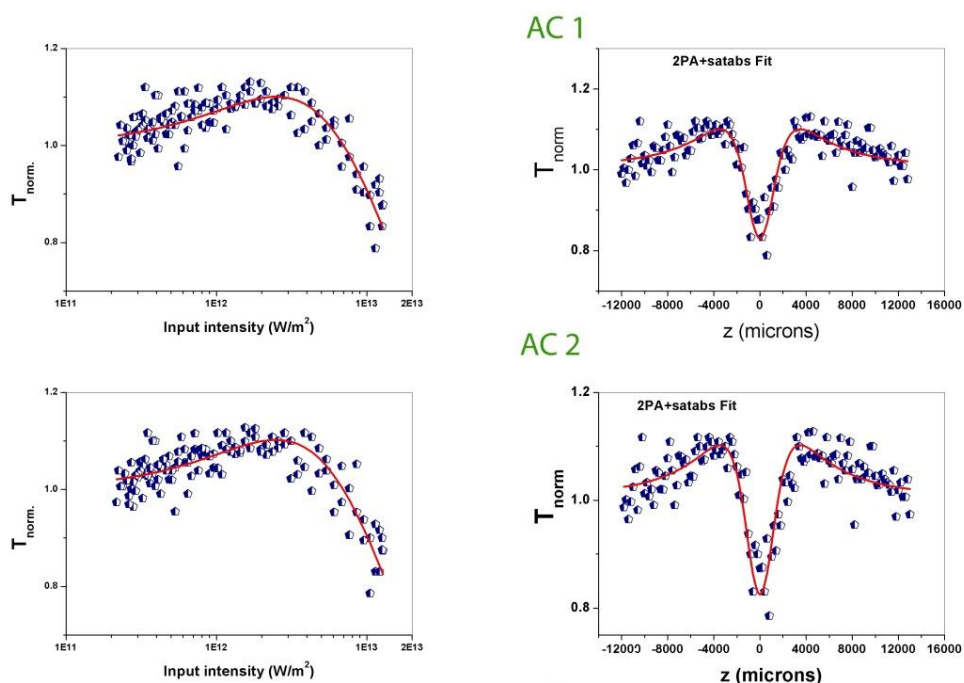


**Figure 3.13: Fluence graph and open aperture Z scan curves of AC1 and AC2**

In our studies, open aperture Z scan curves clearly show that the compound has both SA and RSA. A slight increase in transmittance is observed after which the increase in intensity decreases the transmittance. Since the RSA is the dominating factor, the compounds are good optical limiters. Moreover, due to the switching between SA and RSA, our compounds can be used as optical switches as well. The plot of input laser fluence versus the sample transmission is also given in the figure 3.10. The fluence graphs further proves that both samples are good optical limiters with almost 20-30% optical limiting efficiency.

For the simultaneous switching of FCA and SA, an effective nonlinear absorption coefficient  $\alpha(I)$  with an expression

$$\alpha(I) = \frac{\alpha_0}{1 + \frac{I}{I_s}} + \beta_{\text{eff}}I$$

can be considered. Here  $\alpha_0$  is the unsaturated linear absorption coefficient at the wavelength of excitation,  $I$  is the input laser intensity, ' $I_s$ ' is the saturation intensity (intensity at which the linear absorption drops to half of its original value). ' $\beta_{\text{eff}}$ ' is the effective two photon absorption<sup>28</sup> coefficient, which represents the two-photon like absorption happening in the system (ground state excitation followed by FCA). For a given input laser intensity, the transmitted intensity can be calculated by solving the propagation equation given by:

$$\frac{dI}{dZ'} = \left[ \left( \frac{\alpha_0}{1 + \frac{I}{I_s}} \right) + \beta_{\text{eff}}I \right] I$$

The imaginary part of third order susceptibility  $\text{Im } \chi^{(3)}$ <sup>29</sup> can be solved using the following equation.

$$\text{Im } \chi^{(3)} = \eta_0^2 c^2 \beta / (240\pi^2 \omega)$$

Where  $\eta_0$  is the linear refractive index of the sample solution,  $c$  is the velocity of light in vacuum and  $\omega$  is the angular frequency of radiation

used which is equal to  $2\pi\nu$  where  $\nu=c/\lambda$ . The refractive indexes of samples **AC1** and **AC2** is found to be 1.40 and 1.41 respectively. Table 3.4 below shows the Effective two photon absorption coefficients and the imaginary part of third order susceptibilities of **AC1** and **AC2**.

Sample	Excitation energy ( $\mu\text{J}$ )	Saturation Intensity ( $\text{I}_s$ ) ( $10^{10} \text{ W/m}^2$ )	$\beta_{\text{eff}}(\times 10^{-10} \text{ m/W})$	$\text{Im } \chi^{(3)}(\text{esu})$
<b>AC1</b>	<b>50</b>	<b>300</b>	<b>0.75</b>	<b><math>1.6 \times 10^{-10}</math></b>
<b>AC2</b>	<b>50</b>	<b>300</b>	<b>0.78</b>	<b><math>1.7 \times 10^{-10}</math></b>

**Table 3.5: Two photon absorption coefficients and  $\text{Im}\chi^{(3)}$  of AC1 and AC2**

From the table, the effective two photon absorption coefficient and third order susceptibilities (imaginary part) for **AC1** and **AC2** is found to be in the order of  $0.75 \times 10^{-10}$ ,  $0.78 \times 10^{-10} \text{ m/W}$  and  $1.6 \times 10^{-10}$ ,  $1.7 \times 10^{-10} \text{ esu}$  respectively. This value indicates that the prepared novel oligomers are typically of the order of semiconductors and have good optical limiting<sup>30</sup> natures.

### 3.3.10 Measurement of I-V characteristics

The compounds **AC1** and **AC2** were coated as thin films on top of gold coated glass plates which is the cathode. This forms the Schottky (metal-semiconductor) junction. Ag contacts (anode) were provided on top of the oligomer layers by thermal evaporation. Typical device set-up used is given in the figure 3.14. Probe station employing tungsten probes were used to measure the current-voltage characteristics. The I-V characteristics were analyzed using a Keithley-2450 source meter to confirm the formation of the Schottky junction.

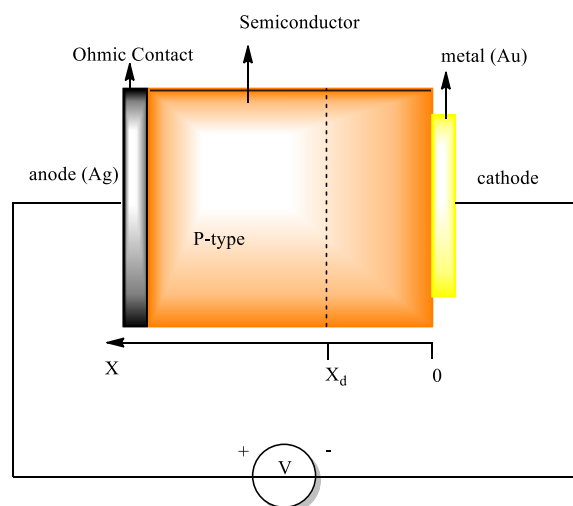


**Figure 3.14: Device set up with configuration Ag/ oligomer/ Au**

The current-voltage characteristics of the devices with configuration Ag/oligomer/Au are shown in the figure 3.15. Forward bias current is obtained when anode is positively biased and cathode is negatively biased. Once a metal-semiconductor junction is formed, the diffusion of charge carriers occurs from either ends until equilibrium is established. Once this equilibrium attains, a barrier potential is created at the junction which in turn depends upon the carrier concentration of the material. Now, when voltage is applied across this junction current flows slowly first till the barrier potential is achieved and when it crosses the barrier potential current flow shows a steep increase even with a small variation of the voltage. This type of a junction like behavior is clearly evident from the I-V graphs shown which in turn ensures the applicability of these oligomers in fabricating PLED's.

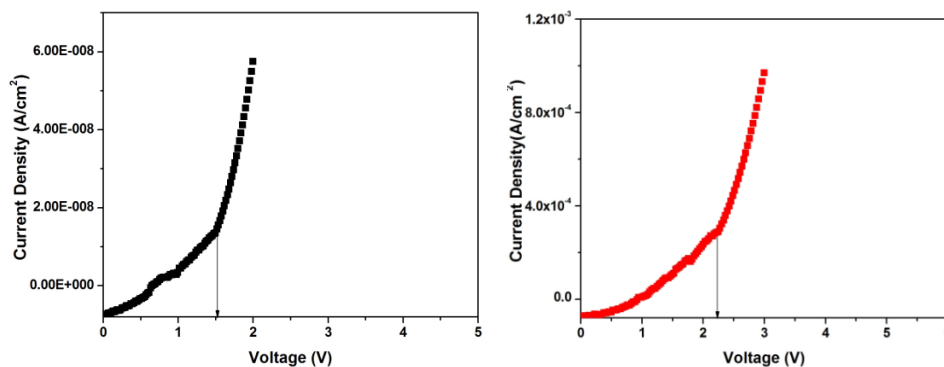


**Figure 3.15: I-V characteristics of Ag/oligomer/Au devices using AC1 and AC2**

Both the compounds show a low onset voltage around 1.5 for AC1 and 2.4 for AC2 and such low onset voltages are advantageous in device fabrication. The energy diagram for construction of both device configurations is given below in the figure 3.16.

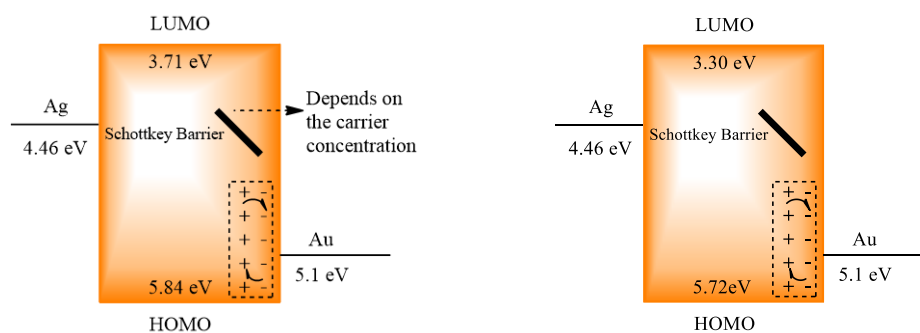


**Figure 3.16: Energy diagram of AC1 and AC2**

The HOMO levels of both the oligomers matches well with the work function of the metal chosen for efficient transport of electrons and holes. Thus, it can be clearly stated that the required energy levels of these materials are fulfilled for device fabrication.



### **3.4 CONCLUSION**

We have synthesized two novel oligomers of bisaromatic cycloalkanones by using direct arylation method. This is probably a novel route for synthesis of oligo ketones. The compounds were characterized using <sup>1</sup>H NMR, IR, Powder XRD, UV-Visible spectra, PL spectra, SEM, TGA and DSC analysis. Computational calculations were done to calculate HOMO and LUMO which in turn reveals the band gap of the synthesized compounds. Both the compounds had band gap in semiconductor range which was further confirmed from cyclic voltammetry studies. The UV-Visible spectra gave the absorption maxima of **AC1** and **AC2** to be in the range of 485 nm and 465 nm respectively. The major emission peak appears at 563 nm and 557 nm for **AC1** and **AC2**. The compounds exhibit intense yellow-orange emission under UV irradiation. The powder XRD spectra reveals a semi-crystalline nature with **AC2** being more amorphous than **AC1** due the unsymmetrical structure and bulky pyrene groups present. From the TGA and DSC curves, we inferred that both the compounds have thermal stability up to 400 °C. SEM images predict the irregular morphology which is in agreement with the poly ketones reported. The Non-linear optical studies were carried using Z scan technique in which both the compounds were found to be excellent optical limiters along with a slight switching from SA to RSA. The synthesized compounds though are oligomers have two photon absorption coefficients in semiconductor range and hence have wide range applications similar to polymers. The measurement of I-V characteristics clearly shows a junction like behavior characteristic for fabricating PLED's.

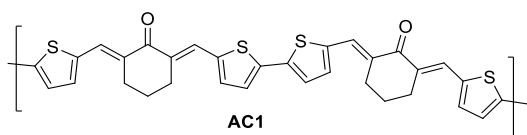
### 3.5 EXPERIMENTAL

All reactions were carried out using oven dried glass wares. All experiments were done with distilled and dried solvents by using standard protocols. All starting materials were purchased from either *Sigma-Aldrich* or *Spectrochem Chemicals* and were used without further purification. Separation and purification of compounds were done by precipitation technique. Infra-red spectra were recorded using *Jasco 4100 FT-IR* spectrometers. The  $^1\text{H}$  NMR spectra was recorded at 400 MHz on a *Bruker Avance III* FT-NMR spectrometer with tetramethylsilane (TMS) as internal standard. Chemical shifts ( $\delta$ ) are reported in parts per million (ppm) downfield of TMS. The Powder X-ray diffraction (XRD) patterns were obtained using a Rigaku Xray diffractometer with Cu  $K\alpha$  radiation (1.542Å). The molecular weight of the synthesized polymers was determined by GPC (Shimadzu Prominence) using a column packed with polystyrene gel beads. Here THF was used as the eluent. The UV-visible absorption spectra were recorded using Thermo Evolution Model 201. Photoluminescence studies were carried out using Flouromax-3 fluorescence spectrophotometer. The glass transition temperature was measured using a Mettler Toledo Differential Scanning Calorimeter 822e and thermal stability was determined using a Perkin Elmer, Diamond TG/DTA system. Computational calculations were done using Density Functional Theory (DFT) with B3LYP/6-31G hybrid functional. The nonlinear optical properties of the samples were investigated using the Z-scan technique employing the second harmonic output (532 nm) of a Q-switched Nd: YAG laser (Minilite, Continuum USA). JEOL model JSM-6390LV Scanning electron Microscope (SEM) was used to generate

surface morphological images of the samples with the resolution of a micrometer.

**3.5.1 Synthesis of oligomer (2E,2'E,6E,6'E)-6,6'-([2,2'-bithiophene]-5,5'-diylbis(methanylylidene))bis(2-((5-methylthiophen-2-yl)methylene)cyclohexanone) (AC1) from (2E,6E)-2,6-bis(thiophen-2-ylmethylene) cyclohexanone (1) and (2E,6E)-2,6-bis((5-bromothiophen-2-yl)methylene)-cyclohexanone (2) using direct arylation method**

A mixture of (2E,6E)-2,6-bis(thiophen-2-ylmethylene)cyclohexanone (1, 0.1 g, 0.53 mmol in 10mL DMF), tetrabutylammonium bromide (0.17 g, 0.53 mmol) and sodium acetate (0.17 g, 2.1 mmol) was stirred at room temperature for 15 minutes. After 15 minutes (2E,6E)-2,6-bis((5-bromothiophen-2-yl)methylene) cyclohexanone (2, 0.23 g, 0.53 mmol) and palladium acetate (0.01 g, 10 mol %) were added. The reaction mixture was stirred at 90 °C for 72 h. After precipitation, the reaction mixture was cooled and poured in to cold methanol. The precipitate was filtered into a thimble and subjected to purification by Soxhlet extraction using methanol, hexane and chloroform as solvents. The product was dissolved in minimum amount of chloroform and precipitated in methanol.

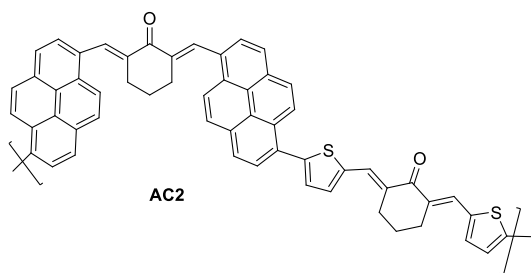


*Oligomer AC1: Yield: 40%;  
M<sub>w</sub>: 1919; PDI: 1.07; IR  
(KBr): 3423, 2922, 1643,  
1583, 1416, 1236, 1135, 784,  
548 cm<sup>-1</sup>; <sup>1</sup>H NMR (CDCl<sub>3</sub>)  
δ 7.99-7.84 (m, 2H), 7.55-  
7.30 (m, 2H), 7.16-7.10 (m,  
1H), 2.97-2.84 (m, 4H), 2.01-  
1.97(m, 2H); Anal. Calcd. for*

H(C<sub>34</sub>H<sub>30</sub>O<sub>2</sub>S<sub>4</sub>)Br : C: 68.09,  
H: 4.98, S: 24.76, 21.40.  
Found: C: 68.19, H: 5.05, S:  
21.42.

**3.5.2 Synthesis of oligomer (AC2) (2E,6E)-2-((3-methyl-3a1,6-dihydropyren-1-yl)methylene)-6-((3-(5-((E)-(E)-3-((5-methylthiophen-2-yl)methylene)-2-oxocyclohexylidene)methyl)thiophen-2-yl)pyren-1-yl)methylene)cyclohexanone (AC2) from (2E,6E)-2,6-bis((5-bromothiophen-2-yl)methylene) cyclohexanone (2) and cyclohexanone ( (2E,6E)-2,6-bis(pyren-2-ylmethylene) cyclohexanone (3) by direct arylation**

(2E,6E)-2,6-bis(pyren-2-ylmethylene)cyclohexanone (**3**, 0.27 g, 0.53 mmol), tetrabutylammonium bromide (0.17 g, 0.53 mmol) and sodium acetate (0.17 g, 2.1 mmol) was stirred in 10 ml DMF at room temperature for 15 minutes. After 15 minutes (2E,6E)-2,6-bis((5-bromothiophen-2-yl)methylene) cyclohexanone (0.23g, 0.53mmol) and palladium acetate (0.01 g, 10 mol %) were added. The reaction mixture was stirred at 90 °C for 72 h. The reaction mixture was cooled and poured in to cold methanol. The precipitate obtained was filtered and purified by Soxhlet extraction using methanol, hexane and chloroform as solvent. The product was dissolved in minimum amount of chloroform and precipitated in methanol.



*Oligomer AC2*: Yield: 50%;  
M<sub>w</sub>: 2178; PDI: 1.07; IR  
(KBr): 3423, 2922, 1643,  
1583, 1416, 1236, 1135, 784,  
548 cm<sup>-1</sup>; <sup>1</sup>H NMR (CDCl<sub>3</sub>):  
δ 8.69 (s, 2H), 7.99-7.84 (m,  
4H), 7.55-7.30 (m, 4H),  
7.16-7.10 (m, 2H), 2.97-2.84

(m, 8H), 2.01-1.97 (m, 4H);  
Anal. Calcd. for  
 $\text{H}(\text{C}_{58}\text{H}_{44}\text{O}_2\text{S}_2)_3\text{Br}$  : C: 83.20,  
H: 5.23, S: 7.56. Found: C:  
83.22, H: 5.30, S: 7.66.

### 3.6 REFERENCES

- 1) Ackermann, L.; Vicente, R.; Kapdi, A. R. *Angew. Chem., Int. Ed.* **2009**, *48*, 9792.
- 2) Bellina, F.; Rossi, R. *Tetrahedron* **2009**, *65*, 10269.
- 3) Lu, W.; Kuwabara, J.; Kanbara, T. *Macromolecules* **2011**, *44*, 1252.
- 4) Fujinami, Y.; Kuwabara, J.; Lu, W.; Hayashi, H.; Kanbara, T. *ACS Macro Lett.* **2012**, *1*, 67.
- 5) Miura, M.; Nomera, M. *Top. Curr. Chem.* **2002**, *219*, 211.
- 6) Labinger, J. A.; Bercaw, J. E. *Nature* **2002**, *417*, 507.
- 7) Glover, B.; Harvey, K. A.; Liu, B.; Sharp, M. J.; Tymoschenko, M. *F.Org. Lett.* **2003**, *5*, 301.
- 8) Grigg, R.; Sridharan, V.; Stevenson, P.; Sukirthalingam, S.; Worakun, T. *Tetrahedron* **1990**, *46*, 4003.
- 9) Yamamoto, T. *NPG Asia Mater.* **2010**, *2*, 54.
- 10) Ohmori, Y.; Uchida, M.; Muro, K.; Yoshino, K. *Jpn. J. Appl. Phys.* **1991**, *30*, L1938.
- 11) Ohmori, Y.; Morishita, C.; Uchida, M.; Yoshino, K. *Jpn. J. Appl. Phys.* **1992**, *31*, L568.
- 12) Braun, D.; Gustaffson, G.; Macbranch, D.; Heeger, A. *J. Appl. Phys.* **1992**, *72*, 164.
- 13) Barbarella, G.; Favaretto, L.; Zanelli, A.; Gigli, G.; Mazzeo, M.; Anni, M.; Bongini, A. *Adv. Funct. Mater.* **2005**, *15*, 664.

- 14) Peripichka, I. I.; Peripichka, I. F.; Bryce, M. R.; Palsson, L. O. *Chem. Commun.* **2005**, 3397.
- 15) Fuks-Janczarek, I.; Ebothe, J.; Miedzinski, R.; Gabanski, R.; Reshak, A. H.; Lapkowski, M.; Motyka, R.; Kityk, I. V.; Suwinski, J. *Laser Phys.* **2008**, *18*, 1056.
- 16) Skala, M. C.; Squirrel, J. M.; Vrotsos, K. M.; Eickhoff, V. C.; Gendron-Fitzpatrick, A.; Eliceiri, K. W.; Ramanujam, N. *Cancer Res.* **2005**, *65*, 1180.
- 17) Belfield, K. D.; Schafer, K. J.; Liu, Y. U.; Liu, J.; Ren, X. B.; Van Stryland, E. W. *J. Phys. Org. Chem.* **2000**, *13*, 837.
- 18) Correa, D. S.; Tayalia, P.; Cosendey, G.; dos Santos, D. S.; Aroca, R. F.; Mazur, E.; Mendonca, C. R. *J. Nanosci. Nanotechnol.* **2009**, *9*, 5845.
- 19) Mendonca, C. R.; Correa, D. S.; Marlow, F.; Voss, T.; Tayalia, P.; Mazur, E. *Appl. Phys. Lett.* **2009**, *95*, 113309.
- 20) Parthenopoulos, D. A.; Rentzepis, P. M. *Science* **1989**, *245*, 843.
- 21) Mendonca, C. R.; Neves, U. M.; De Boni, L.; Andrade, A. A.; dos Santos, D. S.; Pavinatto, F. J.; Zilio, S. C.; Misoguti, L.; Oliveira, O. N. *Opt. Commun.* **2007**, *273*, 435.
- 22) Gao, D.; Agayan, R. R.; Xu, H.; Philbert, M. A.; Kopelman, R. *Nano Lett.* **2006**, *6*, 2383.
- 23) Vivas, M. G.; Nogueira, S. L.; Santos Silva, L.; Barbosa Neto, N. M.; Marletta, A.; Serein-Spirau, F.; Lois, S.; Jarrosson, T.; De Boni, L.; Silva, R. A.; Mendonca, C. R. *J. Phys. Chem. B.* **2011**, *115*, 12687.
- 24) Anand, P. B.; Hasna, K.; Anilkumar, K. M.; Jayalekshmi, S. *Polym. Int.* **2012**, *61*, 1733.
- 25) Alkskas, A. I.; Alhubgeb, A. M.; Azamc, F. *Chinese J. Polym. Sci.* **2013**, *31*, 471.

- 26) Frisch, M.J.; Trucks, G. W.; Schlegel, H. B. Gaussian 09, Revision A.02. Gaussian, Inc., Wallingford, CT **2009**, Gaussian 09, Revision B.01.
- 27) Gao, Y.; Zhang, X.; Li, Y.; Liu, H.; Wang, Y.; Chang, Q. *Optics Commun.* **2005**, *251*, 429.
- 28) Gu, B.; Ji, W.; Patil, P. S.; Dharmaprakash, S. M.; Wang, H. T. *Appl. Phys. Lett.* **2008**, *92*, 091118.
- 29) Li, N.; Xu, Q.; Lu, J.; Xia, X.; Wang, L. *Macromol. Chem.Phys.* **2007**, *208*, 399.
- 30) Sheik-Bahae, M.; Said, A. A.; Wei, T. H.; Hagan, D. J.; Van Stryland, E. W. *IEEE J. Quantum Electr.* **1990**, *26*, 760.





## CHAPTER 4

### *Chemical modification of bis(thiophen-2-ylmethylene)cycloalkanones: Synthesis of thiophene appended hexahydro-2H-indazole derivatives*

---

#### 4.1 Abstract

*In this chapter, we report the synthesis of six thiophene appended hexahydro-2H-indazole derivatives from the corresponding bis(thiophen-2-ylmethylene)cycloalkanones. Not all bis(thiophen-2-ylmethylene)cycloalkanones successfully gave pyrazolines and in order to account for the possible reason for the selective formation of pyrazolines, we used computational methods. Theoretical investigations were carried out using hybrid density functional theory calculations with B3LYP exchange correlational functional and 6-31 + G(d) basis set. We arrived at the energy profile diagram for the formation of pyrazoline, which clearly indicated that the activation energy difference is the major reason behind differential reactivity. We could also predict whether the reaction was exothermic or endothermic.*

---

#### 4.2 INTRODUCTION

Pyrazolines<sup>1-3</sup> are five membered ring heterocycles having two adjacent nitrogen atoms in the ring. 2-Pyrazolines are the most widely studied among the various isomers of pyrazolines. They are active ingredients in various antipyretic, antiepileptic compounds. These are biologically interesting compounds owing to their wide range of pharmacological activities<sup>4-9</sup>. Pyrazolines are fluorescent compounds showing bright blue

or green fluorescence in solution having intramolecular charge transfer<sup>10-13</sup> properties, and generally exhibiting hole transport properties<sup>11-13</sup>. Fused pyrazolines such as indazolines are also important compounds.<sup>14,15</sup>

A common method adopted for the synthesis of pyrazolines involves the reaction of  $\alpha,\beta$ -unsaturated ketones with hydrazines. Reaction with diazomethane also yields pyrazoline.  $\alpha,\beta$ -Unsaturated ketones react with dipolar molecules giving cyclic compounds. It was Fischer and Knoevenagel<sup>16-20</sup> who described the first synthesis of pyrazolines from acrolein and phenylhydrazine. The pyrazoline formation reaction can be catalyzed by acids or bases. The reaction with acids involve intermediate hydrazone formation which cannot be isolated, whereas when the reaction is catalyzed by bases like pyridine or piperidine,  $\beta$ -hydrazino ketones are formed as intermediates instead of hydrazones. In all these reactions, 2-pyrazolines are formed as product, and it is predicted that the product formation typically depends on the  $\alpha,\beta$ -unsaturated moiety and the other parts have almost no influence on the reaction product. Lorand<sup>21</sup> *et al* has synthesised 2-pyrazolines by reacting  $\alpha,\beta$ -unsaturated ketones with semicarbazide or thiosemicarbazide in hot ethanol under acidic conditions<sup>21-23</sup>.  $\alpha,\beta$ -unsaturated ketones contain two electrophilic reaction centers due to which they behave like ambident electrophiles. They undergo 1,2-or 1,4-additions, the latter one occurring predominantly.  $\alpha,\beta$ -Unsaturated ketones are expected to react with phenylhydrazine to give the corresponding *N*-phenylpyrazolines. Various bis(thiophen-2-ylmethylene)cycloalkanones synthesized by us are typical  $\alpha,\beta$ -

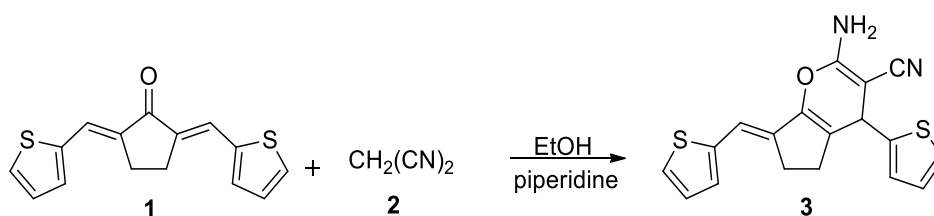
unsaturated ketones and hence are expected to react with phenylhydrazines to give fused pyrazolines. In the present investigation, we carried out the reaction of several bis(thiophen-2-ylmethylene)cycloalkanones with phenylhydrazine. Though we could successfully synthesize six novel pyrazolines from bis(thiophen-2-ylmethylene)cyclohexanones, pyrazoline formation was not observed with other bis(thiophen-2-ylmethylene)cycloalkanones. In order to unravel the reason behind this anomaly, we decided to exploit theoretical methodology to predict the mechanism of formation of pyrazolines and thereby to formulate a reasonable explanation for substrate selectivity exhibited by bis(thiophen-2-ylmethylene)cycloalkanones.

In addition to pyrazoline forming reactions, we attempted structural modification of bis(thiophen-2-ylmethylene)cycloalkanones by subjecting them to Knoevenagel condensation reactions.<sup>24,25</sup> Knoevenagel reaction is the condensation of an aldehyde or ketone with an active methylene compounds to give electron deficient olefins that can act as electron acceptors in intramolecular electron transfer reaction.

### **4.3 RESULTS AND DISCUSSION**

In chapter 3, we reported the synthesis of oligomers of bis(thiophen-2-ylmethylene)cyclohexanones by direct arylation. However, in these oligomers, free carbonyl groups that can potentially enhance intersystem crossing and thereby reduce the quantum efficiency of fluorescence are present. So we decided to modify the carbonyl groups with some other

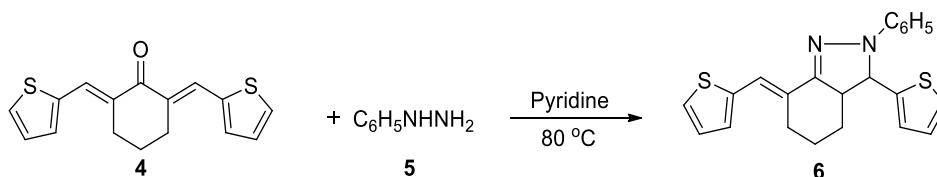
structural entities that are likely to assist holding of the chromophoric systems in well-defined orientations while reducing the intersystem crossing efficiency. Modification of the carbonyl group by reacting with reagents such as hydroxylamines, hydrazines and active methylene compounds appeared feasible. However, we had only limited success with these reactions. In our hands, bis(thiophen-2-ylmethylene)cycloalkanones failed to react with hydroxylamine. Knoevenagel condensation of bis(thiophen-2-ylmethylene)cycloalkanones with malononitrile resulted in the formation of a bicyclic pyran derivative. Pyran formation in the reaction between bis(thiophen-2-ylmethylene)cyclopentanone and malononitrile is shown in Scheme 4.1. Structure of pyran **3** was established on the basis of spectral and analytical data and literature precedence.<sup>25</sup>



**Scheme 4.1**  
Synthesis of bicyclic pyran derivative

As a next attempt of modification of carbonyl group, we carried out the reaction of different bis(thiophen-2-ylmethylene)cycloalkanones with phenylhydrazine. Though bis(thiophen-2-ylmethylene)cyclopentanone and bis(thiophen-2-ylmethylene)cycloheptanone failed to react with phenylhydrazine, successful reaction was observed with bis(thiophen-2-ylmethylene)cyclohexanone. On refluxing with phenylhydrazine in presence of pyridine, bis(thiophen-2-ylmethylene)cyclohexanone (**4**)

afforded the pyrazoline product **6** (Scheme 4.2). Pyrazoline **6** exhibited green fluorescence.



**Scheme 4.2: Synthesis of hexahydro-2H-indazole derivative 6**

In continuation, we examined the reaction between phenylhydrazine and a few bithiophenes listed in Chart 4.1. Among these, pyrazoline formation was successful for bithiophenes **9** and **11** while the remaining bithiophenes remained unreactive towards phenylhydrazine. Rest of the below said reactants failed to give a product.

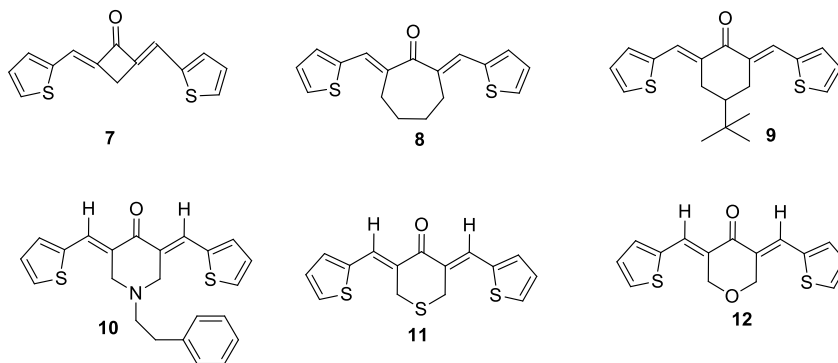
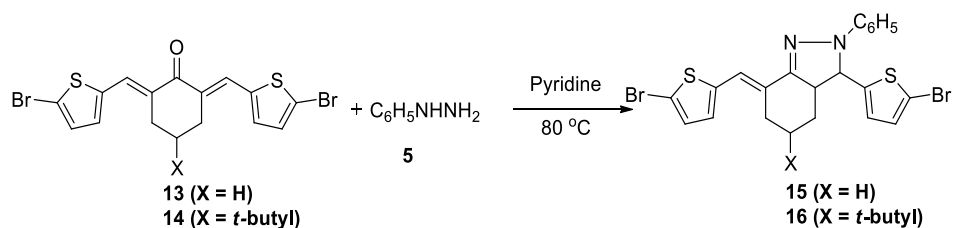


**Chart 4.1: Bithiophenes selected for the reactions**

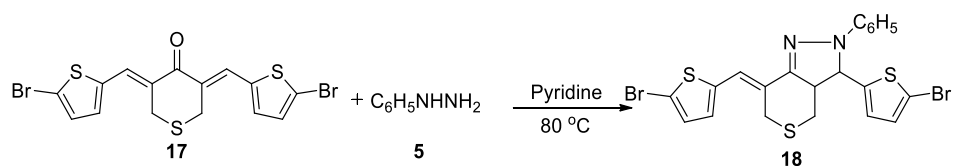
Since our prime focus is on the polymerization of these modified bithiophenes, we proceeded with the preparation of indazolines having 2-bromothiophene units. We accomplished this by reacting suitable 2,6-bis((5-bromothiophen-2-yl)methylene)cyclohexanones such as **13** and **14** with phenylhydrazine to give indazolines **15** and **16** respectively (Scheme

4.3). Incorporation of *t*-butyl group in **14** is intended to enhance solubility of polymers derived thereof.



**Scheme 4.3: Synthesis of hexahydro-2H-indazole derivatives 15,16**

In continuation, we synthesized a 2-bromothiophene appended hexahydrothiopyrano[4,3-*c*]pyrazole appended monomer **16** by the reaction between bithiophene **15** and phenylhydrazine.



**Scheme 4.4: Synthesis of hexahydro-2H-indazole derivative 18**

Next we turned our attention towards deciphering the differential reactivity exhibited by bis(thiophen-2-ylmethylene)cycloalkanones towards phenylhydrazine. In principle, molecules possessing  $\alpha,\beta$ -unsaturated ketone components should react with phenylhydrazine to give pyrazoline derivatives. Literature reports suggest that the mechanism of pyrazoline formation depends on the  $\alpha,\beta$ -unsaturated ketone component alone. However, our findings are only in partial agreement with this generalization. While bis(thiophen-2-ylmethylene)cyclohexanones gave products, the corresponding cyclopentanones and cycloheptanones proved unreactive towards

phenylhydrazine under the conditions employed by us. Even with the six membered rings, structural changes affected the course of reactions. We observed that for heteroatom substituted six-membered ring ketones, nature of the heteroatom controlled reactivity. While pyrazoline formation was observed with cyclohexanone and dihydro-2*H*-thiopyran-4(3*H*)-one derivatives, dihydro-2*H*-pyran-4(3*H*)-one and piperidin-4-one derivatives remained unreactive towards phenylhydrazine. To account for this unusual behavior, we carried out theoretical calculations involving Hybrid density functional theory to find out the energy profile diagram that helps in understanding reaction mechanism.

Generally, potential energy function determines the course of a chemical reaction. For two reactants or say atoms separated by inter nuclear distance  $R$ , coming together to form a diatomic molecule,  $U$  is the potential energy which gives the Potential Energy surface (PES) of the reaction. Reactions usually proceed through a minimum energy path, and the point of maximum potential energy on the minimum energy point is called a transition state. TS is an unstable molecule, the barrier height being the energy difference between TS and reactants. For a multistep reaction, in addition to TS, there are reaction intermediates which are product of one elementary step and reactant to the consecutive step. Reaction intermediates are often short-lived; hence the determination of their structure by spectroscopic techniques is not feasible. Computational methods can be successfully applied to determine the structure and relative energies of these intermediates, so as to predict the mechanism of the reaction.

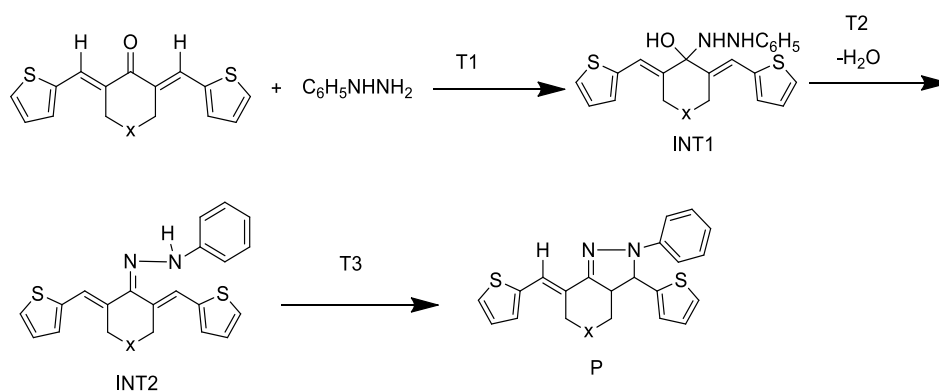
In our study, the theoretical investigation was carried out using Hybrid density functional theory calculations with B3LYP exchange correlational functional and 6-31 + G(d) basis set. DFT theory has been employed widely to study reaction mechanisms. When a reaction mechanism is predicted by theoretical means, an energy profile diagram is generated based on the exact mechanism of the reaction reported, where the reactants in the left passes through various intermediates and transition states forming product in the right. The reactants can successfully form product only if they have the energy to overcome these barriers, the so called activation energy. Generally for all theoretical calculations, it is required that a geometry optimized structure should be generated and the possible intermediates and transition states are generated by computational calculations. This requires extensive task and comparison should be done with experimental data for conclusion. We selected 5 bithiophene systems for our investigation, viz, (2*E*,6*E*)-2,6-bis(thiophen-2-ylmethylene)cyclohexanone (**4**), (2*E*,6*E*)-4-(*tert*-butyl)-2,6-bis (thiophen-2-ylmethylene)cyclohexanone (**9**), (3*Z*,5*Z*)-3,5-bis(thiophen-2-ylmeth ylene)dihydro-2*H*-thiopyran-4(3*H*)-one (**11**), (2*E*,7*E*)-2,7-bis(thiophen-2-ylmethylene)cycloheptanone (**8**) and (3*E*,5*E*)-3,5-bis(thiophen-2-ylmethylene)dihydro-2*H*-pyran-4(3*H*)-one (**12**), the former three being successful pyrazoline reactions and the latter two being unsuccessful reactions.

#### 4.3.1 Mechanism of Pyrazoline formation

The mechanism of pyrazoline formation (Scheme 4.5) is predicted in various literature reports as a three stage process, the first stage being the



addition of more nucleophilic  $\beta$ -nitrogen atom to the C=O group of the ketone, forming an intermediate 1 (INT1). T1 is the transition state in this step. The dehydration step by the loss of water molecule takes place in the second stage, forming an intermediate 2 (INT 2), T2 being its transition state. The third and the last stage involves the attack of the next nucleophilic nitrogen atom followed by an immediate cyclisation forming the product. T3 is the transition state of this stage.



**Scheme 4.5 : Mechanism of pyrazoline formation**

Knowledge of the minima, TS and barrier heights gives a good idea of the reaction mechanism.

### 4.3.2 The Energy Profile Diagrams

#### 4.3.2.1 (*E*)-2-phenyl-3-(thiophen-2-yl)-7-(thiophen-2-ylmethylene)-3,3a,4,5,6,7-hexahydro-2*H*-indazole (6)

The energy profile diagram for the mechanism of formation of (*E*)-2-phenyl-3-(thiophen-2-yl)-7-(thiophen-2-ylmethylene)-3,3a,4,5,6,7-hexahydro-2*H*-indazole calculated by theoretical method is shown below. The diagram clearly shows a three stage mechanism involving two intermediates and three transition states. The activation energy in

each step can be calculated by taking the energy difference between the starting material or any intermediate and their upcoming transition state.

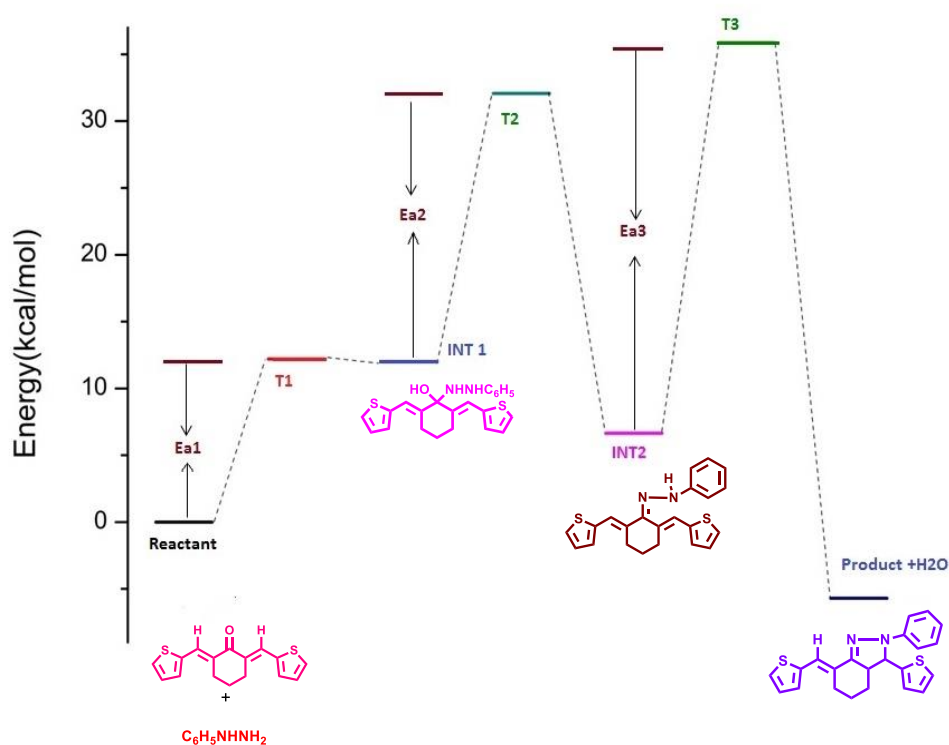


**Figure 4.1: Energy profile diagram of (E)-2-phenyl-3-(thiophen-2-yl)-7-(thiophen-2-ylmethylene)-3,3a,4,5,6,7-hexahydro-2H-indazole (6)**

Since pyrazoline formation is a multistep reaction involving three stages, we can calculate three activation energies, Ea1, Ea2 and Ea3. In the case of the above reaction, Ea1, Ea2 and Ea3 was calculated to be 12.2 Kcal/mol, 20.1 Kcal/mol and 29.1 Kcal/mol respectively. The transition states T1, T2 and T3 can be represented as given below.

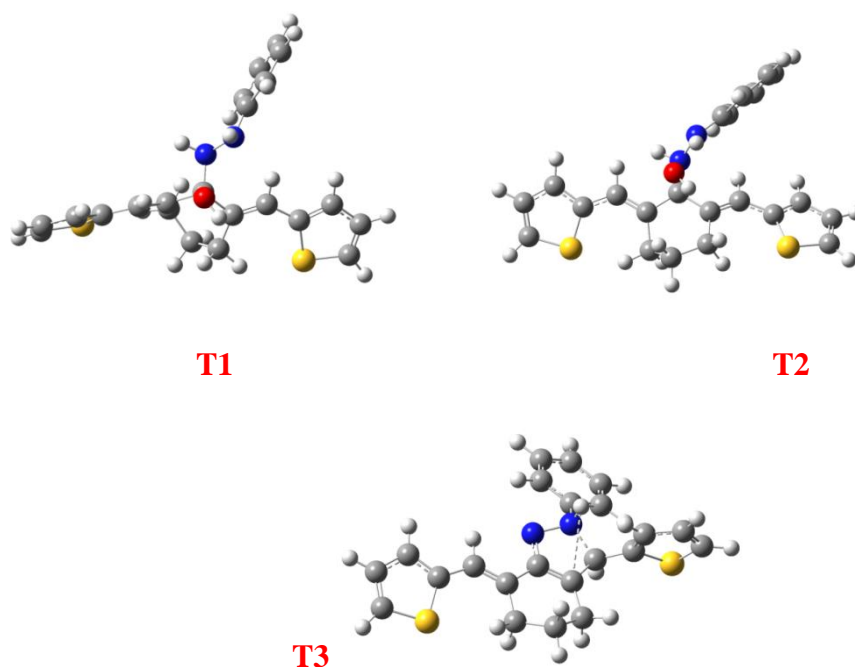


**Figure 4.2: Intermediate Transition states for the formation of (*E*)-2-phenyl-3-(thiophen-2-yl)-7-(thiophen-2-ylmethylene)-3,3a,4,5,6,7-hexahydro-2*H*-indazole (6)**

The feasibility of this reaction had already resulted in the formation of product and hence we investigated the energy profile diagrams of other four reactions which we selected for our study to compare the results obtained.

#### **4.3.2.2 (*E*)-5-(*tert*-butyl)-2-phenyl-3-(thiophen-2-yl)-7-(thiophen-2-ylmethylene)-3,3a,4,5,6,7-hexahydro-2*H*-indazole (19)**

The energy profile diagram is shown below.

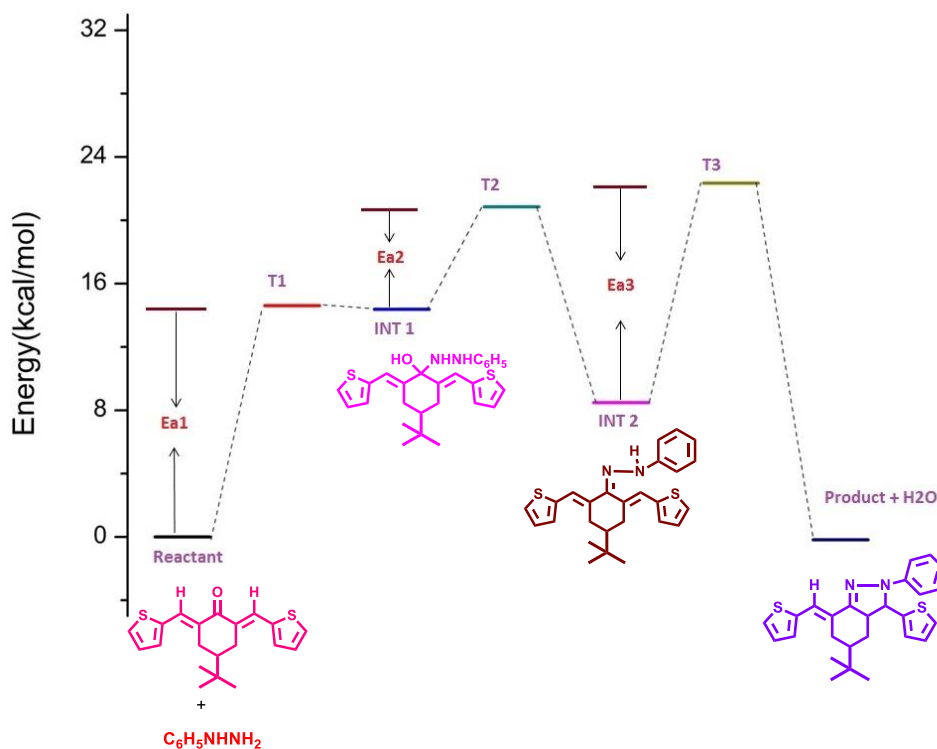
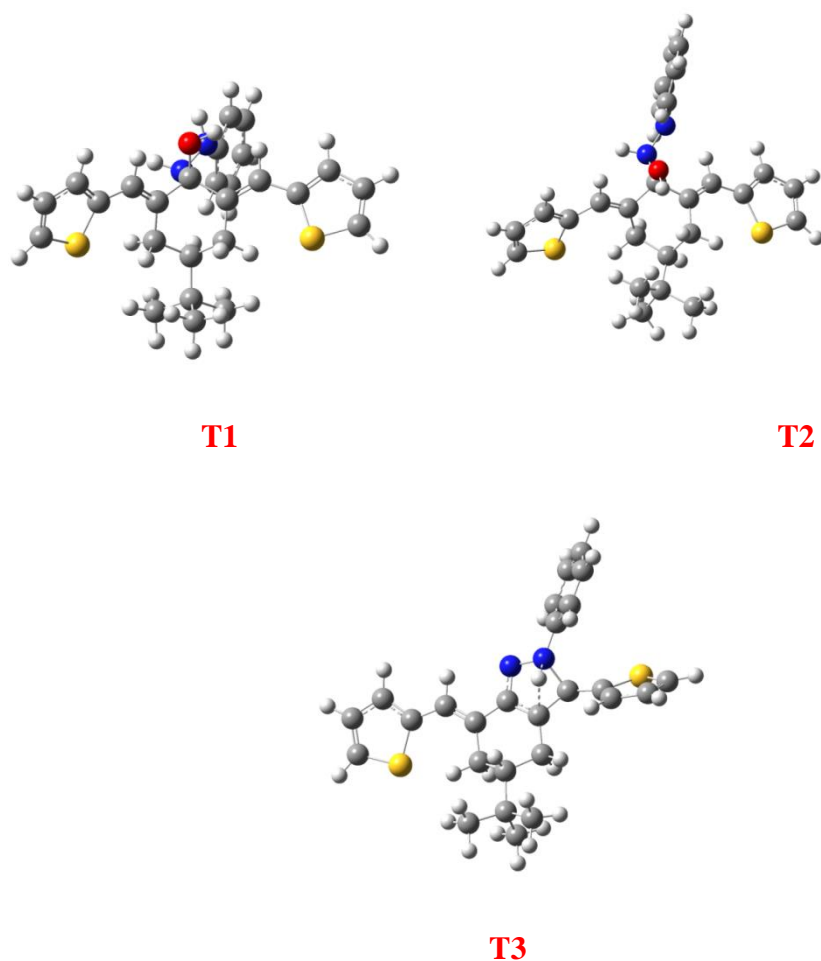


Figure 4.3: Energy profile diagram for the formation of (*E*)-5-(*tert*-butyl)-2-phenyl-3-(thiophen-2-yl)-7-(thiophen-2-ylmethylene)-3,3a,4,5,6,7-hexahydro-2*H*-indazole (19)

For the above reaction the activation energies Ea1, Ea2 and Ea3 were calculated to be 14.6 Kcal/mol, 6.48 Kcal/mol and 13.88 Kcal/mol respectively. The transition states T1, T2 and T3 are shown below.



**Figure 4.4: Intermediate Transition states for the formation (*E*)-5-(tert-butyl)-2-phenyl-3-(thiophen-2-yl)-7-(thiophen-2-ylmethylene)-3,3a,4,5,6,7-hexahydro-2*H*-indazole (19)**

**4.3.2.3 (*Z*)-2-phenyl-3-(thiophen-2-yl)-7-(thiophen-2-ylmethylene)-2,3,3a,4,6,7-hexahydrothiopyrano[4,3-*c*]pyrazole (20)**

The energy profile diagram is shown below.

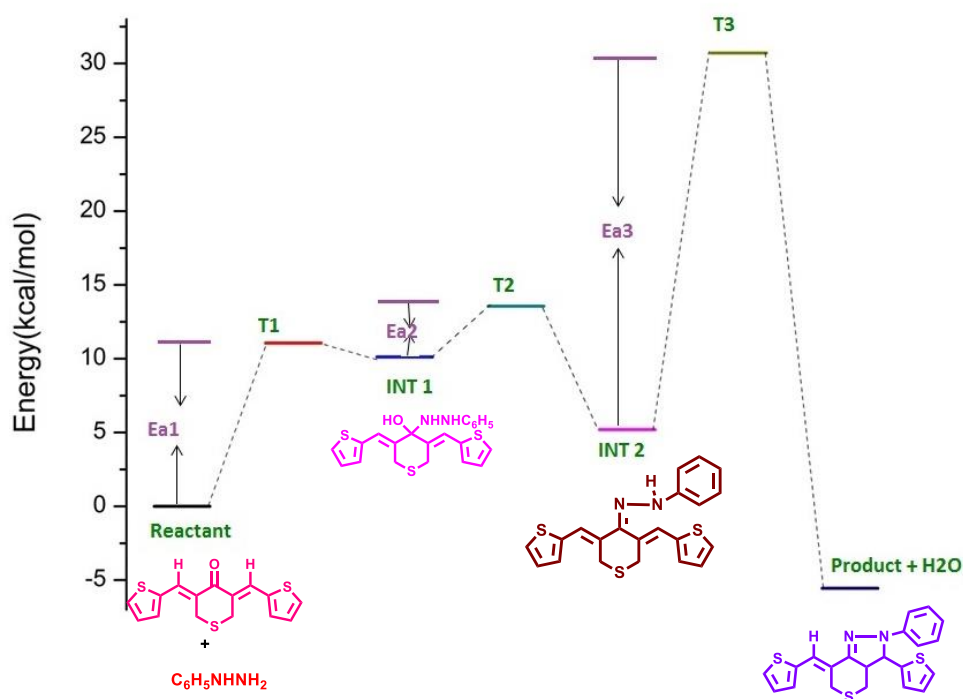


**Figure 4.5:** Energy profile diagram for formation of (Z)-2-phenyl-3-(thiophen-2-yl)-7-(thiophen-2-ylmethylene)-2,3,3a,4,6,7-hexahydrothiopyrano[4,3-c]pyrazole (20)

The activation energies Ea1, Ea2 and Ea3 were found to be 11.1 Kcal/mol, 3.44 Kcal/mol and 25.5 Kcal/mol respectively. Here too the activation energy between the first transition state and the starting material is very small of the order of 11.1 Kcal/mol and the reaction was feasible.

The transition states T1, T2 and T3 are given below.

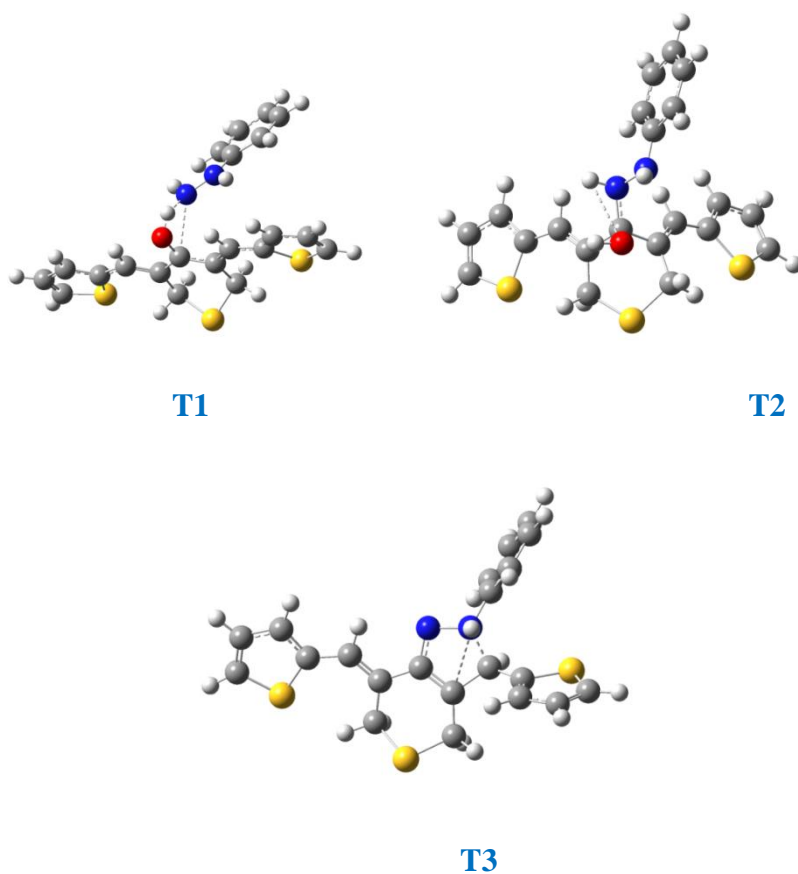


**Figure 4.6: Intermediate Transition states for the formation of (Z)-2-phenyl-3-(thiophen-2-yl)-7-(thiophen-2-ylmethylene)-2,3,3a,4,6,7-hexahydrothiopyrano[4,3-c]pyrazole (20)**

The three above shown energy profile diagrams are those of successful reactions. In the case of the unsuccessful reactions, we have obtained the energy profile diagram as shown below.

#### **4.3.2.4 Reaction of (2E,7E)-2,7-bis(thiophen-2-ylmethylene)cycloheptanone (8) with phenyl hydrazine (5)**

The energy profile diagram is shown in the figure.

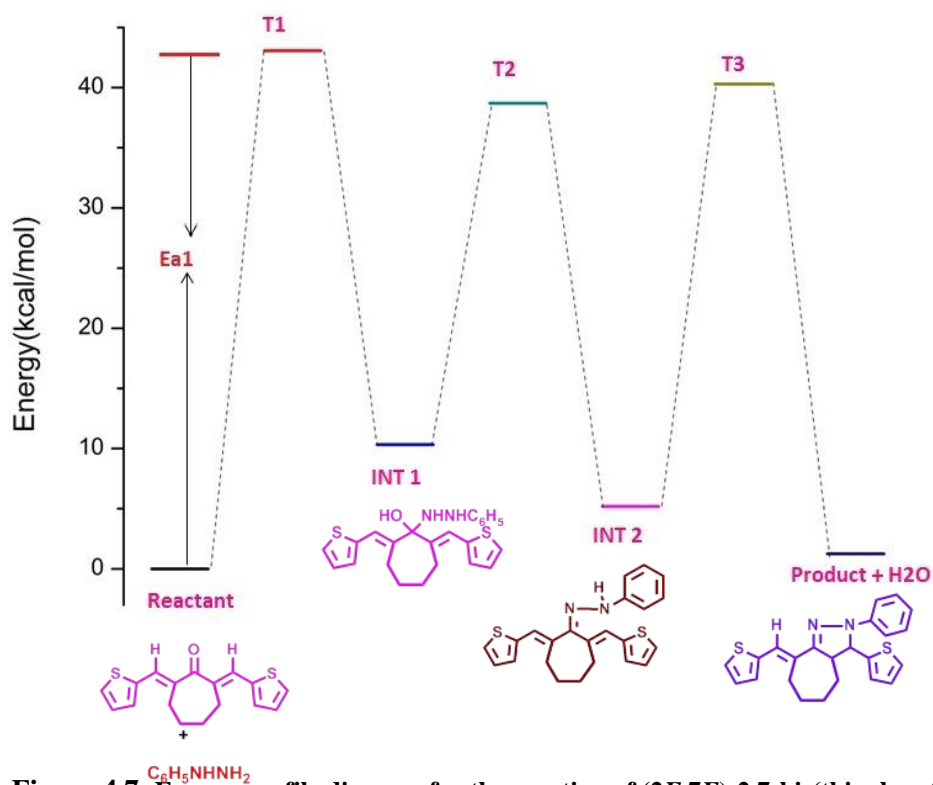


**Figure 4.7:** Energy profile diagram for the reaction of (2*E*,7*E*)-2,7-bis(thiophen-2-ylmethylene)cycloheptanone with phenyl hydrazine

Here the activation energy  $E_{a1}$  was calculated to be 43.1 Kcal/mol, which is a very large value due to which the reactants are unable to attain the intermediate 1 through a transition state T1. Hence the reaction failed to give the product.

In a similar manner, the energy profile diagram of was obtained by theoretical calculations as shown below.

#### 4.3.2.5 Reaction of (3*E*,5*E*)-3,5-bis(thiophen-2-ylmethylene)dihydro-2*H*-pyran-4(3*H*)-one (12) with phenyl hydrazine (5)

The energy profile diagram is given below.



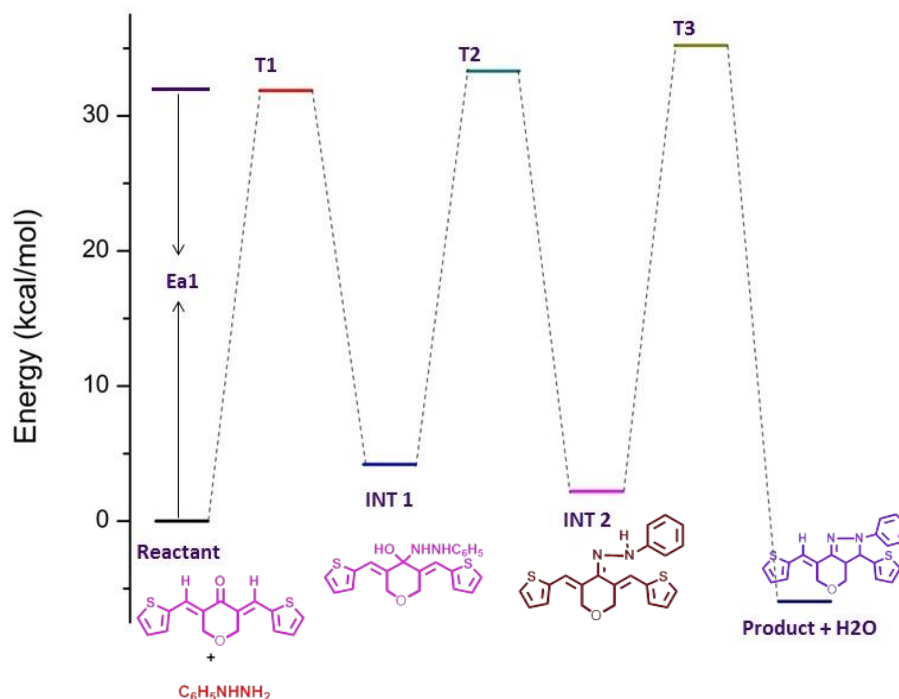


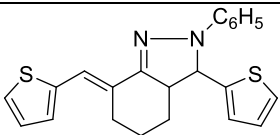
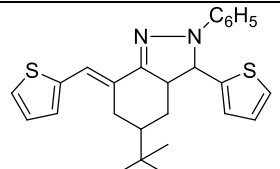
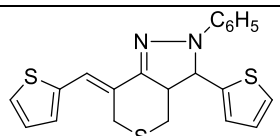
Figure 4.8: Energy Profile diagram for the reaction of (3E,5E)-3,5-bis(thiophen-2-ylmethylene)dihydro-2H-pyran-4(3H)-one with phenyl hydrazine

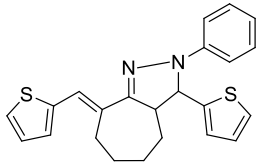
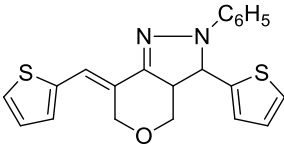
In the case of reaction of (3E,5E)-3,5-bis(thiophen-2-ylmethylene)dihydro-2H-pyran-4(3H)-one (12), similar to (2E,7E)-2,7-bis(thiophen-2-ylmethylene) cycloheptanone (8), the activation energy Ea1 for the first step is a considerably large value due to which the reaction is not feasible. The calculated Ea1 is 31.9 Kcal/mol.

To summarize, we successfully predicted the mechanism of formation of pyrazolines of bithiophene cycloalkanones by computational calculations using hybrid functional theory and it was clearly observed from energy profile diagram that the larger energy difference (Ea1) is the major factor for unsuccessful formation of pyrazolines in certain cases. The activation energies Ea1, Ea2, Ea3 corresponding to three stages of

pyrazoline formation for the selected five reactants are encapsulated in the table below.

Comparison of activation energies for the five reactions clearly depicts that the reaction has become feasible in those cases where the first activation energy  $E_{a1}$  is of the order of 10-15 Kcal/mol as shown in the table 4.1. For the latter two reactions, the  $E_{a1}$  value is of the order of greater than 30 Kcal/mol and overcoming such a huge barrier is a difficult task that resulted in unsuccessful reactions. Both oxygen and sulfur belongs to the same group in the periodic table but sulfur as heteroatom only gave products rather than oxygen or nitrogen. Substitution of sulfur as heteroatom usually increases the feasibility of a reaction which oxygen or nitrogen cannot provide. This factor further contributes to the product formation.

Expected fused pyrazoline product	Ea1 (Kcal/mol)	Ea2 (Kcal/mol)	Ea3 (Kcal/mol)
	12.2	20.1	29.1
	13.8	6.48	14.6
	11.1	3.44	25.5

	<b>43.1</b>	-	-
	<b>31.9</b>	-	-

**Table 4.1: Comparison of activation energies of the selected pyrazoline compounds for study**

From various literature reports<sup>26-29</sup>, the rate determining step in the mechanism of pyrazoline formation has been the addition of second nucleophilic nitrogen atom in the stage 3 whereas polarographic studies even though accounts for a three stage mechanism, rate determining step here is the dehydration in stage 2.

Generally for a multistep reaction, if the energy of products is lower compared with energy of reactants in the energy profile diagram the reaction is considered to be exothermic. In our study, all the energy profile diagrams clearly suggest that the pyrazoline formation is an exothermic reaction. In addition, the enthalpy change for the reaction ( $\Delta H$ ) was calculated. According to Hess's law of heat summation, the enthalpy change is negative for an exothermic reaction and the theoretical data proved to be in agreement with this result.  $\Delta H$  value obtained is summarized in the table below.

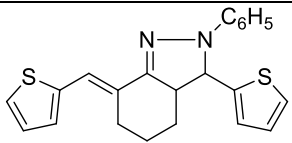
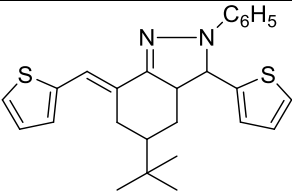
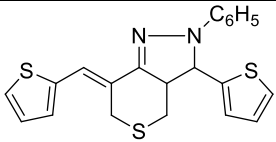
Fused pyrazoline Product	$\Delta H$
	-5.7
	-0.2
	-5.5

Table 4.2: Enthalpy values of fused pyrazoline product

#### 4.4 CONCLUSION

We synthesized six novel indazoline derivatives and one fused pyran derivative as a part of modification of carbonyl group. Owing to the intense fluorescence, we chose pyrazolines for further investigations. The un-reactivity of some bithiophene cycloalkanones towards formation of pyrazolines was noted and thus we focused our studies to mechanism of reaction by theoretical methodology. Hybrid density functional theory B3LYP/6-31G + (d) was used to determine the energy profile diagram choosing five set of reactions, viz, three successful and two unsuccessful towards pyrazoline formation. The Activation energy  $E_{a1}$  was considerably higher of the order of greater than 30 Kcal/mol for unsuccessful reactions and we reasoned that the difficulty to cross this barrier is the prime factor to be considered. The reaction was predicted to

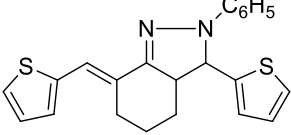
be exothermic in accordance with the energy profile diagram. The heat of formation  $\Delta H$  was also calculated and the negative value further intensified the exothermic nature of the reaction.

## 4.5 EXPERIMENTAL

All reactions were carried out using oven dried glasswares. Dried and distilled solvents were used for synthesis. Starting materials were purchased from either *Sigma-Aldrich* or *Spectrochem Chemicals* and were used without further purification. All compounds were purified by recrystallization from suitable solvents. Infra-red spectra were recorded using *Jasco 4100* and *ABB Bomem (MB Series) FT-IR* spectrometers. The  $^1\text{H}$  NMR spectra was recorded at 400 MHz on a *Bruker Avance III* FT-NMR spectrometer with tetramethyl silane (TMS) as internal standard. Chemical shifts ( $\delta$ ) are reported in parts per million (ppm) downfield of TMS. The theoretical calculations were done using B3LYP/6-31G + (d) theory and all calculations were done using G09 suites of codes. The effect of ethanol solvent was also considered while optimizing the results.

### 4.5.1 Synthesis of (*E*)-2-phenyl-3-(thiophen-2-yl)-7-(thiophen-2-ylmethyl ene)-3,3a,4,5,6,7-hexahydro-2*H*-indazole from (2*E*, 6*E*)-2, 6-bis(thiophen-2-yl-methylene) cyclohexanone (19) .

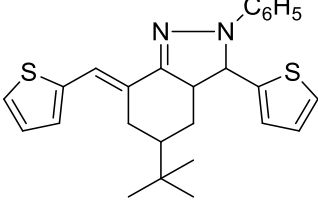
To a mixture of (2*E*,6*E*)-2,6-bis(thiophen-2-yl-methylene)cyclohexanone (**4**, 0.500 g, 1.9 mmol) and phenyl hydrazine (**5**, 0.415 g, 3.8 mmol) in ethanol, a few drops of piperidine was added and the mixture was refluxed overnight. Progress of the reaction was monitored by TLC.

Structure	Physical data
	<p><i>Characterisation data:</i> Yield: 87%, mp: 138-140 °C; IR (KBr): 2930, 2856, 1639, 1548, 1378, 1296 cm<sup>-1</sup>; <sup>1</sup>H NMR CDCl<sub>3</sub>: 7.53-7.52 (m, 1H), 7.33-7.32 (m, 1H), 7.26 (m, 1H), 7.18-7.15 (m, 1H), 7.09-7.07 (m, 4H), 7.06-7.05 (m, 2H), 7.00-6.98 (m, 1H), 6.88-6.84 (m, 1H), 4.81 (d, 1H, 12 Hz), 3.19-3.05 (m, 2H), 2.42-2.33 (m, 1H), 2.22-2.20 (m, 1H), 2.06-2.01 (m, 1H), 1.64-1.53 (m, 2H); <sup>13</sup>C NMR CDCl<sub>3</sub>: 153.4, 147.1, 145.9, 140.2, 129.3, 128.7, 127.6, 127.2, 127.1, 126.5, 125.0, 123.9, 120.8, 119.6, 115.5, 77.3, 77.0, 76.7, 70.2, 57.1, 28.5, 28.5, 23.7; MS <i>m/z</i>: 376 (<i>M</i><sup>+</sup>); Anal. Calcd for C<sub>22</sub>H<sub>20</sub>S<sub>2</sub>N<sub>2</sub>: C: 70.15, H: 5.29, N: 7.32, S: 16.98. Found: C: 70.18, H: 5.35, N: 7.34, S: 17.00.</p>

When reactants were fully consumed, the reaction mixture was cooled overnight and the product crystallized was collected out by filtration, washed with ethanol. The product resulted as fluorescent yellow crystals.

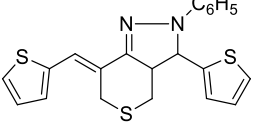
#### 4.5.2 Synthesis of (*E*)-5-(*tert*-butyl)-2-phenyl-3-(thiophen-2-yl)-7-(thiophen-2-ylmethylene)-3,3a,4,5,6,7-hexahydro-2*H*-indazole from (*2E*, *6E*)-2, 6-bis (thiophen-2yl-methylene) *t*-butyl cyclohexanone (**20**).

To a mixture of (*2E*, *6E*)-2, 6-bis (thiophen-2yl-methylene) *t*-butyl cyclohexanone (**9**, 0.7 g, 4.4 mmol) and phenyl hydrazine (5, 0.9 g, 8.8 mmol) in ethanol, a few drops of piperidine were added and refluxed overnight. When reactant was fully consumed, the reaction mixture was cooled and the product crystallised was collected out by filtration, washed with ethanol. The product resulted as fluorescent yellow crystals.

Structure	Physical data
	<p><i>Characterisation data:</i> Yield: 82%, m.p: 176-178 °C; IR (KBr): 3113, 2957, 2858, 1636, 1595, 1497, 1309, 1050, 749 cm<sup>-1</sup>; <sup>1</sup>H NMR: 7.56-7.55 (m,1H), 7.35-7.33 (m, 1H), 7.27-7.26 (m, 1H), 7.21-7.13 (m, 5H), 7.11-7.10 (m, 1H), 7.08-7.06 (m, 1H), 7.02-7.00 (m, 1H), 6.88-6.84 (m, 1H), 4.81 (d,1H), 3.24 (dd, 16 and 12 Hz), 3.13-3.06 (m, 1H), 2.24-2.20 (m, 1H), 2.16-2.08 (m,1H), 1.52-1.36 (m,2H), 0.97 (s, 9H). <sup>13</sup>C NMR: 153.6, 147.2, 146.0, 140.2, 129.5, 128.7, 127.2, 127.1, 127.12, 126.5, 125.0, 123.9, 120.8, 119.8, 115.5, 70.4, 57.5, 45.7, 32.8, 30.1, 29.8, 27.5; MS <i>m/z</i>: 431(<i>M</i><sup>+</sup>); Anal. Calcd for C<sub>26</sub>H<sub>28</sub>S<sub>2</sub>N<sub>2</sub> : C: 72.15, H: 6.52, N: 6.47, S: 14.82, Found: C: 72.01, H: 6.48, N: 6.40, S: 14.81.</p>

#### 4.5.3 Synthesis of (Z)-2-phenyl-3-(thiophen-2-yl)-7-(thiophen-2-ylmethylene)-2,3,3a,4,6,7-hexahydrothiopyrano[4,3-c]pyrazole from (3Z,5Z)-3,5-bis(thiophen-2-ylmethylene) dihydro-2H-thiopyran-4(3H)-one (21).

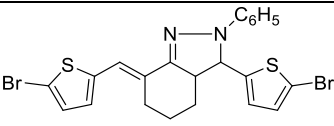
To a mixture of (3*E*,5*E*)-3,5-bis(thiophen-2-ylmethylene)dihydro-2*H*-pyran-4(3*H*)-one (**11**, 0.1 g, 8.8 mmol) and phenyl hydrazine hydrochloride(5, 0.9 g, 8.8 mmol) in ethanol, a few drops of piperidine was added and refluxed overnight. The progress of the reaction was monitored by TLC and the reaction mixture was cooled and the product crystallised was collected out by filtration, washed with ethanol. The product resulted as fluorescent yellow crystals.

Structure	Physical data
	<p><i>Characterisation data:</i> Yield: 80%, m.p: 162-164 °C, IR (KBr): 2922, 2855, 1642, 1492, 1378, 1312, 1058, 753 cm<sup>-1</sup>; <sup>1</sup>H NMR: 7.48 (s, 1H), 7.36 (d, 4.8 Hz), 7.28 (dd, 4.8 and 4 Hz), 7.21-7.15 (m, 5H), 7.10-7.06 (m, 2H), 7.01-6.99 (m, 1H), 6.91-6.87 (m, 1H), 4.81 (d, 1H), 4.01 (d, 1H), 3.65 (dd, <math>J_1 = 14.8</math> and <math>J_2 = 12.8</math> Hz, 1H), 3.54-3.47 (m, 1H), 3.01-2.89 (m, 2H); <sup>13</sup>C NMR: 150.7, 146.5, 144.7, 139.0, 130.0, 128.7, 127.3, 127.2, 126.9, 125.4, 125.15, 124.3, 121.2, 120.1, 115.5, 69.2, 58.1, 30.7, 29.2; MS <math>m/z</math>: 393 (<math>M^+</math>); Anal. Calcd for C<sub>21</sub>H<sub>18</sub>S<sub>3</sub>N<sub>2</sub> : C: 63.92, H: 4.60, N: 7.10, S: 24.38, Found: C: 63.87, H: 4.56, N: 7.10, S: 24.30.</p>

#### 4.5.4 Synthesis of (*E*)-3-(5-bromothiophen-2-yl)-7-((5-bromothiophen-2-yl)methylene)-2-phenyl-3,3a,4,5,6,7-hexahydro-2*H*-indazole from (*2E,6E*)-2,6-bis((5-bromothiophen-2-yl)methylene) cyclohexanone (15).

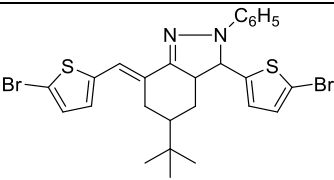
To a mixture of (*2E,6E*)-2,6-bis((5-bromothiophen-2-yl)methylene) cyclohexanone (13, 0.80g, 1.5mmol) and phenyl hydrazine (5, 0.32g, 3.0mmol) in ethanol, a few drops of piperidine was added and refluxed overnight. When reactant was fully consumed, the reaction mixture was cooled and the product crystallised was collected out by filtration, washed with ethanol and dried. The product resulted as fluorescent yellow crystals.



Structure	Physical data
	Characterisation data: Yield: 96%; m.p: 152 °C; IR (KBr): 2930, 2861, 1598, 1489, 1443, 1298, 1181, 1109, 1085, 940, 835 cm <sup>-1</sup> ; <sup>1</sup> H NMR (CDCl <sub>3</sub> ): 7.32 (s, 1H), 7.15-7.09 (m, 2H), 7.09-7.07 (d, 1H), 6.87-6.86 (m, 1H), 6.83-6.82 (d, 1H), 6.78-6.77 (m, 1H), 4.66-4.64 (d, 1H), 2.98-2.95 (m, 2H), 2.77-2.74 (m, 2H), 2.66-2.64 (m, 1H), 1.92-1.88 (m, 2H), MS: <i>m/z</i> : 533 ( <i>M</i> <sup>+</sup> ), Anal. Calcd. for C <sub>22</sub> H <sub>18</sub> Br <sub>2</sub> N <sub>2</sub> S <sub>2</sub> : Found: C: 49.45, H: 3.40, N: 5.24, S: 12.00, Calculated: C: 49.44, H: 3.36, N: 5.03, S: 12.01.

#### 4.5.5 Synthesis of (*E*)-3-(5-bromothiophen-2-yl)-7-((5-bromothiophen-2-yl)methylene)-5-(tert-butyl)-2-phenyl-3,3a,4,5,6,7-hexahydro-2H-indazole from (*2E,6E*)-2,6-bis((5-bromothiophen-2-yl)methylene)*t*-butyl cyclohexanone (16)

To a mixture of (*2E,6E*)-2,6-bis((5-bromothiophen-2-yl)methylene) *t*-butylcyclohexanone(14, 0.89 g, 1.5 mmol) and phenylhydrazine (**5**, 0.32 g, 3.0 mmol) in ethanol, a few drops of piperidine was added and refluxed overnight. The reaction mixture was cooled and the product crystallised was collected out by filtration, washed with ethanol. The product resulted as fluorescent yellow crystals.

Structure	Physical data
	Characterisation data: Yield: 25%; m.p: 164 °C; IR (KBr.): 3067, 2957, 2861, 1596, 1493, 1443, 1369, 1221, 1109, 1044, 965, 890, 837, 793, 692, 568 cm <sup>-1</sup> ; <sup>1</sup> H NMR (CDCl <sub>3</sub> ): δ 7.48 (s, 1H), 7.42-7.41 (s, 1H), 7.34-7.29 (m, 3H), 6.93-6.92 (m, 1H), 6.89-6.88 (m, 1H), 6.80-6.79 (m, 1H), 6.49-6.48 (m, 1H), 3.22-3.19 (d,

	1H), 2.76-2.72 (dd, 1H, 12Hz and 8Hz), 2.38-2.32(dd, 1H 12Hz and 4 Hz ), 2.14-2.08 (m, 1H), 1.78-1.56 (m, 3H), 1.01-1.00 (d, 2H), 0.94-0.91(m, 3H), 0.86-0.82 (m, 3H); <sup>13</sup> C NMR: 148.9, 142.4, 130.1, 129.8, 129.2, 128.5, 128.3, 126.0, 119.6, 115.6, 77.2, 77.0, 76.8, 46.1, 32.7, 29.3, 27.6, 27.4, 22.7; MS: <i>m/z</i> : 589 ( <i>M</i> <sup>+</sup> ); Anal. Calcd. for C <sub>26</sub> H <sub>26</sub> Br <sub>2</sub> S <sub>2</sub> N <sub>2</sub> : C: 52.89, H: 4.44, N: 4.74, S: 10.86; Found: C: 52.86, H:4.24, N: 4.69, S: 10.85.
--	--

**4.5.6 Synthesis of (Z)-3-(5-bromothiophen-2-yl)-7-((5-bromothiophen-2-yl)methylene)-2-phenyl-2,3,3a,4,6,7-hexahydrothiopyrano[4,3-c]pyra zole from (3Z,5Z)-3,5-bis((5-bromothiophen-2-yl)methylene)dihydro-2H-thiopyran-4(3H)-one (18)**

To a mixture of (3Z,5Z)-3,5-bis((5-bromothiophen-2-yl)methylene)dihydro-2H-thiopyran-4(3H)-one (**17**, 0.82 g, 1.5 mmol) and phenyl hydrazine (0.32 g, 3.0 mmol) in ethanol, a few drops of piperidine was added and refluxed overnight. The product resulted as fluorescent yellow crystals.

Structure	Physical data
	<p><i>Characterisation data:</i> Yield: 40%; m.p: 150 °C; IR (KBr): 2830, 1595, 1491, 1422, 1283, 1175, 1054, 966, 889, 751, 694; <sup>1</sup>H NMR (CDCl<sub>3</sub>) δ 7.51 (s, 1H), 7.34-7.26 (m, 2H), 7.19-7.06 (m, 2H), 6.96-6.93 (dd, 2H, 8Hz and 4Hz), 6.90-6.89 (m, 1H), 6.88-6.78 (m, 1H), 6.53-6.52 (d, 1H); <sup>13</sup>C NMR: 150.6, 146.2, 140.5, 130.3, 130.1, 130.0, 129.2, 125.8, 124.7, 121.7, 119.7, 115.7, 114.1, 112.6, 77.2, 77.0, 76.8, 69.3, 57.9, 30.9, 29.2;</p>

	MS: $m/z$ : 551 ( $M^+$ ); Anal. Calcd. for $C_{21}H_{16}Br_2S_3N_2$ : C: 52.86, H:4.24, N: 5.07, S: 17.42, Found: C: 52.83, H: 4.00, N: 5.02, S: 17.40.
--	--

#### 4.6 REFERENCES

- 1) Palaska, E.; Erol, D.; Demirdamar, R. *Eur. J. Med. Chem.* **1996**, *31*, 43.
- 2) Shahar, M. Y.; Siddiqui, A. A.; Ali, M. A. *Bioorg. Med. Chem. Lett.*, **2006**, *16*, 4571.
- 3) Elguero, J.; Goya, P.; Jagerovic, N.; Silva, A. M. S. *Targets Heterocycl. Syst.* **2002**, *6*, 52.
- 4) Bilgin, A. A.; Palaska, E.; Sunal, R.; Guemuesel, D. *Pharmazie* **1994**, *49*, 67.
- 5) Abbady, M. A.; Hebbachy, R. *Indian J. Chem. Sect. B.* **1993**, *32*, 1119.
- 6) Attia, A.; Michael, M. *Acta Chim. Hung.* **1983**, *114*, 337.
- 7) Descacq, P.; Nuhrich, F.; Varache-Beranger, V.; Capdepuy, V.; Devaux, D. *Eur. J. Med.Chem.* **1990**, *25*, 285.
- 8) Ankiwala, M. D. *J. Indian Chem. Soc.* **1990**, *67*, 514.
- 9) Fahmy, A. M.; Hassan, K. M.; Khalaf, A. A.; Ahmed, R. A. *Indian J. Chem. Sect. B.* **1987**, *26*, 884.
- 10) Rahman, A.; Siddiqui, A. A. *IJPSR* **010**, *2*, 165.
- 11) Li, J. F.; Guan, B.; Li, D. X.; Dong, C. *Spectrochim. Acta* **2007**, *68*, 404.
- 12) Bai, G.; Li, J.; Li, D.; Dong, C.; Han, X.; Lin, P. *Dyes Pigm.* **2007**, *75*, 93.

- 13) Lu, Z.; Jiang, Q.; Zhu, W.; Xie, M.; Hou, Y.; Chen, X.; Wang, Z. *Syn. Met.* **2000**, *111*, 465.
- 14) Ali, N. A.; Dar, B. A.; Pradhan, V.; Farooqui, M. *Mini Rev. Med. Chem.* **2013**, *13*, 1792.
- 15) Schmidt, A.; Beutler, A.; Snovydovych, B. *Eur. J. Org. Chem.* **2008**, *354*, 4073.
- 16) Fischer, E.; Knoevenagel, O. *Ann.* **1887**, 239, 194.
- 17) Auwers, K. V.; Muller, K. *Ber.* **1908**, *41*, 4230.
- 18) Auwers, K. V.; Kreuder, A. *Ber.* **1925**, *58*, 1974.
- 19) Auwers, K. V.; Cauer, E. *Ann.* **1929**, *470*, 284.
- 20) Levai, A. *Chemistry of Heterocyclic compounds* **1997**, *33*, 6.
- 21) Lorand, T.; Szabo, D.; Foldesi, A.; Parkanyi, L.; Kalman, A.; Neszmelyi, A. *J. Am. Chem. Soc.* **1985**, *1*, 481.
- 22) Paur, M. S.; Rovnyak, G. C.; Cohen, A. I.; Toeplitz, B.; Gougoutaz, J. *Z. J. Org. Chem.* **1979**, *44*, 2513.
- 23) Rovnyak, G. C.; Shu, V. *J. Org. Chem.* **1979**, *44*, 2518.
- 24) Hu, Z.; Lou, C.; Wang, J.; Chen, C.; Yan, M. *J. Org. Chem.* **2011**, *76*, 3797, 3804.
- 25) a) Inokuma, T.; Hoashi, Y.; Takemoto, Y. *J. Am. Chem. Soc.* **2006**, *128*, 9413. b) Zhao, S. L.; Zheng, C. W.; Zhao, G. *Tetrahedron Asymmetry*, **2009**, *20*, 1046. c) Li, X. F.; Kun, L. F.; Lian, C.X.; Zhong, L.; Chen, Y. C.; Liao, J.; Zhu, J.; Deng, J. G. *Org. Biomol. Chem.* **2008**, *6*, 349. d) Russo, A.; Perfetto, A.; Lattanzi, A. *Adv. Synth. Catal.* **2009**, *351*, 3067. e) Ren, Q.; Gao, Y. J.; Wang, J. *Chem. Eur. J.* **2010**, *16*, 13594.
- 26) Ueda, A.; Ogasawara, K.; Nishida, S.; Ise, T.; Yoshino, T.; Nakazawa, S.; Sato, K.; Takui, T.; Nakasuji, K.; Morita, Y. *Angew. Chem. Int. Ed.* **2010**, *122*, 6333.

- 27) Kubo, T.; Katada, Y.; Shimizu, A.; Hirao, Y.; Sato, K.; Takui, T.; Uruichi, M.; Yakushi, K.; Haddon, R. C. *J. Am. Chem. Soc.* **2011**, 133, 14240.
- 28) Suchchar, S. P.; Singh, A. K. *J. Indian Chem. Soc.* **1985**, 62, 142.
- 29) Ferres, H.; Hamdam, M. S.; Jackson, W. R. *J. Chem. Soc. B.* **1971**, 1892.



## Chapter 5

### **Synthesis and study of third order non-linear optical properties and Schottky junction characteristics of a few thiophene based polymers synthesized through Stille coupling and direct arylation reactions**

---

#### *5.1 Abstract*

*This chapter describes the synthesis of novel yellow light emitting polymer and oligomer of (E)-3-(thiophen-2-yl)-7-((5-thiophen-2-yl)methylene)-2-phenyl-4,5,6,7-tetrahydro-2H-indazoles by Stille coupling and direct arylation method. Our prime focus is to investigate the difference in nature of products formed and their properties when subjected to the two different polymerization techniques. All new polymers were characterized using NMR, IR, Powder XRD, UV-Visible and PL spectra, SEM, Cyclic Voltammetry and AFM studies. Computational methods were adopted to estimate band gaps of these materials. Non-linear optical studies were carried out using Z-scan technique. The measurement of I-V characteristics shows the formation of Schottky junction making them suitable materials for fabricating PLEDs.*

---

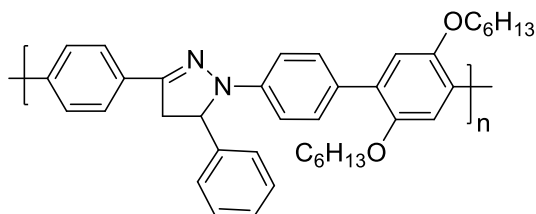
#### **5.2 INTRODUCTION**

Stille coupling<sup>1,2</sup> and direct arylation<sup>3-6</sup> methods are versatile techniques used for carbon-carbon bond forming process in organic chemistry. Stille coupling employs palladium promoted coupling of organotin compounds and is advantageous<sup>7-10</sup> in the sense that it requires mild conditions and produces high yield of products. The use of palladium as catalyst gives tolerance to many functional groups. High molecular weight products are formed by proper choice of solvents that could stabilize Pd catalyst. The reaction involves three stages.

- a) Oxidative Insertion in which the electrophilic carbon reacts with Pd(0) complex forming Pd(II).
- b) Transmetallation where the transfer occurs between two metal centers, i.e, the transfer of substituent from tin center to palladium thus forming a palladium complex which incorporates both the fragments that are to be coupled.
- c) Reductive elimination where the product is generated with recycle of the catalyst.

Both Pd(0) and Pd(II) can be tolerated for Stille reactions but with Pd (II) as catalyst the reduction to Pd(0) by organostannanes is a crucial step. The transfer of substituent from tin complex to palladium center is a slow process with high selectivity. Even though this is good traditional coupling reaction being used for years, the toxicity of organostannanes involved is a major disadvantage. Compared with Stille coupling, direct arylation bears the advantage of less toxicity but here regioselectivity is a factor to be considered. However, if the reactive site is specific, this problem can be overruled. As already discussed previous chapters, thiophene<sup>11-14</sup> based oligomers<sup>15,16</sup> and polymers are being widely explored owing to their interesting applications in devices and non-linear optics<sup>17</sup>. Fang<sup>18</sup> and co-workers have effectively synthesized highly photoluminiscent and electrochemically active polymers having 2-pyrazoline units in the chain as shown below.



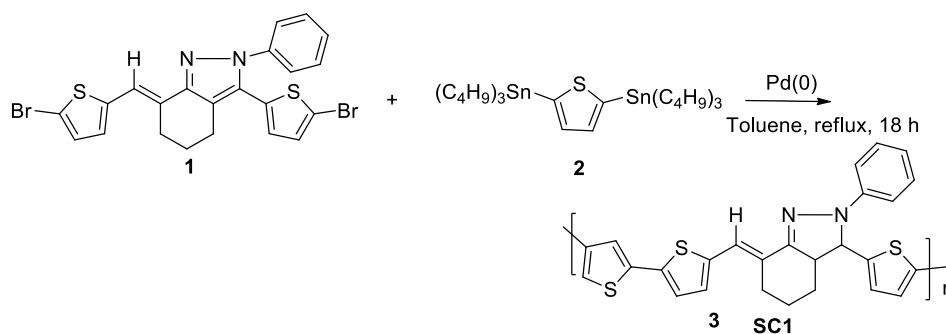


In the present study, we tried to synthesize a few novel organic materials incorporating pyrazoline ring so as to study their applications in non-linear optics and optoelectronic devices.

### 5.3 RESULTS AND DISCUSSION

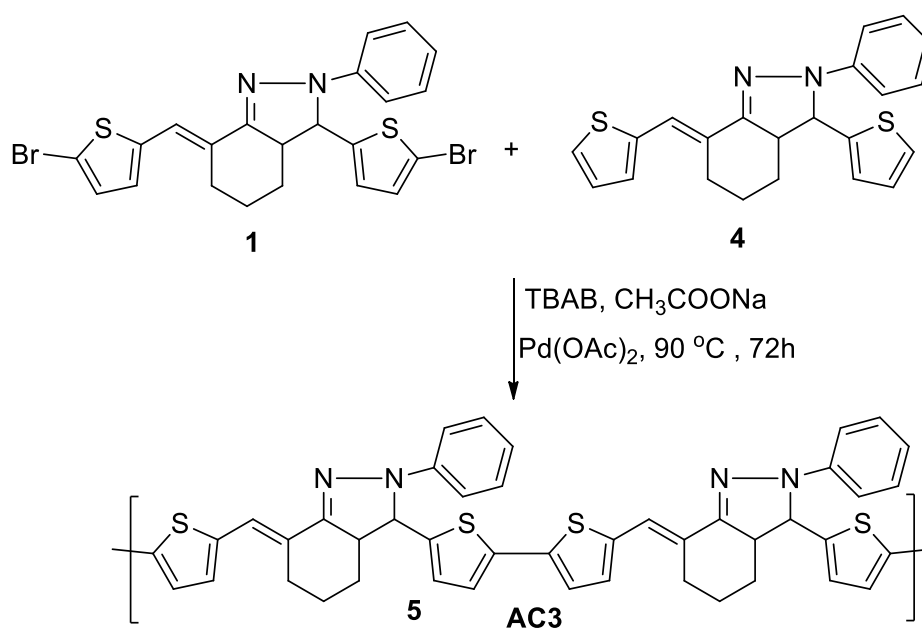
We synthesized two novel yellow light emitting materials **SC1** and **AC3** by polymerization of hexahydro-2*H*-indazole derivatives using Stille coupling and direct arylation techniques. The scheme of synthesis of **SC1** is shown below (Scheme 5.1). Scheme for synthesis of precursors **1** and **2** are described in sections 4.2.2 and 4.2.5 of Chapter 4 of this thesis.

Gel permeation chromatographic(GPC) analysis was carried out to determine the molecular weight of the product **SC1**.  $M_w$  and  $M_n$  was found to be 6358 and 5225 with PDI of 1.22. Thus **SC1** has 15 repeating units and it can be considered as a polymer.



Scheme 5.1: Synthesis of polymer SC1

In continuation, we carried out direct arylation reaction between monomers **1** and **4** to give oligomer **AC3** as shown in Scheme 5.2.



Scheme 5.2: Synthesis of oligomer **AC3**

GPC analysis revealed the *M<sub>w</sub>* and *M<sub>n</sub>* values to be 2489 and 2478 with PDI 1.004. Thus the formed material was an oligomer with good PDI value. The low molecular weight may be attributed to the steric effect of two bulky pyrazoline rings present in one unit. In the case of **SC1**, the thiophene ring imparts much more flexibility to the system as a whole which leads to increased molecular weight. The structure was confirmed by <sup>1</sup>H NMR and IR spectra.



C-H stretching is indicated by the peaks  $2926\text{cm}^{-1}$  and  $2932\text{cm}^{-1}$  for **SC1** and **AC3** respectively.

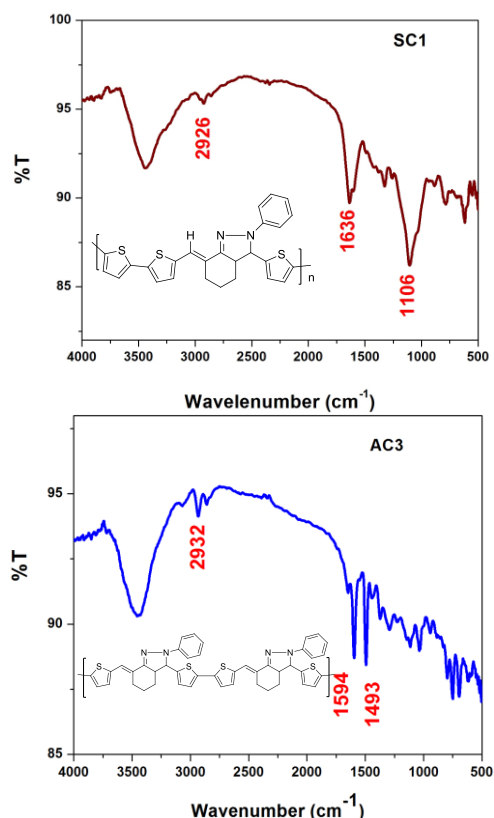
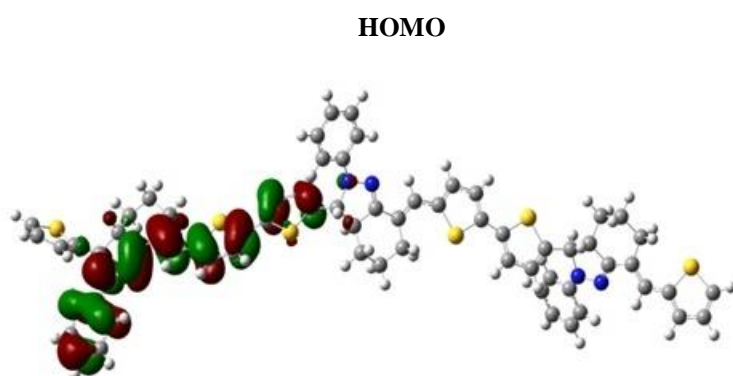
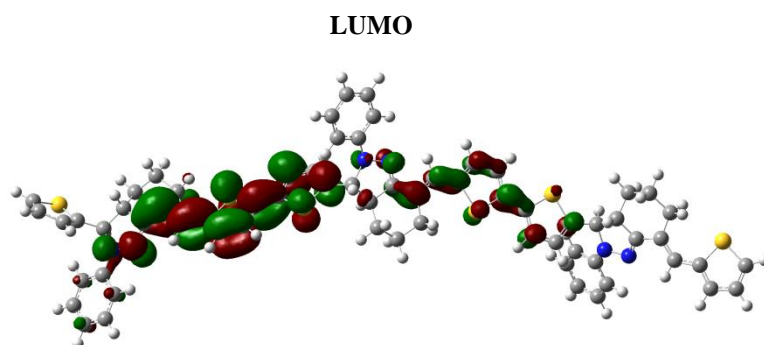
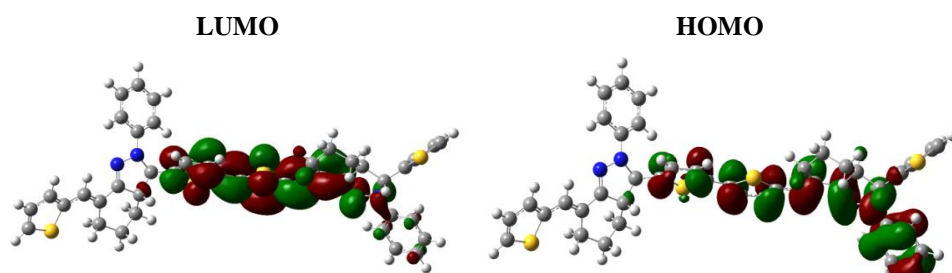


Figure 5.2: FTIR spectra of SC1 and AC3

### 5.3.3 Theoretical interpretation of influence of chain length on band gap of SC1 and AC3

In the case of oligomers **AC1**, **AC2** (Chapter 3) and **AC3** synthesized by direct arylation, almost three repeating units were obtained. By using computational calculations, we inferred that further increase in number of units have negligible effect on the band gaps of the compounds. This was

optimized using hybrid density functional theory and AC3 compound was taken as reference.



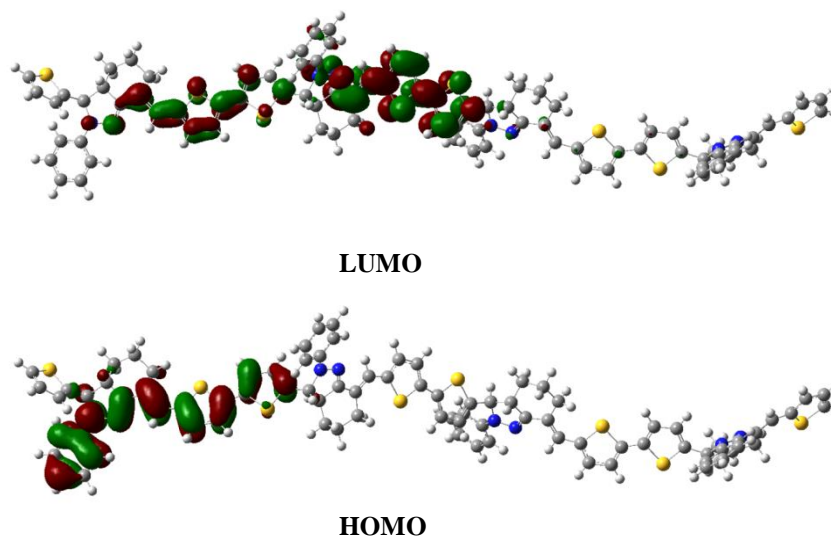


**Figure 5.3: Representative frontier orbitals of two, three and four repeating units of AC3 basic unit**

The representative frontier molecular orbitals corresponding to the basic structure of AC3 having two repeating, three repeating and four repeating units are given above in figure 5.3.

	HOMO (eV)	LUMO (eV)	E <sub>g</sub> (eV)
<b>2 unit</b>	<b>-4.68</b>	<b>-1.76</b>	<b>2.42</b>
<b>3 unit</b>	<b>-4.69</b>	<b>-1.78</b>	<b>2.41</b>
<b>4 unit</b>	<b>-4.69</b>	<b>-1.79</b>	<b>2.40</b>

**Table 5.1: Comparison of band gaps**

The table gives the band gaps estimated for oligomers having 2, 3 and 4 repeating units which reveals that the increase in number of units have negligible influence in the band gap of the compounds, all lying in the semiconductor range. Thus it is inferred that further increase in the chain length of such units may not alter band gap of the molecule.

### 5.3.4 POWDER X-RAY DIFFRACTION

Powder XRD depicts the crystalline nature of the compounds which in turn describes its molecular arrangement. Figure shows the Powder XRD of SC1 and AC3.

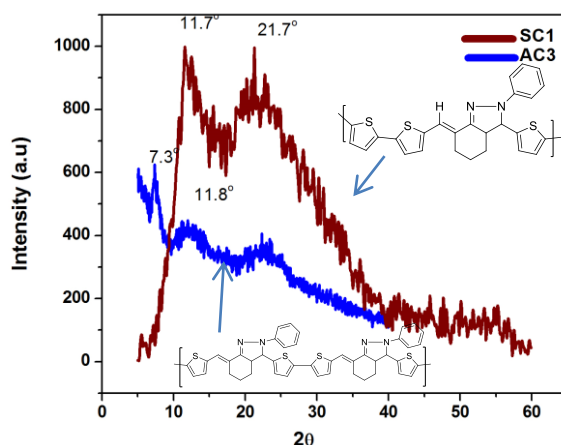


Figure 5.4: Powder X-ray diffraction spectra of SC1 and AC3

SC1 shows two sharp peaks at  $2\theta$  values  $11.7^\circ$  and  $21.7^\circ$ . The peak is sharp at the top while broad towards bottom. The XRD spectra of AC3 show a sharp peak at  $2\theta$  value  $7.3^\circ$  while the peak at  $11.8^\circ$  is broad. The sharp peak indicates the crystalline nature of the compound whereas the broad peak is an indication of amorphous nature of the compound. Both sharp and broad peaks in our compounds thus show its semi-crystalline nature.

### 5.3.5 UV-VISIBLE AND PHOTOLUMINISCENCE SPECTRA

UV-visible and PL spectra provide valuable information on electronic structure of the compound.

Figure 5.5 shows the UV-Visible and PL spectra of the monomer 1.

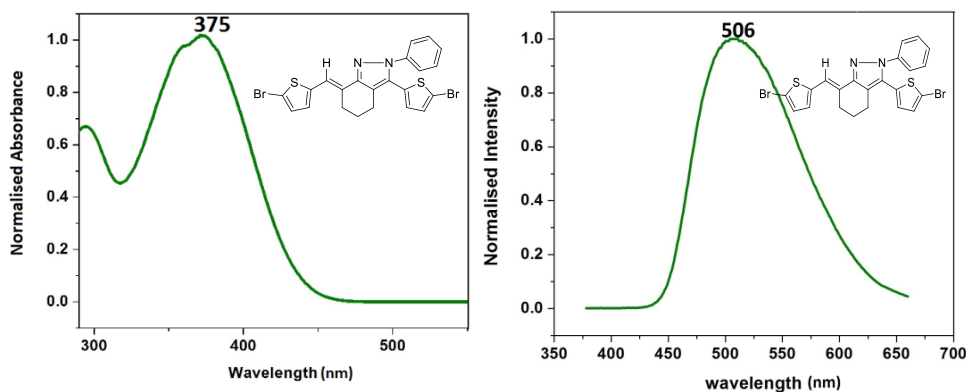


**Figure 5.5: UV-Visible and PL spectra of monomer pyrazoline**

The monomer shows an absorption maximum at 375 nm and an emission at 506 nm. Under UV irradiation at 350 nm, monomer exhibited green emission in solution state and greenish yellow emission in solid state.



**Figure 5.6: Solid state emission of monomer pyrazoline under UV irradiation**

The spectrum of polymer and oligomer is given below. **SC1** and **AC3** show absorption maxima at 444 and 420 nm which corresponds to  $\pi$ - $\pi^*$  transition. The emission spectra of these compounds are at 555 nm and 545 nm which lies in the UV-visible region.



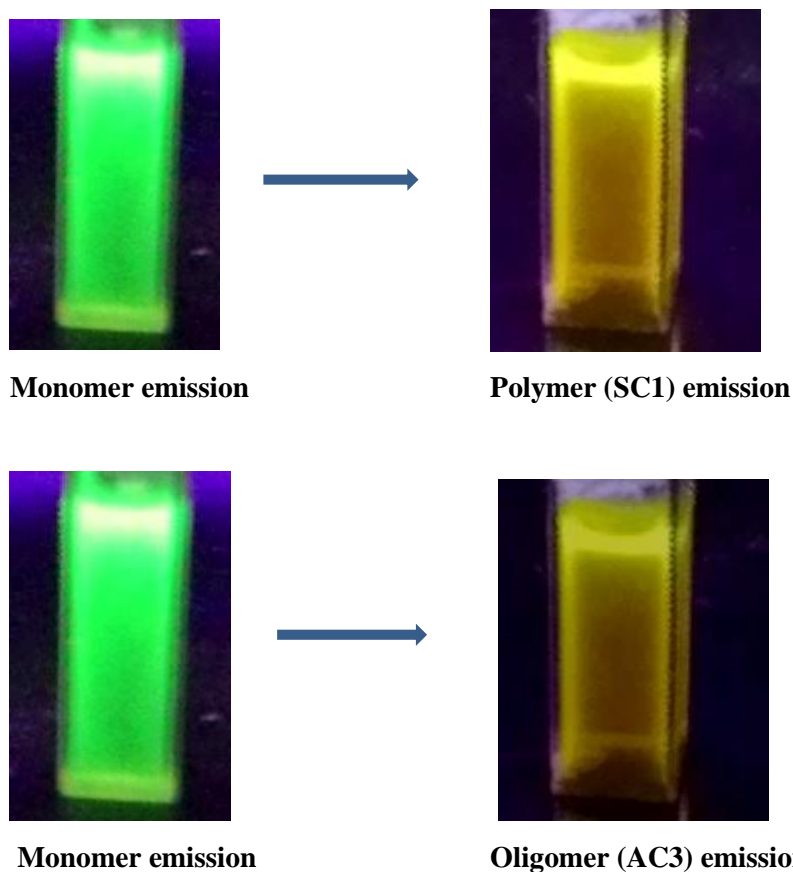


Figure 5.7: Emission of monomer, polymer and oligomer in solution state under UV irradiation

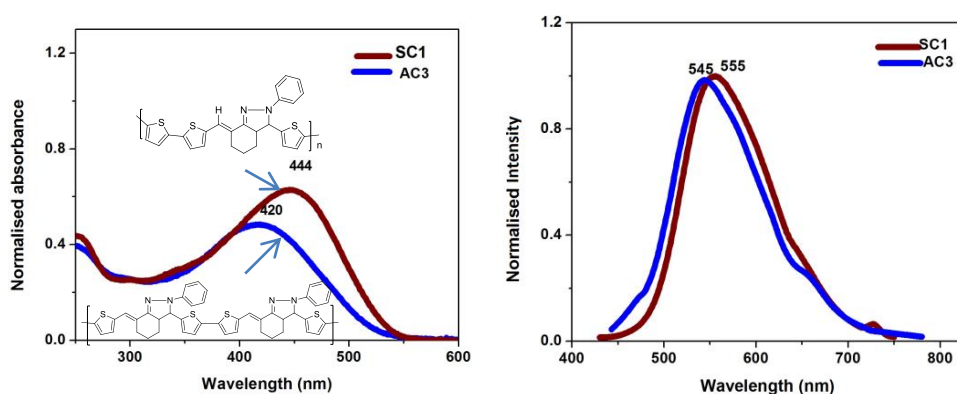


Figure 5.8: UV-Visible and PL spectra of SC1 and AC3

Compared with the monomer a red shift of 49 nm for the polymer and 39 nm for the oligomer is obtained. Under UV irradiation, a strong yellow emission is observed for polymer and a weak yellow emission for oligomer. Emission spectra ( $\lambda_{\text{ex}} = 350 \text{ nm}$ ) of **SC1** and **AC3** are also presented in Figure 5.8. Photographs showing solution state fluorescence of monomer, oligomer and polymer are also shown in Figure 5.7.

### 5.3.6 SCANNING ELECTRON MICROSCOPY

Scanning electron Microscopy is used to generate the surface morphology of a compound in micrometer realm. The SEM images of powdered **SC1** and **AC3** are given below. Both **SC1** and **AC3** have a uniform arrangement as seen from SEM data. The polymer **SC1** shows a bean like structure considering individual units while that of **AC3** shows some kind of circular flake like morphology. The structures of polymer and oligomer of pyrazoline, however, shows considerable difference in their arrangement with polymer having a distinguishable surface resolution compared with oligomer.

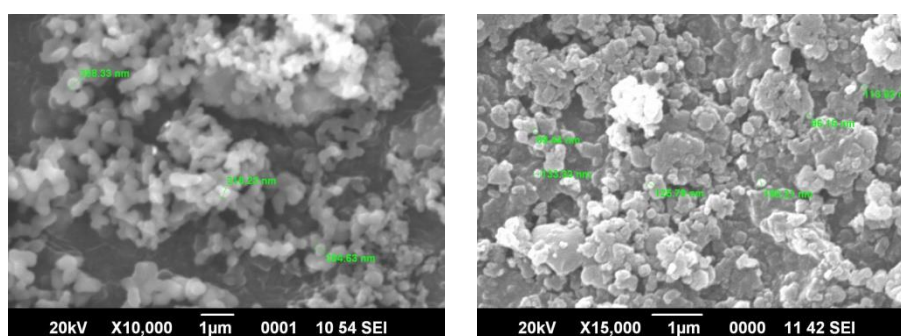
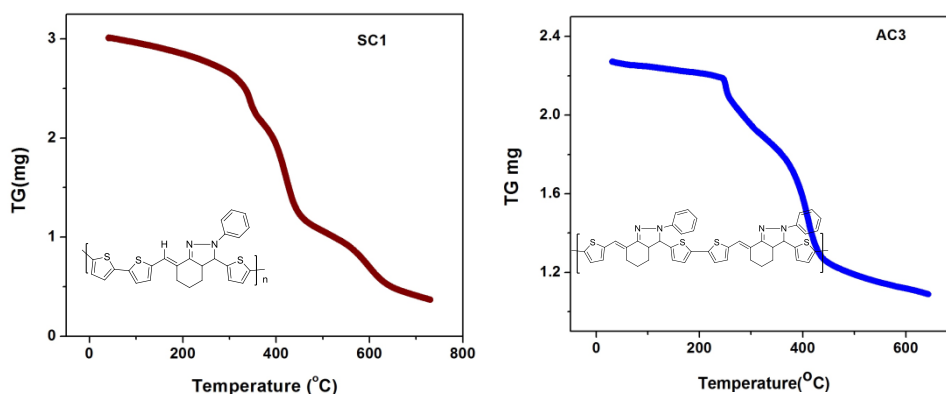


Figure 5.9: SEM images of **SC1** and **AC3**

### 5.3.7 THERMAL GRAVIMETRIC ANALYSIS

The thermal stability of the compounds was determined using TGA studies. TGA gives information regarding percentage weight loss of the compounds. Polymer SC1 gave 20% weight loss around 345 °C, 61% weight loss around 420 °C and 77% weight loss around 596 °C, which indicates that the compound is stable up to 600 °C. The first weight loss indicates the melting temperature of the polymer and the second and third weight loss may be the scission of C=C bonds by oxidation. The presence of more thiophene units has considerably increased the thermal stability of the polymer of the order of 600 °C. The oligomer AC3 on the other hand, shows two weight losses, one being 8 % weight loss around 200 °C and 42% weight loss around 400 °C, being thermally stable up to 400 °C, similar to the oligo ketones synthesized by direct arylation.



**Figure 5.10: TGA curves of SC1 and AC3**

Polymer	Percentage weight loss			Oligomer	Percentage weight loss	
	344 °C	420 °C	596 °C		200 °C	400 °C
SC1	20%	61%	77%	AC3	8%	42%

**Table 5.2: Percentage weight losses of SC1 and AC3**

### 5.3.8 DIFFERENTIAL SCANNING CALORIMETRY

DSC plot gives information regarding the physical and chemical changes of a sample during heating. We carried out DSC analysis to find out the glass transition temperature ( $T_g$ ) and melting temperature of the synthesized compounds. From the DSC data  $T_g$  of **SC1** and **AC3** were found to be 100 °C and 122 °C. The melting temperatures were obtained at 345 °C and 256 °C which are in agreement with the first decomposition curves of TGA analysis.

Compounds	$T_g$ (°C)	$T_m$ (°C)
SC1	100 °C	345 °C
AC3	122 °C	256 °C

**Table 5.3:  $T_g$  and  $T_m$  of SC1 and AC3**

### 5.3.9 ATOMIC FORCE MICROSCOPY

AFM<sup>19</sup> studies reveal the surface resolution of sample in nanometer realm. AFM performs three functions, viz, force measurement, imaging

and manipulation. In the imaging technique, the measurement of the force which the sample exerts on the probe is used to generate a three dimensional image of the sample at high resolution. The sample moves in a raster scan pattern with respect to tip and the height of the probe from sample is measured based on probe-sample interaction.

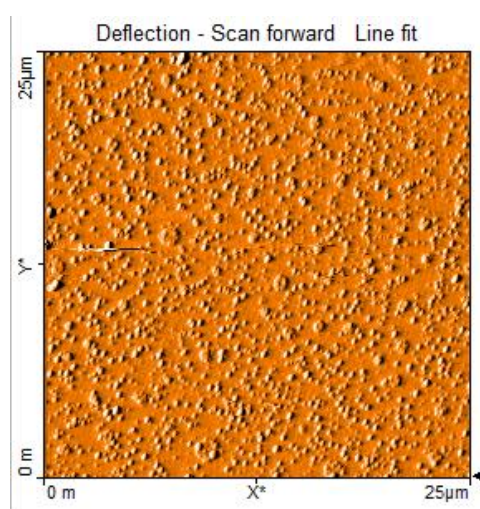


**Figure 5.11: AFM image of SC1**

In our study the polymer sample was spin casted to form a thin uniform film and this was subjected to AFM studies. The image is given above in Figure 5.11. The image shows a uniform distribution of polymer in nanometer resolution. The particles are well oriented and evenly arranged. Spin casting of oligomer is a difficult task and hence no AFM was recorded for **AC3**.

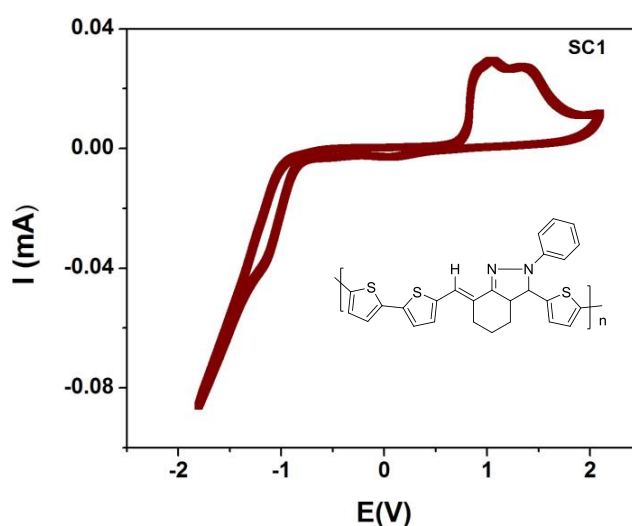
### **5.3.10 CYCLIC VOLTAMMETRY**

Cyclic voltammetric studies using a BAS CV50W voltammetric analyser were performed to determine the electrochemical band gap of synthesised materials. We have employed a three electrode system which consists of

a Standard Calomel Electrode (SCE) (Ag/AgCl electrode), working electrode and a counter electrode similar to the samples done before. The general set up is given in detail in chapter 3 section 3.2.9. The  $E_{\text{HOMO}}$  and  $E_{\text{LUMO}}$  can be calculated using the equations below which in turn gives the band gaps of the synthesised compounds.

$$\begin{aligned} \text{HOMO} &= -(E_{\text{ox-on}} - E_{\text{foc}}) - 4.8 \text{ eV} \\ \text{LUMO} &= -(E_{\text{red-on}} - E_{\text{foc}}) - 4.8 \text{ eV} \\ E_{\text{g}}^{\text{EC}} &= E_{\text{HOMO}} - E_{\text{LUMO}} \end{aligned}$$

Oxidation ( $p$  doping) or reduction ( $n$  doping) occurs during the forward and reverse scans. In the case of **AC3** reduction peak could not be confirmed from CV graph, hence we also attempted the Differential pulse voltammetry. The DPV graph for reduction is shown in Figure 5.13. The Cyclic Voltammograms of **SC1** and **AC3** are shown below:



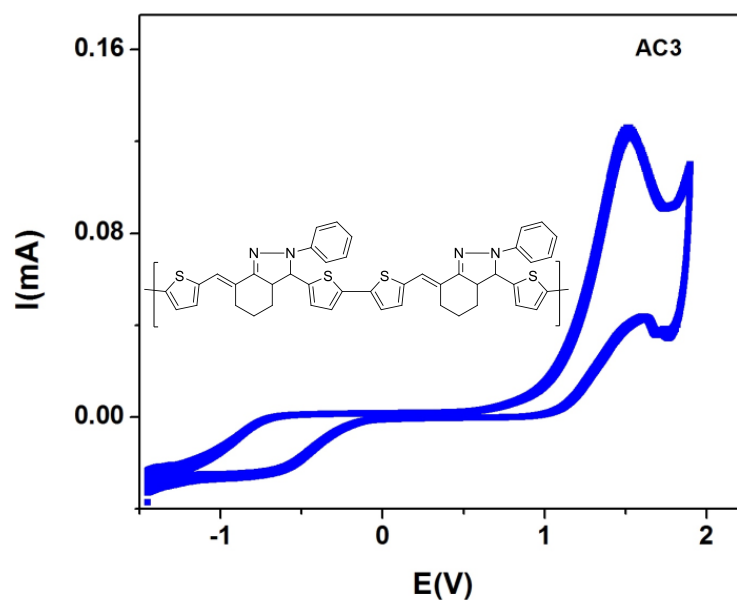


Figure 5.12: Cyclic Voltammogram of SC1 and AC3

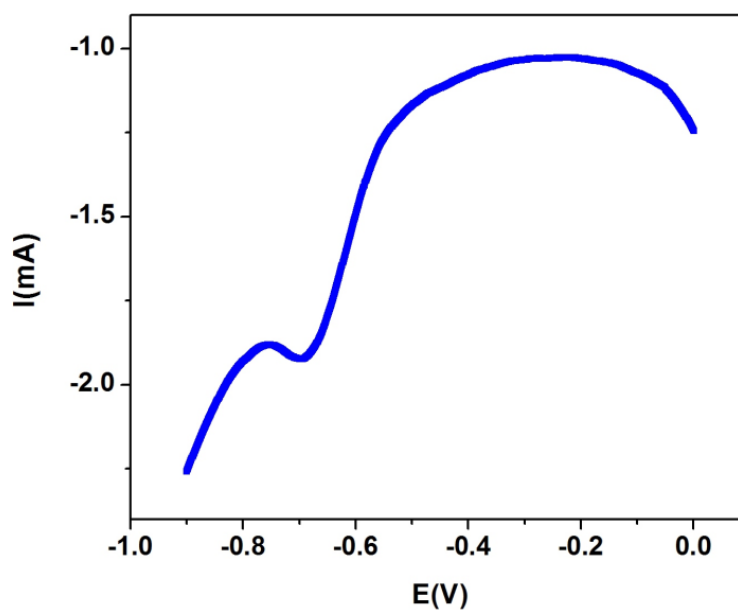


Figure 5.13: DPV curve for reduction of AC3

The HOMO, LUMO and electrochemical band gap ( $E_g^{EC}$ ) are displayed in the table below.

Compound	$E_{ox,on}(V)$	$E_{re,on}(V)$	HOMO (eV)	LUMO (eV)	$E_g^{EC}(eV)$
SC1	0.99	-1.11	-5.33	-3.23	2.1
AC3	1.51	-0.65	-5.85	-3.69	2.16

Table 5.4: Electrochemical data for SC1 and AC3

The electrochemical band gap is found to be almost in agreement with the optical band gap calculated from UV which is in the range of 2.23 and 2.40 for SC1 and AC3.

### 5.3.11 THEORETICAL METHODOLOGY

Band structure of SC1 was calculated using periodic boundary calculation by HSE06/6-31G(d) theory using the unit cell taken from the central portion of the optimized tetramer and is depicted in the Figure 5.14. Red line represents the translational vector. The geometry and energy levels of AC3 was calculated using B3LYP/6-31G(d) theory. The stationary points are characterized by frequency calculation. All calculations were done using G09 suites of codes.

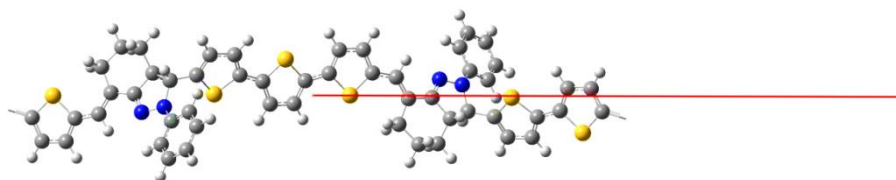
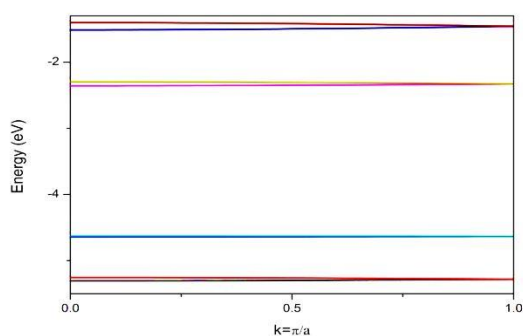


Figure 5.14: Unit cell of SC1 for the PBC/HSE06/6-31G (d) calculation



Four occupied and four unoccupied crystal orbitals were selected for study. The band structure of **SC1** is shown in **Figure 5.15**.



**Figure 5.15: Band structure of SC1**

The HOCO occurs at -4.63 eV and LUCO occurs at -2.36eV. The theoretical band gap of the polymer was found to be 2.27eV. Energy levels and density of states of **AC3** is shown in Figure 5.16. The HOMO and LUMO of **AC3** occurs at -4.83 eV and -2.11 eV respectively. The energy gap is calculated to be 2.72 eV for **AC3**.

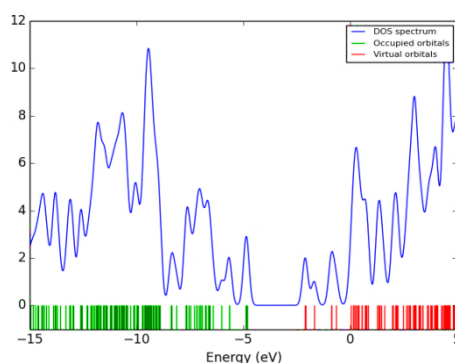


**Figure 5.16: Energy level diagram and DOS of AC3**

Polymer	HOCO	LUCO	Eg <sup>DFT</sup> (eV)	Eg <sup>UV</sup> (eV)
SC1	-4.63	-2.36	2.27	2.23

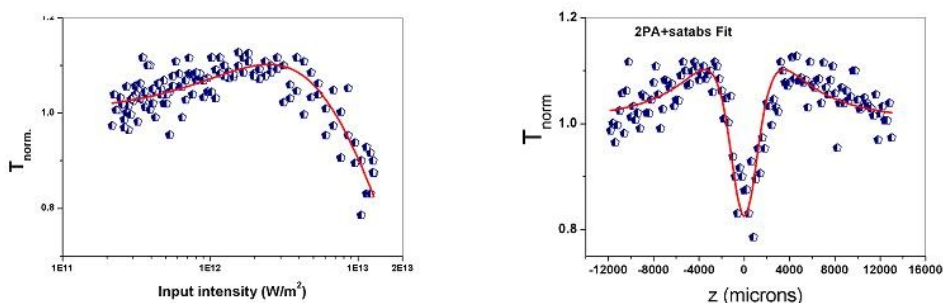
Oligomer	HOMO	LUMO	Eg <sup>DFT</sup> (eV)	Eg <sup>UV</sup> (eV)
AC3	-4.83	-2.11	2.72	2.40

Table 5.4: Comparison of band gaps of SC1 and AC3

A slight difference in band gap is due to the calculations in solution state and gaseous state.

### 5.3.12 NON LINEAR OPTICS

The third order non-linear optical studies of the compounds were carried out using Z-scan technique (explained in chapter 3 section 3.2.10). A peak in the curve indicates saturable absorption (SA) and valley in the curve indicates reverse saturable absorption (RSA). From the open aperture Z scan curves it is possible to plot a graph between input laser fluence and sample transmission. In the case of **SC1** and **AC3**, the fluence graph indicates optical limiting behavior as given in figure 5.17.



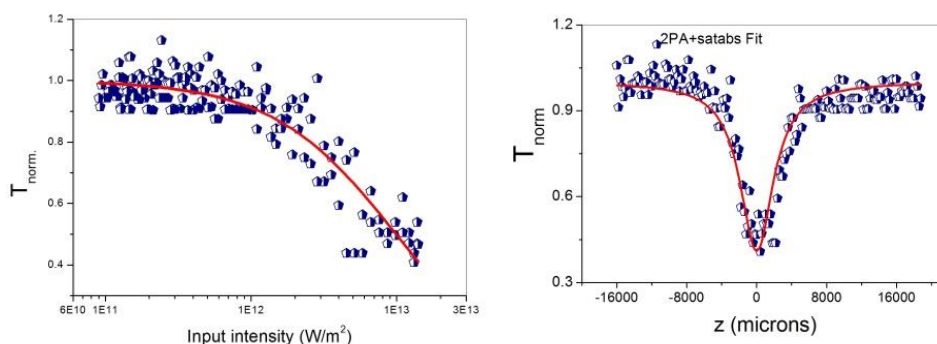


**Figure 5.17: Fluence graph and open aperture Z scan curves of SC1 and AC3**

From the graph, it can be clearly seen that the polymer **SC1** has a peak and valley in the curve indicating both SA and RSA. Whereas for **AC3**, the peak SA is absent, this means that there is no increase in transmittance observed at any particular laser intensity. RSA is the only dominating factor which indicates optical limiting character alone. For **SC1**, even though RSA has the major role to play, SA is also observed due to which they can be opted as optical limiters and optical switches. The effective two photon absorption coefficient value is larger for **AC3** which reveals that compared with polymer; the oligomer is the best optical limiter. The table shows the  $\beta_{\text{eff}}$  and  $Im \chi^{(3)}$  values of **SC1** and **AC3**.

Sample	Excitation energy ( $\mu\text{J}$ )	Saturation Intensity ( $I_s$ ) ( $10^{-10} \text{ W/m}^2$ )	$\beta_{\text{eff}} (\times 10^{-10} \text{ m/W})$	$Im \chi^{(3)} (\text{esu})$
<b>AC3</b>	<b>50</b>	<b>500</b>	<b>1.90</b>	$4.0 \times 10^{-10}$
<b>SC1</b>	<b>50</b>	<b>300</b>	<b>0.78</b>	$1.7 \times 10^{-10}$

**Table 5.5: Two photon absorption coefficients and  $Im\chi^{(3)}$  of SC1 and AC3**

### 5.3.13 Measurement of I-V characteristics

I-V characteristics of **SC1** and **AC3** were measured based on the device set up given in chapter 2 section 3.2.12. Forward bias current was obtained when anode was positively biased and cathode was negatively biased. The current-voltage characteristic for Ag/polymer or oligomer/Au device configuration is given below in the figure 5.18. Here it can be clearly seen that once the barrier potential is achieved, there is a sharp increase in the current even for a small variation of voltage. This potential is called the Knee voltage or threshold voltage. Both the compounds show a junction like behavior which is typical for fabrication of PLED's. This in turn also ensures that the materials synthesised are semiconducting in nature.

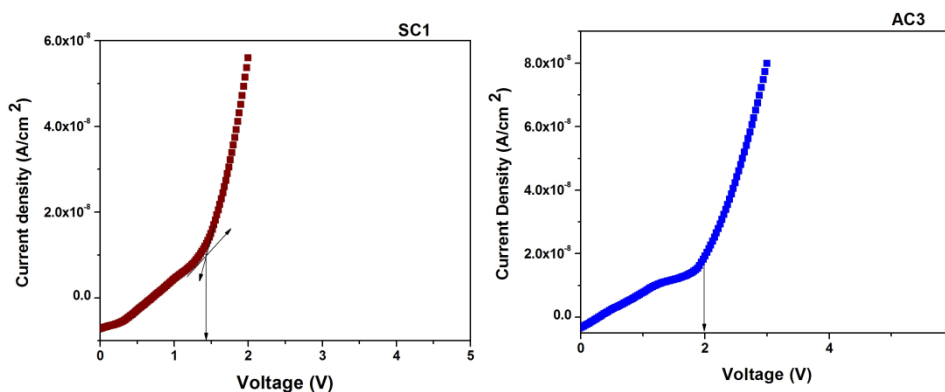


**Figure 5.18: I-V characteristics of Ag/oligomer/Au devices using SC1 and AC3**

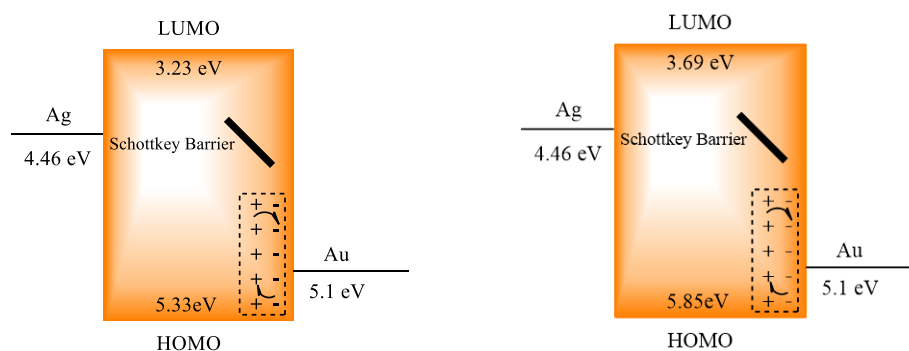


**Figure 5.19: Energy diagram of Ag/(a)polymer or (b)oligomer/Au device configuration using SC1 and AC3**

The energy diagram for Ag/polymer or oligomer/Au device configuration using **SC1** and **AC3** are given in the figure 5.19 below. The HOMO levels of the materials matches well with the work function of the metal to ensure the flow of electrons and holes for the formation of junction.

## 5.4 CONCLUSIONS

We synthesised two novel materials, **SC1** and **AC3**, which are yellow emitting polymer and oligomer by Stille coupling and direct arylation methods. Both the materials are hexahydro-2*H*-indazole derivatives of bithiophene cyclohexanone system which is probably a novel route and novel approach towards pyrazoline chemistry. There are many reports for the synthesis of polymers incorporating pyrazoline units having photoconductive applications and hence we have tried synthesizing such kind of materials with pyrazolines from  $\alpha,\beta$ -unsaturated ketones. The structure of the compounds was confirmed by  $^1\text{H}$  NMR and IR data. The

absorption and emission peaks were determined from UV-Visible and PL spectra. The major absorption peaks for SC1 and AC3 were at 444 nm and 420 nm and the emission peaks were at 555 nm and 545 nm. Surface morphology in micrometer and nanometer realm was obtained from SEM and AFM studies. The electrochemical band gap was calculated from Cyclic voltammetry which shows that the compounds are semiconductors. The optical band gap was determined from UV spectra and the theoretical band gap was established using hybrid theory calculations by B3LYP/6-31G(d) and HSE06/6-31G(d) theory. The band gaps calculated are all in semiconductor range and the slight variation is due to the calculations in different states like solid, solution and gaseous states. The non-linear optical studies were carried out using Z-scan technique which confirms the compounds to be good optical limiters. The polymer SC1 shows switching between SA and RSA whereas the oligomer AC3 shows RSA alone with high two photon absorption coefficient due to which AC3 can be opted for as the best optical limiter. The I-V graphs of the device set up with Ag/polymer or oligomer/ Au configuration ensures the applicability of these materials for fabricating PLED's.

## 5.5 EXPERIMENTAL

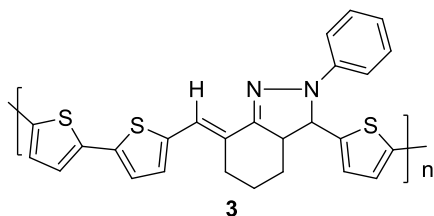
All reactions were done in dry glasswares. Chemicals were purchased from sigma Aldrich or spectrochem and used without further purification. Infra-red spectra were recorded using *Jasco 4100 FT-IR* spectrometers. A *Bruker Avance III* FT-NMR spectrometer with tetramethyl silane (TMS) as internal standard was used to record  $^1\text{H}$  NMR at 400 MHz. Chemical

shifts ( $\delta$ ) are reported in parts per million (ppm) downfield of TMS. The Powder X-ray diffraction (XRD) patterns were obtained using a Rigaku X-ray diffractometer with Cu K $\alpha$  radiation (1.542 Å). The molecular weight of the synthesized polymers was determined by GPC, (Shimadzu-Prominence) using a Column packed with polystyrene gel beads and THF was used as the eluent. The UV-visible absorption spectra were recorded using Thermo Evolution Model 201. Photoluminescence studies were carried out using Fluoromax-3 fluorescence spectrophotometer. The glass transition temperature was measured using a Q100 Differential Scanning Calorimeter and thermal stability was determined using Q50 Thermal Gravimetric Analyser at a rate of 10 °C/ min under nitrogen atmosphere. Computational calculations were done using Density Functional Theory (DFT) with B3LYP/6-31G and HSE06/6-31G(d) hybrid functional. The nonlinear optical properties of the samples were investigated using the Z-scan technique employing the second harmonic output (532 nm) of a Q-switched Nd: YAG laser (Minilite, Continuum USA). JEOL model JSM-6390LV Scanning electron Microscope (SEM) was used to generate surface morphological images of the samples with the resolution of a micrometer.

#### **5.5.1 Synthesis of polymer (SC1) (3) of (*E*)-3-(5-bromothiophen-2-yl)-7-((5-bromothiophen-2-yl) methylene) -2-phenyl-3,3a,4,5,6,7-hexahydro-2*H*-indazole using Stille coupling**

To a mixture of Pd(PPh<sub>3</sub>)<sub>4</sub> (0.05 g, 0.043 mmol), (*E*)-3-(5-bromothiophen-2-yl)-7-((5-bromothiophen-2-yl)methylene)-2-phenyl-3,3a,4,5,6,7-hexahydro-2*H*-indazole (**1**, 0.095 g, 0.0019 mmol) and 2,5-bis(tributyl)stannylthiophene (**2**, 0.12 g, 0.18 mmol) taken in a three

necked RB flask, freshly distilled toluene (5 mL) was added. Under a positive pressure of N<sub>2</sub>, the reactants were heated to reflux until the black metallic palladium precipitated. The mixture was then cooled to room temperature and then poured into 50mL methanol. Sequential extraction of precipitated polymer was performed using methanol, hexane and THF. The polymer was dissolved in minimum amount of THF and re-precipitated from methanol.



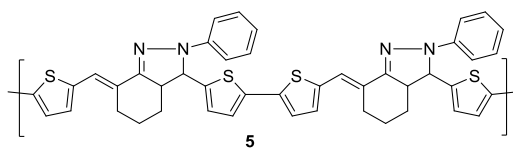
*Characterization data:* Yield: 40%; M<sub>w</sub>: 6358; PDI: 1.47; IR (KBr): 3878, 3419, 2962, 2354, 1596, 1384, 1261, 1021 cm<sup>-1</sup>; <sup>1</sup>H NMR (CDCl<sub>3</sub>): δ 7.13-7.04 (m, 3H), 7.00-6.98 (m, 3H), 6.90-6.76 (m, 1H), 5.89 (s, 1H), 5.22 (s, 1H), 4.76-4.62 (m, 1H), 3.82 (s, 1H), 3.18-3.08 (m, 1H), 2.27-2.14 (m, 2H), 1.47 (m, 4H), 1.36 (d, 2H).

### 5.5.2 Synthesis of Oligomer (*E*)-3-(5-methylthiophen-2-yl)-7-((5'-((*E*)-7-((5-methyl thio phen-2-yl)methylene)-2-phenyl-3,3a,4,5,6,7-hexahydro-2H-indazol-3-yl)-[2,2'-bithio phen]-5-yl)methylene)-2-phenyl-3,3a,4,5, 6,7-hexahydro-2H-indazole (AC3) (**5**) by direct arylation method.

A mixture of (*E*)-2-phenyl-3-(thiophen-2-yl)-7-(thiophen-2-ylmethylene)-3,3a,4,5,6,7-hexahydro-2H-indazole (**5**, 0.078 g, 0.53 mmol in 10 mL DMF), tetrabutylammonium bromide (0.17 g, 0.53 mmol) and sodium acetate (0.17 g, 2.1 mmol) was stirred at room temperature for 15 minutes. After 15 minutes, added (*E*)-3-(5-bromothiophen-2-yl)-7-((5-bromothiophen-2-yl)methylene)-2-phenyl-3,3a,4,5,6,7-hexahydro-2H-indazole (**1**, 0.120 g, 0.53 mmol) and palladium acetate (0.01 g, 10 mol %)



and the mixture was stirred at 90 °C for 72 h. The reaction mixture was cooled and poured in to cold methanol. The precipitate was collected by filtration. The polymer was purified by Soxhlet extraction by using methanol, hexane and CHCl<sub>3</sub> as solvent. The product was dissolved in minimum amount of chloroform and precipitated in methanol.



*Characterization data:* Yield: 53%; M<sub>w</sub>: 2489; PDI: 1.00; IR (KBr): 3426, 2928, 1596, 1493, 1321, 1107, 1032, 751, 695 cm<sup>-1</sup>; <sup>1</sup>H NMR (CDCl<sub>3</sub>): δ7.44-7.39 (m, 2H), 7.14-7.09 (m, 5H), 7.01-6.97 (m, 3H), 6.93-6.78 (m, 3H), 4.73-4.63 (m, 3H), 3.09-3.03 (m, 4H), 2.31-2.28 (d, 2H), 2.14-2.10 (d, 2H), 2.00-1.97 (d, 2H).

## 5.6 REFERENCES

- 1) Stille, J. K. *Angew. Chem.* **1986**, 98, 504.
- 2) Stille, J. K. *Angew. Chem.Int. Ed. Engl.* **1986**, 25, 508.
- 3) Ackermann, L.; Vicente, R.; Kapdi, A. R. *Angew. Chem., Int. Ed.* **2009**, 48, 9792.
- 4) Bellina, F.; Rossi, R. *Tetrahedron* **2009**, 65, 10269.
- 5) Lu, W.; Kuwabara, J.; Kanbara, T. *Macromolecules* **2011**, 44, 1252.
- 6) Fujinami, Y.; Kuwabara, J.; Lu, W.; Hayashi, H.; Kanbara, T. *ACS Macro Lett.* **2012**, 1, 67.
- 7) Agrofoglio, L. A.; Gillaizeau, I.; Saito, Y. *Chem. Rev.* **2003**, 103, 1875.
- 8) Farina, V.; Krishnamurthy, V.; Scott, W. J. *Org. React.* **1997**, 50, 1.
- 9) Baldwin, J. V.; Adlington, R. M.; Ramcharitar, S. H. *Tetrahedron* **1992**, 48, 2957.

- 10) Kalivretenos, A.; Stille, J. K.; Hegedus, L. S. *J. Org. Chem.* **1991**, *56*, 2883
- 11) Yamamoto, T. *NPG Asia Mater.* **2010**, *2*, 54.
- 12) Ohmori, Y.; Uchida, M.; Muro, K.; Yoshino, K. *Jpn. J. Appl. Phys.* **1991**, *30*, L1938.
- 13) Ohmori, Y.; Morishita, C.; Uchida, M.; Yoshino, K. *Jpn. J. Appl. Phys.* **1992**, *31*, L568.
- 14) Braun, D.; Gustaffson, G.; Macbranch, D.; Heeger, A. *J. Appl. Phys.* **1992**, *72*, 164.
- 15) Barbarella, G.; Favaretto, L.; Zanelli, A.; Gigli, G.; Mazzeo, M.; Anni, M.; Bongini, A. *Adv. Funct. Mater.* **2005**, *15*, 664.
- 16) Peripichka, I. I.; Peripichka, I. F.; Bryce, M. R.; Palsson, L. O. *Chem. Commun.* **2005**, 3397.
- 17) Vivas, M. G.; Nogueira, S. L.; Santos Silva, L.; Barbosa Neto, N. M.; Marletta, A.; Serein-Spirau, F.; Lois, S.; Jarrosson, T.; De Boni, L.; Silva, R.A.; Mendonca, C. R. *J. Phys. Chem. B.* **2011**, *115*, 12687, 12693.
- 18) Fang, Q.; Jiang, B.; Xu, B.; Cao, A. *Macromol.Rapid.Commun.* **2004**, *25*, 1856.
- 19) Sharifi-Viand, A.; Ghasem-Mahjani, M.; Moshrefi, R.; Jafarian, M. *Vacuum* **2015**, *114*, 17.

## **Summary and Conclusions**

This section summarises the general outline of the work done in this thesis. The thesis entitled “**DESIGN AND SYNTHESIS OF SOME NOVEL YELLOW AND GREEN LIGHT EMITTING ORGANIC MATERIALS FOR APPLICATION IN NON-LINEAR OPTICS AND RELATED STUDIES**” deals with the synthesis of some novel light emitting organic materials and exploiting the possibility of exploring them in various fields like non-linear optics and polymeric light emitting diodes (PLED’s). We have chosen thiophene *viz.*, bithiophene cycloalkanones as the basic skeleton for synthesis and the advantages and applicability of thiophene based oligomers and polymers in the present era are very well stated in chapter 1. Though biological activities of bithiophene cycloalkanones has widely been investigated, their application as monomers for synthesis of oligomers and polymers has not been exploited yet. In this context, with limited literature reports on such materials, we have tried synthesising some organic materials that can be used as promising candidates in the field of optoelectronics.

In chapter 2, several bithiophene cycloalkanones are synthesised using four classes of spacers. Incorporation of such rigid spacers into the thiophene backbone offers a more planar conformation with diminished steric effect so that maximum delocalisation of  $\pi$  electrons can be achieved. They also experience less neighbouring interactions when compared with polythiophenes. We have presented the spectral data’s of novel compounds only and selected ones where used for polymerisation. The basic polymerisation techniques used for synthesis of polythiophenes like Stille coupling, direct arylation etc. can also be employed for

synthesis of oligothiophenes and so as said selected monomers were subjected to polymerisation using these methods. For bithiophene cycloalkanones, however, Stille coupling seemed to be inefficient and hence we have opted for direct arylation method and synthesised two oligomers both of which are bright yellow-orange emitting and these materials were completely characterised using  $^1\text{H}$  NMR, FTIR, Powder XRD, SEM, TGA, DSC, UV-Visible, PL, GPC, Cyclic voltammetry and computational analyses. All these results are presented in chapter 3. The third non-linear optical properties of the material revealed their optical limiting nature. The Schottky diode characteristics of the material were studied by measurement of I-V characteristics which in turn also ensures the applicability of these materials in optoelectronics despite its low degree of polymerisation.

In continuation, derivatives of bithiophenes *viz.*, pyrazolines were synthesised by their reaction with phenyl hydrazine. We observed that structure of bithiophene cycloalkanones played a decisive role in their efficacy for conversion into pyrazoline derivative, while bithiophene cyclohexanones and some of their derivatives reacted smoothly, other bithiophene cycloalkanones completely failed to give the product. Hence, we investigated the mechanism of formation of pyrazolines by theoretical methods. Computational calculations carried out using B3LYP hybrid functional was found to be in agreement with the experimental data. The results are based on energy profile diagrams and such an approach is considered to be an innovative idea in pyrazoline chemistry. The results are provided in chapter 4.

The pyrazolines are intense green light emitting compounds with promising optoelectronic applications and we extended our studies to polymerisation of these pyrazoline incorporated moiety using Stille coupling and direct arylation methods, resulting in the formation of novel polymer and oligomer which are presented in chapter 5 of this thesis. All characterisations were done as before and third order non-linear optical properties and I-V measurement ensured the applicability of these materials in devices.

Our studies helped us to conclude that despite being oligomers, our materials have equal probability of application in optoelectronic devices like polymers. The scope of our synthesis can be extended to various other derivatives of these materials; probably no one has yet explored the application of these light emitting materials in devices.

*Summary and Conclusions*

---

**List of Publications**

- 1) **C. Nithya**, M. Sithambaresan, S. Prathapan, M.R. PrathapachandraKurup, “(2*E*,7*E*)-2,7-Bis[(thiophen-2-yl)methylidene]cycloheptanone”, *Acta Cryst.* **2014**, *E70*, o722.
- 2) **C. Nithya**, M. Sithambaresan, M. R. Prathapachandra Kurup, “Crystal structures of (1*E*,4*E*)-1,5-bis(5-bromothiophen-2-yl)-2,4-dimethylpenta-1,4-dien-3-one and (*E*)-4-(5-bromothiophen-2-yl)-1,3-diphenylbut-3-en-2-one”, *Acta Cryst.* **2016**, *E72*, 199-202.
- 3) **Nithya C.**, Abhilash A., Jayalekshmi S., Unnikrishnan P. A. and Prathapan S. “Synthesis of (1*Z*,3*E*,4*Z*,6*E*)-1,3,4-tris(thiophen-2-ylmethylene)-6-(thiophen-3-yl)methylene tetra hydro-pentalene-2,5(1*H*,3*H*)-dione”, *MATCON 2016 International Conference on Materials for the Millennium* January 14 -16, 2016. (ISBN 978-93-80095-738)
- 4) **Nithya C.**, Abhilash A., Jayalekshmi S., Unnikrishnan P. A. and Prathapan S. “Synthesis and determination of optoelectronic properties of (*E*)-3-(5-bromothiophen-2-yl)-7-((5-bromothiophen-2-yl) methylene)-2-phenyl-3,3a,4, 5,6,7-hexahydro-2*H*-indazole and a polymer derived thereof”, *MATCON 2016 International Conference on Materials for the Millennium* January 14 -16, 2016. (ISBN 978-93-80095-738)
- 5) **Nithya C.**, Saumya T. S., Unnikrishnan P.A. and Prathapan S. “Regioselectivity and Mechanism for Synthesis of (1*Z*,3*E*,4*Z*,6*E*)-1,3,4-tris (thiophen-2-ylmethylene)-6-(thiophen-3-ylmethylene)tetrahydro-pentalene-2,5(1*H*,3*H*)-dione and (1*E*,4*E*)-

1,4-bis(anthracen-9-ylmethylene)tetrahydropentalene-2,5  
(1H,3H)-dione” *Journal of Materials Chemistry C*, (under  
preparation).

- 6) **Nithya Chakingal**, Anand Puthirath Balan, Abhilash Ayyappan,  
Mahesh Kumar, M. V., Reji Philip, Jayalekshmi Sankaran and  
Prathapan Sreedharan, “Synthesis, non-linear optical studies and  
Schottky diode characterization of few thiophen based materials  
synthesised using Stille and direct arylation methods” *Dyes and  
Pigments* (under preparation).

### **Poster presentations**

- 1) Synthesis of pyrazolines from Bisthiophene cycloalkanones,  
**Poster Presentation, C. Nithya** and S. Prathapan, CTriC 2013  
National seminar at Cochin University of Science and  
Technology, Kerala, India.
- 2) Synthesis of Bisthiophene cycloalkanones, **Poster Presentation,**  
**C. Nithya**, P. A. Unnikrishnan and S. Prathapan. CTriC 2014  
National seminar at Cochin University of Science and  
Technology, Kerala, India.





**DEPARTMENT OF APPLIED CHEMISTRY  
COCHIN UNIVERSITY OF SCIENCE AND TECHNOLOGY  
KOCHI- 682 022, KERALA, INDIA**

*March 2017*